IEEE Standards

IEEE Std 1110™-2002
(Revision of
IEEE Std 1110-1991)

1110™

IEEE Guide for Synchronous Generator Modeling Practices and Applications in Power System Stability Analyses

IEEE Power Engineering Society

Sponsored by the
Electric Machinery Committee

IEEE

Published by
The Institute of Electrical and Electronics Engineers, Inc.
3 Park Avenue, New York, NY 10016-5997, USA

11 November 2003

Print: SH95058
PDF: SS95058

Recognized as an
American National Standard (ANSI)

IEEE Std 1110™-2002(R2007)
(Revision of
IEEE Std 1110-1991)

IEEE Guide for Synchronous Generator Modeling Practices and Applications in Power System Stability Analyses

Sponsor

Electric Machinery Committee
of the
IEEE Power Engineering Society

Reaffirmed 24 April 2008
Approved 26 February 2002

American National Standards Institute

Reaffirmed 27 September 2007
Approved 11 November 2002

IEEE-SA Standards Board

Abstract: Categorizes three direct-axis and four quadrature-axis models, along with the basic transient reactance model. Discusses some of the assumptions made in using various models and presents the fundamental equations and concepts involved in generator/system interfacing. Covers, generally, the various attributes of power system stability, recognizing two basic approaches. The first is categorized under large disturbance nonlinear analysis; the second approach considers small disturbances, where the corresponding dynamic equations are linearized. Applications of a range of generator models are discussed and treated. The manner in which generator saturation is treated in stability studies, both in the initialization process as well as during large or small disturbance stability analysis procedures is addressed. Saturation functions that are derived, whether from test data or by the methods, of finite elements are developed. Different saturation algorithms for calculating values of excitation and internal power angle depending upon generator terminal conditions are compared. The question of parameter determination is covered. Two approaches in accounting for generator field and excitation system base quantities are identified. Conversion factors are given for transferring field parameters from one base to another for correct generator/excitation system interface modeling, Suggestions for modeling of negative field currents and other field circuit discontinuities are included.
Keywords: modeling practices, saturation practices, stability data determination and application, synchronous generator stability models

The Institute of Electrical and Electronics Engineers, Inc.
3 Park Avenue, New York, NY 10016-5997, USA

Print: ISBN 0-7381-3481-3 SH95058
PDF: ISBN 0-7381-3482-1 SS95058

IEEE Standards documents are developed within the IEEE Societies and the Standards Coordinating Committees of the IEEE Standards Association (IEEE-SA) Standards Board. The IEEE develops its standards through a consensus development process, approved by the American National Standards Institute, which brings together volunteers representing varied viewpoints and interests to achieve the final product. Volunteers are not necessarily members of the Institute and serve without compensation. While the IEEE administers the process and establishes rules to promote fairness in the consensus development process, the IEEE does not independently evaluate, test, or verify the accuracy of any of the information contained in its standards.

Use of an IEEE Standard is wholly voluntary. The IEEE disclaims liability for any personal injury, property or other damage, of any nature whatsoever, whether special, indirect, consequential, or compensatory, directly or indirectly resulting from the publication, use of, or reliance upon this, or any other IEEE Standard document.

The IEEE does not warrant or represent the accuracy or content of the material contained herein, and expressly disclaims any express or implied warranty, including any implied warranty of merchantability or fitness for a specific purpose, or that the use of the material contained herein is free from patent infringement. IEEE Standards documents are supplied "**AS IS**."

The existence of an IEEE Standard does not imply that there are no other ways to produce, test, measure, purchase, market, or provide other goods and services related to the scope of the IEEE Standard. Furthermore, the viewpoint expressed at the time a standard is approved and issued is subject to change brought about through developments in the state of the art and comments received from users of the standard. Every IEEE Standard is subjected to review at least every five years for revision or reaffirmation. When a document is more than five years old and has not been reaffirmed, it is reasonable to conclude that its contents, although still of some value, do not wholly reflect the present state of the art. Users are cautioned to check to determine that they have the latest edition of any IEEE Standard.

In publishing and making this document available, the IEEE is not suggesting or rendering professional or other services for, or on behalf of, any person or entity. Nor is the IEEE undertaking to perform any duty owed by any other person or entity to another. Any person utilizing this, and any other IEEE Standards document, should rely upon the advice of a competent professional in determining the exercise of reasonable care in any given circumstances.

Interpretations: Occasionally questions may arise regarding the meaning of portions of standards as they relate to specific applications. When the need for interpretations is brought to the attention of IEEE, the Institute will initiate action to prepare appropriate responses. Since IEEE Standards represent a consensus of concerned interests, it is important to ensure that any interpretation has also received the concurrence of a balance of interests. For this reason, IEEE and the members of its societies and Standards Coordinating Committees are not able to provide an instant response to interpretation requests except in those cases where the matter has previously received formal consideration.

Comments for revision of IEEE Standards are welcome from any interested party, regardless of membership affiliation with IEEE. Suggestions for changes in documents should be in the form of a proposed change of text, together with appropriate supporting comments. Comments on standards and requests for interpretations should be addressed to:

Secretary, IEEE-SA Standards Board
445 Hoes Lane
P.O. Box 1331
Piscataway, NJ 08855-1331
USA

Note: Attention is called to the possibility that implementation of this standard may require use of subject matter covered by patent rights. By publication of this standard, no position is taken with respect to the existence or validity of any patent rights in connection therewith. The IEEE shall not be responsible for identifying patents for which a license may be required by an IEEE standard or for conducting inquiries into the legal validity or scope of those patents that are brought to its attention.

Introduction

(This introduction is not part of IEEE Std 1110-2002, IEEE Guide for Synchronous Generator Modeling Practices and Applications in Power System Stability Analyses.)

The Joint Working Group on Determination and Application of Synchronous Machine Models for Stability Studies was formed in 1973. The scope of the Working Group was updated in 1986 and its purpose was stated:

"Define synchronous machine models, particularly for solid iron rotor machines, for use in stability studies, and recommend standard methods for determining the values of parameters for use in these models by calculation and/or test. Assess the effect of magnetic saturation on these parameters. Devise and recommend analytical methods for incorporating such machine models, including representation of saturation, into stability programs."

The Joint Working Group was responsible for two particular IEEE Committee Reports on the subject of machine modeling. The first was published in PA & S in 1980. In 1983, the Working Group (W/G) organized a one-day symposium on the subject of machine modeling and generator stability data acquisition at the IEEE PES Winter Power Meeting. Following publication of our second IEEE committee report in March 1986 (vol. EC-1), the group and the two committees to whom we then reported (PSE and Electric Machinery) suggested that application be made to the New Standards Committee (NesCom) of the Standards Board for permission to publish a guide outlining the work which we had sponsored over the past ten to fifteen years. A Project Authorization Request was made through the Power System Engineering Committee, which was approved by the IEEE Standards Board on December 12, 1985. This occurred at the December 12, 1985 meeting of NesCom, and the request was issued as Projection Authorization Request (PAR) number P1110.

The membership of the Joint Working Group remained essentially unchanged between 1986 and 1991, when the complete document was approved as a guide by the IEEE Standards Board in 1991 (IEEE Std 1110-1991).

With the publication of IEEE Std 1110 in 1991, the Joint Working Group had discharged its original mandate and so was disbanded. Its principal thrust was then subsequently organized under the PES Electric Machinery Committee (EMC). One of the newer Working Groups in the EMC also involved a merging of IEEE Std 115™ and IEEE Std 115A™, which related to test procedures for synchronous machines. This second W/G project was completed in 1995 and this new standard consists of two portions. The first portion was subtitled "Acceptance and Performance Testing." The second portion included a lengthy example consisting of the many steps followed in parameter determination for machine stability analysis. Both sudden short-circuit test data and test data from frequency response measurements were used in Part II.

The Synchronous Machinery Subcommittee recommended, with the publishing, especially of Part II of IEEE Std 115, in 1995, that a review of the related IEEE Std 1110 was very much in order.

In 1996 a new PAR was approved. Its form and outline are about the same as the 1991 document, but many clauses have been completely rewritten. The older (1991) document had the title "IEEE Guide for Synchronous Generator Modeling Practices in Stability Analysis." The new guide has the title "IEEE Guide for Synchronous Generator Modeling Practices and Applications in Power System Stability Analyses."

It should be noted that one of the Joint Working Group members, Charles Concordia, had made an interesting prediction in the discussion of his 1960 paper on solid cylindrical rotor synchronous machines. This prediction stated "by a more detailed consideration of actual rotor configurations, equations amenable to attack by frequency response techniques may be obtained." This prediction has been verified in the two standards produced, namely IEEE Std 1110-1991 and IEEE Std 115-1995.

Charles Concordia was a key member of the Working Group, which produced the 1991 IEEE Std 1110 document. He also was involved prior to 1991 in suggested improvements in the "first" guide after it was published. Therefore, the current Working Group wishes to highlight his many contributions by dedicating this latest guide in his honor.

The present Working Group (W/G 7 of Synchronous Machinery S/C) wishes to acknowledge the material and physical inputs to the guide recently made by Ms. Patricia Doherty, administrative assistant with The Edward S. Rogers Sr. Department of Electrical and Computer Engineering at the University of Toronto, as she was instrumental in producing the final manuscript.

At the time this complete draft was submitted by W/G 7 of the Synchronous Machinery S/C, its structure and its membership were as follows:

Paul L. Dandeno, *Chair*

Prabha S. Kundur, *Co-Chair*

Stephen D. Umans, *Secretary*

Innocent Kamwa, *Co-Secretary*

Haran Karmaker
Sheppard Salon
Ahmed El-Serafi
Manoj Shah

The Working Group especially acknowledges the contributions of its Chair, Paul L. Dandeno, who passed away shortly before the publication of this standard. Paul received the IEEE Power Engineering Society (PES) Individual Service Award in 1984; the PES Outstanding Working Group Award for IEEE Std 115 in 1996; and the IEEE Nikola Tesla Award in 1998. This standard is dedicated to his memory.

The following members of the balloting committee voted on this standard. Balloters may have voted for approval, disapproval, or abstention.

Paul Anderson
William Anderson
Edwin Averill
S. Cherukupalli
Guru Dutt Dhingra
Paul L. Dandeno
Roger Daugherty
James Edmonds
Franklin Emery
Nirmal Ghai
Randall Groves
Adrienne Hendrickson
Gary Heuston
Innocent Kamwa
Haran Karmaker
Prabha S. Kundur
Jesus Martinez
James Michalec
Gary Michel
Daleep Mohla
Lon W. Montgomery
Krste Najdenkoski
Nils E. Nilsson
James Ruggieri
Maurice Secrest
Ahmed El-Serafi
Gerald Vaughn

When the IEEE-SA Standards Board approved this guide on 11 November 2002, it had the following membership:

James T. Carlo, *Chair*

James H. Gurney, *Vice Chair*

Judith Gorman, *Secretary*

Sid Bennett
H. Stephen Berger
Clyde R. Camp
Richard DeBlasio
Harold E. Epstein
Julian Forster*
Howard M. Frazier
Toshio Fukuda
Arnold M. Greenspan
Raymond Hapeman
Donald M. Heirman
Richard H. Hulett
Lowell G. Johnson
Joseph L. Koepfinger*
Peter H. Lips
Nader Mehravari
Daleep C. Mohla
William J. Moylan
Malcolm V. Thaden
Geoffrey O. Thompson
Howard L. Wolfman
Don Wright

*Member Emeritus

Also included are the following nonvoting IEEE-SA Standards Board liaisons:

Alan Cookson, *NIST Representative*
Satish K. Aggarwal, *NRC Representative*

Catherine Berger/Don Messina
IEEE Standards Project Editors

CONTENTS

IEEE Guide for Synchronous Generator Modeling Practices and Applications in Power System Stability Analyses

1. Overview and objectives

1.1 Introduction

The basic techniques for studying the stability of interconnections of synchronous generators stem from the late nineteenth century and the early years of last century. The key concept of transforming stator variables into quantities rotating in synchronism with the rotor was developed by Blondel [B1],[1] Park ([B62], [B63]), and others and remains the basis for synchronous machine analysis to this day.

To some extent, the techniques developed in those early years remained relatively untouched until the last three or four decades of the twentieth century. Although it was in theory possible to develop relatively complex generator models prior to this time, limited computational capability meant that such models were impractical for use in large-scale stability studies. However, with the advent of the digital computer, the picture changed significantly and computational capability continues to grow at a rapid rate. In addition, the growing complexity of electric power systems combined with the advent of more sophisticated generator and system controls, such as high-speed, solid-state excitation systems, greatly increased the demands on stability programs.

In response, the latter part of the twentieth century saw an increased interest in synchronous generator modeling. This interest took many forms. For example, initial investigations attempted to correlate the performance of synchronous machine models with the measured performance of specific machines following transient disturbances on a power system (Chorlton and Shackshaft [B6], Dandeno et al. [B12]). Other investigators developed alternate techniques for determining machine parameters (Manchur et al. [B57]). The objective of this and related work, which continues to this day, is to improve the existing capability to analyze and predict the dynamic behavior of electric power systems. This work becomes increasingly important with the ever-increasing demands being placed on power systems as they continue to grow in size and complexity and as deregulation significantly modifies the way these systems are operated and controlled.

The objective of this guide is to summarize available practices in synchronous machine models used in power system stability studies. As will be discussed, computational capability has increased to the point that

[1]The numbers in brackets correspond to those of the bibliography in Annex A.

it is possible to model generators (along with their excitation systems and other controls) with a significant level of detail, subject to the availability of the appropriate data from which to form the model.

1.2 Specialized problems in stability not discussed in this guide

This guide does not attempt to recommend specific procedures for machine representation in non-standard or atypical cases such as generator tripping and overspeed operation or models for harmonics or unbalanced operation. Similarly, modeling suggestions for subsynchronous resonance (SSR) studies are documented in Dandeno and Iravani [B9] and IEEE [B35]. Recent investigations have shown that models developed from small-signal analyses, based on standstill-frequency-response data, are also adequate for SSR investigations. This applies to situations where third-order models have been found to be necessary to cover the frequency spectrum from 15 Hz to 50 Hz (IEEE [B35]).

1.3 Overview of the guide

Clause 3 discusses the various categories of stability studies which are commonly performed during power system studies and the corresponding synchronous generator modeling requirements. Clause 4 then reviews some of the basic principles of synchronous generator modeling and discusses the range of models which can be used in the study of synchronous generator dynamic behavior as is summarized in Table 1 of Clause 4. This clause emphasizes the point that a model is uniquely determined only when both its structure (e.g., the number of assumed conducting paths in the rotor) and its parameters (as obtained from test data or analytical techniques) are specified. Clause 5 next presents guidelines as to how the various models discussed in Clause 4 can be applied to the various types of stability studies which are discussed in Clause 3.

Clause 6 then discusses the effects of saturation on the performance of synchronous machines and various techniques which have been developed for incorporating these effects in synchronous generator models. Included in Annex D is the development of direct- and quadrature-axis saturation functions. Because saturation is an inherently nonlinear phenomenon while the commonly-used generator models are linear, the techniques used for incorporating saturation effects into generator models are somewhat ad hoc. This is an area in which further investigation is clearly required.

Finally, Clause 7 discusses the techniques which have been developed for obtaining parameters for synchronous generator models. Such parameters are found either by test, as described in IEEE Std 115™-1995, or from calculations by manufacturers.[2] The issue of the translation of parameters from the inductances and resistances of d- and q-axis models to transient and estrangement reactances and time constants or to transfer functions form is also discussed.

2. References

This guide shall be used in conjunction with the following publication. If the following publication is superseded by an approved revision, the revision shall apply.

IEEE Std 115-1995, IEEE Guide: Test Procedures for Synchronous Machines, Part I—Acceptance and Performance Testing, and Part II—Test Procedures and Parameter Determination for Dynamic Analysis.[3, 4]

[2]Information on references can be found in Clause 2.
[3]The IEEE standards or products referred to in Clause 2 are trademarks owned by the Institute of Electrical and Electronics Engineers, Incorporated.
[4]IEEE publications are available from the Institute of Electrical and Electronics Engineers, 445 Hoes Lane, P.O. Box 1331, Piscataway, NJ 08855-1331, USA (http://standards.ieee.org/).

3. Classification of power system stability and synchronous machine modeling requirements

3.1 General background

Traditionally, power system stability studies focused on the system's ability to maintain synchronous operation following a severe disturbance. However, with continuing growth in interconnections, more use of new technologies, and the increased need to operate power systems in highly stressed conditions, other forms of stability have emerged as greater sources of concern than in the past.

Clearly, instability in a power system may be manifested in many different ways depending on the system configuration, operating mode, and form of disturbance. Analysis of stability problems, including identifying essential factors that contribute to instability and devising methods of improving stable operation, is greatly facilitated by classification into appropriate categories. These are based on the following considerations:

— The physical nature of the resulting instability, i.e., the main system parameters in which instability can be observed;
— The size of disturbance considered, impacting on the applicable method of analysis.

Based on the physical nature of the phenomena, power system stability may be classified into three main categories: (a) rotor-angle stability, (b) voltage stability, and (c) frequency stability (Kundur and Morrison [B51], Kundur [B54]).

3.2 Rotor-angle stability

Rotor-angle stability (or **angle stability**) is concerned with the ability of interconnected synchronous machines of a power system to remain in synchronism under normal operating conditions and after being subjected to a disturbance. A fundamental factor in this aspect of stability is the manner in which the torque or power outputs of the synchronous machines vary as their rotors oscillate. The mechanism by which synchronous machines maintain synchronism with one another is through the development of restoring torques whenever there are forces tending to accelerate or decelerate the machines with respect to each other.

The change in electromagnetic torque of a synchronous machine following a perturbation can be resolved into two components: (i) a synchronizing torque component, in phase with the rotor-angle deviation, and (ii) a damping torque component, in phase with the speed deviation. Lack of sufficient synchronizing torque results in aperiodic instability, whereas lack of damping torque results in oscillatory instability. Loss of synchronism can occur between one machine and the rest of the system, or between groups of machines, possibly with synchronism maintained within each group after separating from each other.

For convenience in analysis and for gaining insight into the nature of stability problems, it is useful to characterize angle stability into the following subcategories based on the size of disturbance considered:

a) **Large-disturbance angle stability**, commonly referred to as **transient stability,** is concerned with the ability of the power system to maintain synchronism when subjected to a severe disturbance, such as a transient fault on a transmission circuit, or loss of a large generator. The resulting system response involves large excursions of generator rotor angles and is influenced by the nonlinear power-angle relationship of synchronous machines. Usually, the disturbance alters the system such that the post-disturbance conditions will be different from those prior to the disturbance. Instability is in the form of an aperiodic drift of the rotor angle due to insufficient synchronizing torque. In large power systems, transient instability may not always occur as first swing instability associated with a single mode; it could be the result of increased peak deviation caused by superposition of

several modes of oscillation causing large excursions of rotor angle beyond the first swing. The period of interest in transient stability is usually limited to about 3 to 5 seconds following the disturbance.

b) **Small-disturbance angle stability** is concerned with the ability of the power system to maintain synchronism under small disturbances such as those that continually occur in the normal operation of the power system. The disturbances are considered to be sufficiently small that linearization of system equations is permissible for purposes of analysis. Small-signal analysis using linear techniques provides valuable information about the inherent dynamic characteristics of the power system. Instability that may result can be of two forms: (i) increase in rotor angle through a non-oscillatory or aperiodic mode due to lack of synchronizing torque, or (ii) rotor oscillations of increasing amplitude due to lack of sufficient damping torque.

In present-day power systems, the small-disturbance angle stability problem is usually one of insufficient damping of oscillations. The stability of the following types of oscillations is of concern:

— Local-plant-mode oscillations, associated with units in a power plant swinging against the rest of the power system.
— Inter-area-mode oscillations, associated with the swinging of a group of generators in one area against a group of generators in another area.
— Torsional-mode oscillations, associated with the turbine-generator shaft system rotational components of individual generators.

3.3 Voltage stability

Voltage stability is concerned with the ability of a power system to maintain steady acceptable voltages at all buses in the system under normal operating conditions and after being subjected to a disturbance. Instability that may result occurs in the form of a progressive fall or rise of voltage of some buses with only moderate excursions of generator angles. The main factor causing voltage instability is the inability of the power system to maintain a proper balance of reactive power throughout the system. This is significantly influenced by the characteristics of system loads and voltage control devices, including generators and their excitation system.

As in the case of angle stability, it is useful to classify voltage stability into the following two subcategories based on the size of disturbance considered:

a) **Large-disturbance voltage stability** is concerned with a system's ability to maintain steady voltages following severe disturbances. The evaluation of stability usually requires the examination of the dynamic performance of the power system over a period of time sufficient to capture the interactions of such devices as under-load transformer tap changers and generator field-current limiters. The study period may extend from a few seconds to several minutes.
b) **Small-disturbance voltage stability** is concerned with a system's ability to maintain steady voltages following small perturbations, such as incremental changes in load. Small disturbance analysis using linear techniques gives valuable voltage-stability related information from a system-wide perspective and clearly identifies areas that have potential problems.

3.4 Frequency stability

Frequency stability is concerned with the ability of a power system to maintain the frequency within a nominal range following a severe system upset, which may or may not result in the system being divided into subsystems (electrical islands). It depends on the ability to restore balance between system generation and load with minimum loss of load.

Analysis of frequency stability is carried out using time-domain simulations that include all appropriate fast and slow dynamics sufficient for modeling the control and protective systems that respond to large frequency excursions as well as the accompanying large shifts in voltages and other system variables. In the case of large interconnected power systems, simulations required may include severe disturbances beyond the normal design criteria, which result in cascading and splitting of the power system into a number of separate islands with generators in each island remaining in synchronism. Stability in this case is a question of whether or not each island will reach an acceptable state of equilibrium with minimum loss of load.

Over the course of a disturbance that results in frequency instability, the characteristic times of the processes and devices that are activated by the large shifts in frequency and other system variables will range from a few seconds, corresponding to the responses of devices such as generator controls, to several minutes, corresponding to the responses of devices such as prime mover energy supply systems and load voltage regulators.

3.5 Modeling requirements for synchronous machines

Synchronous machines may be modeled in as much detail as possible in the study of most categories of power system stability. This includes appropriate representation (subject to the availability of data) of the dynamics of the field circuit, excitation system, and rotor damper circuits (Kundur [B54]). With today's computing tools, there is no pressing need to simplify models for specific types of studies. In addition, experience has shown that critical problems may be masked by the use of simplified models which are sometimes perceived to be acceptable for a particular type of study.

For the analysis of many voltage-stability and frequency-stability problems using time-domain simulations, the study periods are in the range of tens of seconds to several minutes. To improve computational efficiency of such long-term dynamic simulations, instead of simplifying the models by neglecting fast dynamics, it is better to use singular perturbation techniques to separate fast and slow dynamics and appropriately approximate the fast dynamics (Xu et al. [B82]).

Notwithstanding the above, it is important to recognize the following special requirements in representing synchronous machines for different categories of stability studies:

a) For large-disturbance rotor-angle stability analysis, particularly for generators with high-initial-response excitation systems, magnetic saturation effects should be accurately represented at flux levels corresponding to normal operation all the way up to the highest values experienced with the excitation at its ceiling. With discontinuous excitation controls, such as those described in Lee and Kundur [B56] and Taylor et al. [B74], the excitation remains at its ceiling for about two seconds leading to very high flux levels. If saturation effects are understated, the results of analysis would be overly optimistic.
   It is particularly important to represent the dynamics of the field circuit, as it has a significant influence on the effectiveness of excitation system in enhancing large-disturbance rotor-angle stability.
b) For small-disturbance rotor-angle stability analysis, accurate representation of the field circuit as well as the rotor damper circuits is important.
c) For voltage stability studies, the voltage control and reactive power supply capabilities of generators are of prime importance. During conditions of low system voltages, the reactive power demand on generators may exceed their field-current limits. In such situations, usually the generator field currents are automatically limited by overexcitation limiters, further aggravating the situation and possibly leading to voltage instability (Kundur [B54]). Therefore, the generator models should be capable of accurately determining the transient field currents and accounting for the actions of field-current limiters.
d) Frequency stability problems are generally associated with inadequacies in equipment response and poor coordination of control and protection equipment. Stability is determined by the overall

response of the system as evidenced by its mean frequency, rather than relative motions of machines. The generator models used should be capable of accurately representing, under conditions of large variations in voltage and frequency, the responses of control and protective devices, such as the voltage regulator, power system stabilizer, V/Hz limiter and protection, and over-excitation and under-excitation limiters.

4. Types of models available

4.1 Introduction

Synchronous generators are most commonly constructed with a three-phase armature winding on the stator (although other polyphase arrangements are also found) and an excitation winding (known as the field winding) on the rotor. In addition, synchronous generator rotors include other conducting paths in which currents can be induced during a transient. In some cases, these conducting paths are intentionally included by the designer; e.g., pole-face damper windings. In other cases, they are inherent to the machine design, such as in the case of the currents which can be induced in the rotor body of a solid-rotor turbogenerator.

Early on in the process of developing techniques for the analysis of synchronous machines, it was recognized that analyses can be greatly simplified if they are performed in a reference frame rotating with the rotor. For such analyses, the armature currents and voltages are transformed into two sets of orthogonal variables, one set aligned with the magnetic axis of the field winding, known as the rotor **direct axis (d-axis),** and a second set aligned along the rotor at a position 90 electrical degrees from the field-winding magnetic axis. This second axis is known as the rotor **quadrature axis (q-axis).**

Much of the simplification associated with such an approach stems from two key features of this analysis:

1) Under steady-state operating conditions, all of the currents and fluxes, including both those of rotor windings and the transformed armature windings, have constant (dc) values.
2) By choosing the two axes 90 electrical degrees apart, fluxes produced by currents in the windings on one axis do not produce flux linkages in the windings on the other axis. Thus, these sets of windings are orthogonal. This greatly simplifies the flux-current relationship of the model and gives rise to a model structure consisting of two independent networks, one for the direct axis and one for the quadrature axis.

To illustrate the use of this transformation (often referred to as the **d-q-0** or **Park** transformation), consider a machine consisting only of a three-phase armature winding and a cylindrical rotor with only a field winding. Using generator notation, in which the reference direction for terminal current is chosen to be out of the machine terminals, the flux-current relations for this machine can be written in the form:

$$\begin{bmatrix} \Psi_a \\ \Psi_b \\ \Psi_c \\ \Psi_{fd} \end{bmatrix} = \begin{bmatrix} L_a & L_{ab} & L_{ab} & L_m\cos\theta \\ L_{ab} & L_a & L_{ab} & L_m\cos\left(\theta-\frac{2\pi}{3}\right) \\ L_{ab} & L_{ab} & L_a & L_m\cos\left(\theta+\frac{2\pi}{3}\right) \\ L_m\cos\theta & L_m\cos\left(\theta-\frac{2\pi}{3}\right) & L_m\cos\left(\theta+\frac{2\pi}{3}\right) & L_f \end{bmatrix} \begin{bmatrix} -i_a \\ -i_b \\ -i_c \\ i_{fd} \end{bmatrix} \quad (1)$$

and the voltage equations can be written in the form:

$$\begin{bmatrix} v_a \\ v_b \\ v_c \\ e_{fd} \end{bmatrix} = \begin{bmatrix} R_a & 0 & 0 & 0 \\ 0 & R_a & 0 & 0 \\ 0 & 0 & R_a & 0 \\ 0 & 0 & 0 & R_{fd} \end{bmatrix} \begin{bmatrix} -i_a \\ -i_b \\ -i_c \\ i_{fd} \end{bmatrix} + \frac{d}{dt} \begin{bmatrix} \psi_a \\ \psi_b \\ \psi_c \\ \psi_{fd} \end{bmatrix} \tag{2}$$

In these equations:

Ψ is the winding flux linkage
i is the winding current
ν is the armature-winding voltage
e_{fd} is the field voltage
L_a is the armature-phase self inductance
L_{ab} is the armature phase-phase mutual inductance
L_m is the peak armature-phase to field-winding mutual inductance
L_f is the field-winding self inductance
R_a is the armature phase resistance
R_{fd} is the field-winding resistance
θ is the electrical angle between the magnetic axis of phase a and the magnetic axis of the field winding ($\left(\frac{N_p}{2}\right)$ times the mechanical angle between these axes) where N_p is the number of magnetic poles.

Subscripts *a*, *b*, *c*, and *fd* refer to the three armature phases and the field winding respectively.

The time dependence of the inductance matrix of Equation (1) can be clearly seen when one substitutes the fact that under steady-state operating conditions the rotor angle has the time dependence

$$\theta = \left(\frac{N_p}{2}\right)\omega_m t = \omega t \tag{3}$$

where

ω_m is the rotor mechanical angular velocity
ω is the rotor electrical angular velocity

With *S* representing a variable to be transformed, the d-q-0 transformation can be written as [5]

$$\begin{bmatrix} S_d \\ S_q \\ S_0 \end{bmatrix} = \sqrt{\frac{2}{3}} \begin{bmatrix} \cos\theta & \cos\left(\theta - \frac{2\pi}{3}\right) & \cos\left(\theta + \frac{2\pi}{3}\right) \\ -\sin\theta & -\sin\left(\theta - \frac{2\pi}{3}\right) & -\sin\left(\theta + \frac{2\pi}{3}\right) \\ \frac{1}{\sqrt{2}} & \frac{1}{\sqrt{2}} & \frac{1}{\sqrt{2}} \end{bmatrix} \begin{bmatrix} S_a \\ S_b \\ S_c \end{bmatrix} \tag{4}$$

[5]The transformation as presented here is one of a number of alternative forms of the dq transformation. The form presented here has the advantage of being unitary (i.e., the transformation matrix and its inverse matrix are the transpose of each other) and it is also power-invariant in that the total power is simply the sum of the *ui* products, $p = v_d i_d + v_q i_q$. This transformation also results in a symmetrical inductance matrix of Equation (7).

$$\begin{bmatrix} S_a \\ S_b \\ S_c \end{bmatrix} = \sqrt{\frac{2}{3}} \begin{bmatrix} \cos\theta & -\sin\theta & \frac{1}{\sqrt{2}} \\ \cos\left(\theta - \frac{2\pi}{3}\right) & -\sin\left(\theta - \frac{2\pi}{3}\right) & \frac{1}{\sqrt{2}} \\ \cos\left(\theta + \frac{2\pi}{3}\right) & -\sin\left(\theta + \frac{2\pi}{3}\right) & \frac{1}{\sqrt{2}} \end{bmatrix} \begin{bmatrix} S_d \\ S_q \\ S_0 \end{bmatrix} \tag{5}$$

Applying this transformation to the flux-current relationship of Equation (1) gives

$$\begin{bmatrix} \Psi_d \\ \Psi_q \\ \Psi_{fd} \\ \Psi_0 \end{bmatrix} = \begin{bmatrix} L_a - L_{ab} & 0 & \sqrt{\frac{3}{2}} L_m & 0 \\ 0 & L_a - L_{ab} & 0 & 0 \\ \sqrt{\frac{3}{2}} L_m & 0 & L_f & 0 \\ 0 & 0 & 0 & L_{al} \end{bmatrix} \begin{bmatrix} -i_d \\ -i_q \\ i_{fd} \\ -i_0 \end{bmatrix} \tag{6}$$

which can be rewritten in the form

$$\begin{bmatrix} \Psi_d \\ \Psi_q \\ \Psi_{fd} \\ \Psi_0 \end{bmatrix} = \begin{bmatrix} L_d & 0 & L_{af} & 0 \\ 0 & L_q & 0 & 0 \\ L_{af} & 0 & L_f & 0 \\ 0 & 0 & 0 & L_{al} \end{bmatrix} \begin{bmatrix} -i_d \\ -i_q \\ i_{fd} \\ -i_0 \end{bmatrix} \tag{7}$$

Similarly, the transformed voltage equations[6] are

$$v_d = -i_d R_a - \left(\frac{N_p}{2}\right) \omega_m \psi_q + \frac{d\psi_q}{dt} \tag{8}$$

$$v_q = -i_q R_a + \left(\frac{N_p}{2}\right) \omega_m \psi_q + \frac{d\psi_q}{dt} \tag{9}$$

$$e_{fd} = i_{fd} R_f + \frac{d\psi_{fd}}{dt} \tag{10}$$

$$v_0 = -i_0 R_a + \frac{d\psi_0}{dt} \tag{11}$$

In these equations subscripts *d* and *q* refer to the direct- and quadrature-axis equivalent armature windings respectively. Note the presence of an additional term, known as the **zero-sequence component** and indicated by the subscript 0. This term is analogous to the zero-sequence term in symmetrical-component analyses. The zero-sequence component plays a relatively minor role in stability studies (in fact, no role at

[6]When written for per-unit quantities rather than actual quantities, these equations must be modified with the terms $\left(\frac{N_p}{2}\right)\omega_m$ replaced by $\left(\frac{\omega_m}{\omega_{m0}}\right)$ where ω_{m0} is the synchronous mechanical angular velocity of the rotor and $\frac{d}{dt}$ replaced by $\frac{1}{\omega_0}\frac{d}{dt}$ where ω_0 is the synchronous electrical frequency.

all in studies which assume balanced operating conditions) and hence is neglected in most introductory discussions of stability analyses.

Note that, as is discussed above, there is no time dependence in the transformed inductance matrix. In addition, it can be clearly seen that the two axes are decoupled; currents in the direct axis produce only direct-axis fluxes and quadrature-axis currents produce only quadrature-axis fluxes.

In addition to the electrical equations given above, modeling of a synchronous machine requires an expression for the electromechanical torque to be used in the calculation of the machine mechanical dynamics. In terms of dq variables, the electromechanical torque can be calculated as:

$$T = \left(\frac{N_p}{2}\right)(\psi_d i_q - \psi_q i_d) \tag{12}$$

This modeling concept forms the basis for all but the simplest of synchronous machine models. Hence, most of the models discussed in this clause, and indeed in this guide, are based upon direct- and quadrature-axis representations of the synchronous machine. These representations may take a number of forms: equivalent circuits, transfer functions, flux-current and voltage relationships, etc. Each of these forms is equivalent and will give the same results; the choice of the representation is typically based upon user preference.

Note that the direct- and quadrature-axis models presented here represent the direct and quadrature axes as being magnetically uncoupled [as can been seen from the inductance matrices of Equation (6) and Equation (7)]. This representation is based upon the assumption that currents in one axis do not produce flux in the other axis (or produce any changes in the flux in the other axis). In reality, magnetic nonlinearities (magnetic saturation) will produce some degree of coupling between the axes. Although models that neglect this coupling have been found to be adequate for many studies, work is currently underway to develop techniques for incorporating the effects of magnetic nonlinearities in both steady-state and transient analyses.

Finally, as will be discussed later in this clause, in addition to the field winding, it is common to represent other current paths in the rotor, such as damper windings, both on the direct and quadrature axes. It will be shown that the equations presented here can readily be extended to include these additional windings.

4.2 Terminology

For the purposes of this document, it is helpful to specify the following terminology:

- **Model structure:** The basic form or configuration of a model constitutes its structure. This structure can be combined with model parameters whose values are initially unspecified. A model structure is characterized both by its form (e.g., lumped-parameter equivalent circuit, transfer function, differential-equation representation, etc.) as well as by its order (i.e., the number of equivalent rotor windings).
- **Model parameter values:** Synchronous-machine-model parameter values are derived from the characteristics of actual machine behavior. Although these characteristics may take many forms, the following two basic categories are common:
  1) Test data obtained from measurements, or
  2) Analytic “data” obtained from sophisticated analyses that simulate the detailed internal electromagnetic phenomena which occur in the machine. A common technique for performing such analyses is that of the finite-element method. Using this technique, it is possible to solve for the details of the magnetic flux distributions within synchronous machines, including the nonlinear effects of magnetic saturation as well as the effects of eddy currents and rotor motion.

— **Model:** A complete synchronous-machine model consists of the combination of a model structure and a set of parameter values. Thus, for example, the same model structure in combination with parameter values obtained by different test methods and under different machine operating conditions could yield models which differ sufficiently that the machine behavior predicted by these models could be noticeably different. This is due to the fact that synchronous machines are inherently complex (nonlinear, high-order, etc.) and the conventional models are relatively simple (lumped-parameter, low-order, and linear, with adjustments made to approximate the effects of nonlinearities).

A given model can appear in various equivalent representations, e.g., in the form of an equivalent circuit or in the form of a transfer function, among others. These representations are identical, provided that the following conditions are met:

— The model parameters for each form of the model have been determined from the same set of tests or analytically derived data.
— The order of each representation is the same.
— Modifications to the element/parameter values to account for nonlinearities such as saturation effects are typically made after the nominal values for each of the model parameters have been determined. These saturation modifications must be made in such a fashion as to insure that the behavior of the various forms of the model representation remain consistent.

This clause discusses the various model structures that are commonly used to represent synchronous machines in stability analyses. Later clauses discuss the various methods that can be used to derive parameter values for these model structures.

4.3 Direct-axis model structures

The direct axis of a synchronous machine includes two terminal pairs (ports). These correspond to the direct-axis equivalent armature winding and the field winding. An accurate representation of the direct axis must fully account for the characteristics of both of these terminals.

The simplest direct-axis representation assumes that there are no other current paths in the direct axis other than the direct-axis armature winding and the field winding. However, it is well known that damper-winding currents (in the case of salient-pole machines) or rotor-body currents (in the case of solid-rotor machines) play a significant role in determining the characteristics of the direct axis. Hence, the most common direct-axis model includes an additional winding, known as the direct-axis damper winding.

Part (a) of Figure 1 shows the equivalent-circuit representation for the direct-axis model with a single damper winding. This equivalent circuit includes an ideal transformer, representing the fact that there are differing numbers of turns on the armature and field winding, just as is the case for the primary and secondary windings of a transformer. The variables e'_{fd} and i'_{fd} correspond to the actual values of field voltage and current that would be measured at the field-winding terminals. The variables e_{fd} and i_{fd} correspond to the values of field voltage and current reflected to the armature winding through the field to direct-axis armature winding turns ratio, N_{afd}.

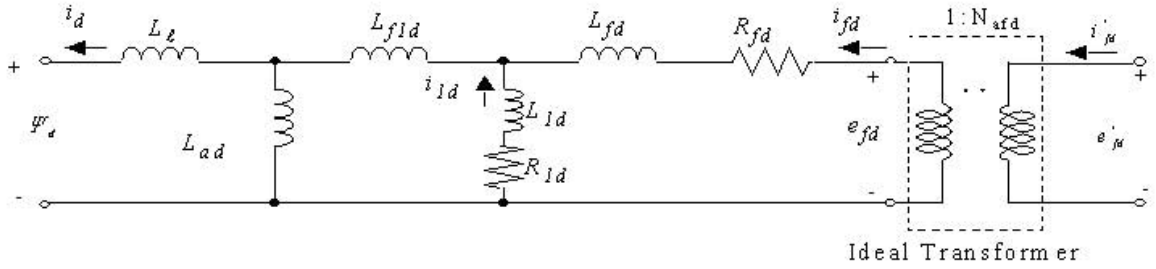

(a) D-axis equivalent circuit including ideal transformer

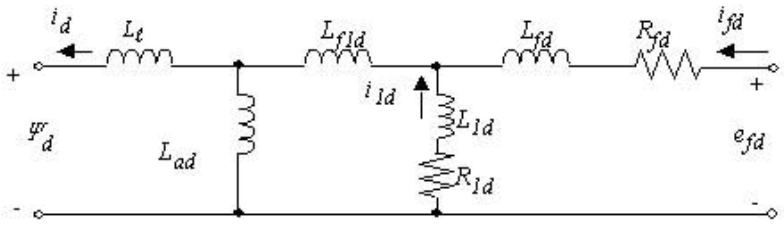

(b) Per-unit d-axis equivalent circuit without ideal transformer

Figure 1—D-axis equivalent circuits including a single d-axis damper winding

It is common to represent synchronous machines using a per-unit representation, rather than actual units, in which case an ideal transformer may or not be required, depending upon the choice of the base for the per-unit system. Whether in actual units or in per unit, the ideal transformer is typically left out of the equivalent circuit, resulting in the equivalent circuit of part (b) of Figure 1 in which the field voltage and current are as reflected to the armature winding. Care must be taken to relate these reflected values to the actual values. The choice of the field-winding base values is equivalent to selecting a turns ratio in the equivalent circuit of part a of Figure 1.

The direct-axis equivalent circuit of part (b) of Figure 1 can be expressed in the alternate forms of a flux-current relationship or a transfer function. The flux-current relationship is

$$\begin{bmatrix} \psi_d \\ \psi_{1d} \\ \psi_{fd} \end{bmatrix} = \begin{bmatrix} L_d & M_{d1d} & M_{fd} \\ M_{d1d} & L_{11d} & M_{f1d} \\ M_{fd} & M_{f1d} & L_{ffd} \end{bmatrix} \begin{bmatrix} -i_d \\ i_{1d} \\ i_{fd} \end{bmatrix} \tag{13}$$

where

$$L_d = L_l + L_{ad} \tag{14}$$

$$L_{11d} = L_{1d} + L_{f1d} + L_{ad} \tag{15}$$

$$L_{ffd} = L_{fd} + L_{f1d} + L_{ad} \tag{16}$$

$$M_{d1d} = L_{ad} \tag{17}$$

$$M_{fd} = L_{ad} \tag{18}$$

$$M_{f1d} = L_{f1d} + L_{ad} \tag{19}$$

(L_{mf1d} may also be used alternatively to M_{f1d})

Note that the "differential-leakage" inductance L_{f1d} accounts for the fact that the mutual inductance between the field winding and the armature winding is not necessarily equal to that between the field winding and the damper winding: $L_{f1d} = M_{f1d} - L_{ad}$. For turbogenerators L_{f1d} is often found to be positive while for salient-pole machines, L_{f1d} is usually negative. This reflects the different physical couplings between the field circuit and the equivalent rotor body circuits in turbogenerators as compared to hydrogenerators.

The corresponding voltage equations will be those of Equation (8), Equation (9), and Equation (10), with the addition of an equation for the d-axis damper winding.

$$v_{1d} = 0 = i_{1d}R_{1d} + \frac{d\psi_{1d}}{dt} \tag{20}$$

where R_{1d} represents the resistance of the d-axis damper winding. Note that the d-axis damper-winding voltage is equal to zero because the damper winding is an internally shorted winding with no external terminals.

Note also that the torque of Equation (12) remains unchanged independent of the number of damper windings included in the representation.

The transfer function representation for this model structure consists of a set of three Laplace transforms relating the terminal quantities of the d-axis two-port network. The choice of the three transforms which define the properties of the network is not unique and many choices are possible. However, common practice has settled on the following three transfer functions:

Direct-axis operational inductance:

$$L_d(s) \equiv -\left.\frac{\psi_d}{i_d}\right|_{e'_{fd}=0} = L_d\left[\frac{(1+T_{1d}s)(1+T_{2d}s)}{(1+T_{3d}s)(1+T_{4d}s)}\right] \tag{21}$$

Field-to-armature-winding current transfer relation:

$$sG(s) \equiv \left.\frac{i'_{fd}}{i_d}\right|_{e'_{fd}=0} = sG_0\left[\frac{(1+T_{5d}s)}{(1+T_{3d}s)(1+T_{4d}s)}\right] \tag{22}$$

Field-winding input impedance:

$$Z_{fd}(s) \equiv -\left.\frac{e'_{fd}}{i'_{fd}}\right|_{\psi_d=0} = N_{afd}^2 R_{fd}\left[\frac{(1+T_{1d}s)(1+T_{2d}s)}{(1+T_{6d}s)}\right] \tag{23}$$

Note that the second and third of these transfer functions have been defined in terms of actual field quantities rather than referred quantities, although this choice is not required.

If field-terminal effects are not of interest (for example, if the field winding is excited from a constant-voltage source) or if it is not possible to make measurements at the field-winding terminals, the direct axis can be considered to be a single-port network and it is not necessary to determine transfer functions which relate the field winding to the armature. In such a case, the direct axis is simply described by the direct-axis operational inductance $L_d(s)$. This in fact was the basis for the traditional approach in which generator models were developed based upon armature-terminal open- and short-circuit tests. It must be understood that although direct-axis models developed under such conditions include a representation for the field-winding, there is no reason to expect that the model will properly represent the effects of changes in the field voltage or current on the machine behavior.

In the equivalent-circuit representation of part a of Figure 1 there are eight unknown parameters. On the other hand, in the transfer function representation of Equation (21), Equation (22), and Equation (23), there are nine measurable parameters; six time constants and three coefficients. Thus, it would appear that by external measurements, one could determine all of the parameters of the equivalent circuit, including values for the turns ratio and the armature leakage inductance. However, this is not the case, and in fact only seven of the nine parameters can be determined independently.

This is similar to the issues which arise when determining the parameters for the equivalent circuit of a transformer. It can be readily shown that, although the turns ratio is typically set equal to the nominal voltage ratio of the transformer (or perhaps the voltage ratio as measured under open circuit conditions), this choice is arbitrary and in fact, any ratio can be selected. The terminal characteristics of the transformer equivalent circuit, based upon any particular choice of turns ratio in combination with a self-consistent set of the remaining equivalent-circuit parameters, will be indistinguishable for those of any other choice of turns ratio. Similarly, it is not possible to make a terminal measurement which will uniquely determine the proportion of leakage inductance to be allocated to the primary versus the secondary windings.

The implication of this fact is that, for the purposes of making an equivalent circuit, it is not possible to make a set of measurements at the generator terminals that will uniquely determine all of the values of the equivalent-circuit parameters. One is always free to pick two parameter values arbitrarily (one parameter plus the field-winding base current for the equivalent circuit of part b of Figure 1). In spite of these arbitrary choices, the resultant model will have uniquely defined terminal characteristics, an essential feature of a useful model.

It is common practice to choose the value of the armature leakage inductance L_l as the free parameter when making equivalent-circuit models for synchronous machines. It is possible to choose this value totally arbitrarily without affecting the validity of the resultant model. The parameter-determination procedure is such that the remaining model parameter values are calculated in a self-consistent fashion such that the terminal behavior of the model will be the same, independent of the choice of the value of the armature leakage inductance. However, it is common (and indeed recommended) practice to choose a value equal to or close to the manufacturer-supplied leakage-inductance value (which is often based upon an analysis of the flux distribution within the machine when it is operating under rated operating conditions).

As is discussed in 4.2, the various representations presented here for the direct-axis model are equivalent and can be used interchangeably. This fact is reinforced in 7.4 which presents some of the equations which translate model parameters from one form to another.

In addition to the d-axis model discussed above, other models with varying numbers of damper windings on the direct axis are commonly used. Table1 shows some of the most commonly used models in equivalent-circuit form (along with commonly used quadrature-axis models). The model-numbering scheme for the various models is of the form “MODEL N.M,” where “N” is an integer which represents the number of equivalent rotor windings on the direct axis and “M” is an integer which represents the number of equivalent rotor windings on the quadrature axis. Thus Model 2.1 represents the direct axis of the rotor with two windings (the field winding and a direct-axis damper winding) and the quadrature axis with a single damper winding.

These models range from a “first-order” representation, which includes only the field winding on the rotor direct axis, to a “third-order” representation which includes the field winding and two equivalent damper-winding circuits. Their equivalent forms, flux-current and voltage relationships and transfer-function representations, are similar to those presented for the second-order, single-damper-winding model which has been discussed in some detail in this clause and hence they will not be presented here.

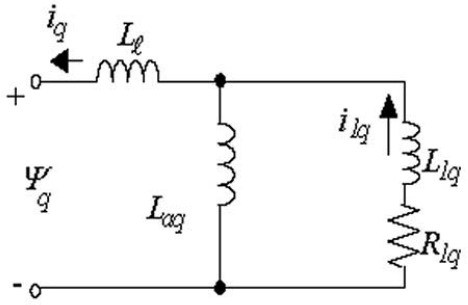

Figure 2—Q-axis equivalent circuit including a single q-axis damper winding

4.4 Quadrature-axis model structures

Because there is no rotor winding with terminals on the quadrature axis, the quadrature axis need be represented only as a single-port network. In addition to the quadrature-axis armature winding, varying numbers of damper windings can be included in the quadrature-axis model. Table 1 shows some of the commonly used quadrature-axis model structures.

The flux-current relations for the quadrature-axis models are directly analogous to those presented earlier for the direct-axis. For example, for the model which includes a single damper winding in the quadrature axis, the equivalent circuit is shown in Figure 2 and the flux-current relationship is given by

$$\begin{bmatrix}\Psi_q\\ \Psi_{1q}\end{bmatrix} = \begin{bmatrix}L_q & M_{q1q}\\ M_{q1q} & L_{11q}\end{bmatrix}\begin{bmatrix}-i_q\\ i_{1q}\end{bmatrix} \tag{24}$$

and the voltage equations consist of Equation (9) in combination with an equation for the q-axis damper winding voltage:

$$v_{1q} = 0 = i_{1q}R_{1q} + \frac{d\Psi_{1q}}{dt} \tag{25}$$

Because the quadrature-axis network has but a single port, only a single transfer function is required.

Quadrature-axis operational inductance:

$$L_q(s) \equiv -\frac{\Psi_q}{i_q} = L_q\left[\frac{(1+T_{1q}s)}{(1+T_{2q}s)}\right] \tag{26}$$

Note that this transfer function is first order in this case because there is but a single damper winding on the quadrature axis in this form of the model.

The representations for the various forms of the quadrature-axis models found in Table 1 are sufficiently similar that there is no need to present a detailed discussion here. They can be derived in analogous form, simply by changing the number of equivalent damper windings included in the representation.

Table 1—Selection of generator models of varying degrees of complexity

CONSTANT ROTOR FLUX LINKAGES	THEVENIN EQUIVALENT			
D-AXIS / Q-AXIS	NO EQUIVALENT DAMPER CIRCUIT	ONE EQUIVALENT DAMPER CIRCUIT	TWO EQUIVALENT DAMPER CIRCUITS	THREE EQUIVALENT DAMPER CIRCUITS
FIELD CIRCUIT ONLY	MODEL 1.0	MODEL 1.1	NOT CONSIDERED	NOT CONSIDERED
FIELD CIRCUIT + ONE EQUIVALENT DAMPER CIRCUIT	NOT CONSIDERED	MODEL 2.1	MODEL 2.2	MODEL 2.3
FIELD CIRCUIT + TWO EQUIVALENT DAMPER CIRCUITS	NOT CONSIDERED	NOT CONSIDERED	NOT CONSIDERED	MODEL 3.3

4.5 Constant-voltage-behind-reactance model

The simplest model that can be used to represent a synchronous machine represents the machine by a constant voltage and a single series reactance. In the steady state, this representation includes the synchronous reactance and the "voltage behind synchronous reactance," which is proportional to the field current supplied to the generator. In this representation, saliency is neglected and the synchronous reactance is set equal to the direct-axis synchronous reactance of the machine.

Similar models can be made for transient (and subtransient) conditions. The transient model consists of the transient reactance (saliency is again neglected) and the "voltage behind transient reactance," which is assumed to remain constant for the duration of any transient under study. This reactance, along with open-circuit and short-circuit time constants, is typically found on manufacturer's data sheets, derived from simple closed-form or finite-element analyses, or it can be obtained from tests (IEEE Std 115-1995). A transient model of this type is assumed to be valid for the initial time period of an electromechanical transient and can be used to roughly estimate the first-swing stability of a synchronous machine.

Since the voltages and currents of these models are not resolved into direct- and quadrature-axis components, this model structure is placed outside the matrix of Table 1. During a transient simulation, the magnitude of the model's internal voltage is kept constant, but the internal angle is changed corresponding to the rotational dynamics of the generator rotor. Advantages of this simple model are that the interfacing of the generator and network equations can be accomplished more quickly during transient simulations and that it requires relatively little data. Thus, this "constant-voltage-behind-transient-reactance" model has virtually replaced Model 1.0 of Table 1 in cases where simple generator models are accepted. However, unlike the case with Model 1.0, exciter action cannot be represented.

4.6 Field-winding per-unit systems

Figure 1 presents two forms of the direct-axis equivalent circuit. Part (a) of Figure 1 includes an ideal transformer which represents the turns ratio between the field winding and the direct-axis equivalent winding. In this figure, i'_{fd} and e'_{fd} represent the actual field current and voltage applied to the field winding while i_{fd} and e_{fd} represent the field current and voltage as referred to the direct axis through the field to direct-axis armature winding turns ratio, N_{afd}. Part (b) of Figure 1 shows the corresponding equivalent circuit in per unit. Consistent with general practice, the per-unit equivalent circuit does not include an ideal transformer. Thus, the per-unit field current and voltage in part (b) of Figure 1 are simply the referred values of the field current and voltage of part (a) of Figure 1 divided by the base current and voltage of the armature winding.

Based upon the equivalent circuit of part (b) of Figure 1, it is clear that the per-unit field current corresponding to 1.0 per-unit direct-axis flux (and hence 1.0 per-unit open-circuit terminal voltage) is equal to $1.0/L_{ad}$ (or equivalently $1.0/X_{ad}$ since L_{ad} and X_{ad} are equal in per unit). In other words, 1.0 per-unit field current will produce an open-circuit per-unit terminal voltage equal to X_{ad} in per unit. This choice of per-unit system for the field current is commonly referred to as the reciprocal per-unit system (Rankin [B65]). Note that for this choice of field-winding base current, the per-unit field voltage under normal operating conditions (equal to $i_{fd} \times R_{fd}$) is quite small since typically R_{fd} is quite small.

Other choices of base-field current and voltage are possible. The data bases of many computer programs define base field current as that required to produce rated open-circuit terminal voltage on the air-gap line. This is known as the non-reciprocal base. Similarly, excitation-systems analyses may define base field voltage as that required to produce rated terminal voltage. As is always the case when interconnecting components whose per-unit parameter values are determined on different bases, the user must be careful to perform the appropriate per-unit system conversion. Clearly for example, if models of the form of part (b) of Figure 1 are to be used, all field-winding quantities must be expressed in terms of the reciprocal per-unit system.

4.7 Generator to power system interfacing

Methods of interfacing the generator and network equations are not presented in this guide in any detail. Kundur and Dandeno [B50] describe one possible approach that permits incorporation of any of the generator stability models discussed in this clause into network computations. Refer to Figure 3.

In a typical analysis program, a synchronous reference frame for the network is selected, typically at the so-called “swing” or reference bus. The network equations are solved by load-flow methods, assuming that the voltages at the machine buses are known. At any given time step, the fluxes within the machine and its rotor angle are assumed to remain constant and the machine terminal voltages must be found consistently with the internal conditions of the machine (as represented by one of the various models described in this clause). Often this process requires some iteration between the network equations and the machine representation.

Once a consistent solution has been found, new values for the machine terminal currents and output power can be determined. These then can be used to solve the machine differential conditions for the rotor angle and fluxes for the next time step and the process is repeated until the simulation is complete.

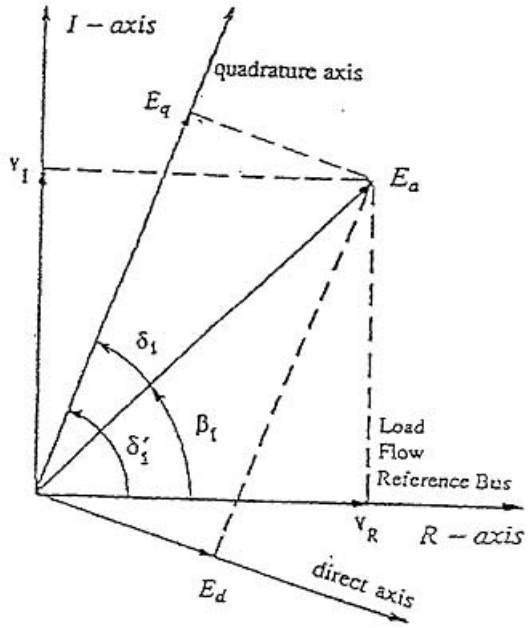

Figure 3—Relationship between d and q axes and real and imaginary axes

5. Application of generator models in stability studies

5.1 General

The representation of synchronous generators in a system stability study depends on the purpose and nature of the study, the physical construction of the rotor, availability of data, and computational considerations.

Power system stability studies are generally conducted for one of the following purposes:

1) **Power system planning and design:** To aid in decisions regarding future transmission network requirements, equipment specifications, and selection of parameters for control and protective systems.

2) **Power system operation:** To determine operating limits and determine the need for arming emergency controls or special protection schemes.
3) **Post-disturbance analysis:** To simulate events following major system disturbances or blackouts.

Power system planning studies involve assessment of alternative expansion plans. For new generation that is being considered at the initial stages of planning, generator data is not available; therefore, typical data is used dependent on the size and type of generating unit being considered. Once the generator manufacturer is chosen and design information is available, a generator model based on design data should be used. This is particularly true for power system design studies for selection of control and protection system parameters. It is often in the design of excitation controls, such as the power system stabilizer, that the most severe demands are made on generator modeling (Kundur [B54].

Power system operating studies should be based on the best available generator models. Preferably, these should be derived from appropriate tests on the generators. State-of-the-art computing tools for on-line dynamic security assessment are capable of simulating in real-time large interconnected power systems with generators and other devices modeled in detail (IEEE [B37]).

Major system disturbances are occasionally experienced by virtually all power systems. Simulation of such events for “post-mortem” analysis can be quite demanding in terms of equipment modeling. However, simulation of such events helps to uncover many shortcomings in system design. Comparison of the results of simulation of such events with measured responses provide the best means of validating analytical tools and models used to represent the power system.

5.2 Modeling considerations based on categories of stability

Planning, design and operating studies investigate the different categories of system stability described in Clause 3. Usually, the focus is on rotor-angle stability and voltage stability.

5.2.1 Transient stability

Transient (angle) stability assessment involves the analysis of power system performance when subjected to a severe fault. Power systems are designed and operated so as to be stable for a set of contingencies referred to as the design contingencies. These contingencies are selected on the basis that they have significant probability of occurrence given the large number of elements comprising the power system.

In transient-stability studies, the important issues are:

— Calculation of generator power or torque during the fault period.
— Calculation of post-fault generator power, angle, and voltage for a period of up to several seconds after the fault cleared.

The transient response of a synchronous generator is significantly affected by the dynamics of the rotor electrical circuits, and the models used should appropriately represent their effects. However, as discussed in Clause 4 (and Annex C), the dynamics of the generator stator circuits and the effect of rotor speed variations on the stator voltages are neglected in large-scale stability studies.

Unbalanced faults are simulated using symmetrical components. The generator is modeled in detail in the positive-sequence network. The combined effects of the negative- and zero-sequence networks are represented by applying an equivalent impedance between the neutral and the point of fault in the positive-sequence network (Kundur [B54]).

The above representation does not account for the effects of dc offsets and negative-sequence components of the armature currents. The corresponding braking torque due to rotor resistive losses is generally neglected in large-scale stability studies. The negative-sequence braking torque is usually small and its neglect introduces a slight degree of conservatism. The dc braking torque is neglected on the basis that most multiphase faults are sequentially developed; that is, they start as single-phase faults and quickly develop into multi-phase faults such that there is very little dc offset in the phase currents (Kundur [B54]).

For accurate assessment of transient stability, it is essential to adequately represent the dynamics of the field circuit and the influence of the excitation system. The largest time constant in the denominator of the transfer function of the direct-axis model reflects the field time constant. The effective field time constant is increased slightly with higher-order models. An accurate knowledge of the magnitude and phase of $L_d(s)$ and $sG(s)$ over a frequency range from 0.1 Hz to 10 Hz is useful in determining the representation of the field circuit.

The number of rotor circuits required to adequately represent damper-circuit effects depends on the physical construction of the generator rotor. This is discussed in 5.3.

The most practical and universally used method of transient stability analysis is time-domain simulation. In this approach the nonlinear differential equations representing the dynamics of the power system are solved using step-by-step numerical integration. One of the considerations in the selection of the order of the generator model (i.e., number of circuits used to represent the damper-circuit effects) is the maximum allowable integration time step. Higher-order models usually have smaller time constants, thereby requiring smaller time steps and increasing computational effort.

5.2.2 Small-disturbance angle stability

Small-disturbance stability assessment involves the examination of the ability of the power system to maintain synchronous operation when subjected to small perturbations. The modeling of the power system, including synchronous generators, is very much similar to that for transient stability analysis. Only balanced operation is considered and the system equations may be linearized for purpose of analysis.

Modal analysis based on eigenvalue/eigenvector computations is the most effective method of assessing small-disturbance angle stability (Kundur et al. [B55]).

Generator models used for small-disturbance stability assessment should accurately account for damper-circuit effects, field circuit dynamics, and excitation control. Except for increasing the total number of states slightly, higher-order generator models with small time constants do not significantly increase the computational effort for eigenvalue calculations.

One of the effective means of enhancing small-signal stability is the use of power system stabilizers (Kundur [B54]). Design of power system stabilizers should be based on detailed and accurate generator models. Kundur et al. [B52] highlight the problems experienced in designing and tuning power system stabilizers for a thermal power plant whose generators have continuous slot wedges and damper windings.

5.2.3 Voltage stability

Voltage stability assessment is concerned with the ability of the power system to maintain steady voltages at all buses after being subjected to a disturbance.

Large-disturbance voltage stability is analyzed using extended time-domain simulations capturing the interactions of such devices as under-load transformer tap changers and generator field-current limiters. The study period of interest may extend from several seconds to tens of minutes. The simulation programs are essentially enhanced transient-stability programs with models for transformer tap changers and field-current limiters (Morison [B61]). The emphasis in synchronous generator modeling is on its ability to supply

reactive power and control voltage with due consideration to field-current and armature-current limits (Kundur [B54]). Representation of damper-circuit effects is not very important for voltage stability analysis.

To speed up time-domain simulations for voltage stability analysis, quasi-dynamic analysis is used (Van Cutsem [B78]). The focus of such analysis is on the evolution of system response driven by slow dynamics associated with transformer tap changers, field-current limiters, and switched capacitors. Fast dynamics, such as those associated with generator rotor circuits and excitation system, are captured by solving associated steady-state equations.

Small-disturbance voltage stability can be effectively studied using static analysis (Morison et al. [B61]). Steady-state models are used for generators with appropriate representation of their reactive power capability limits.

5.2.4 Frequency stability

Frequency stability analysis is concerned with the assessment power system performance following a severe system upset resulting in a significant imbalance between generation and load. Severe system upsets generally result in large excursions of frequency, power flows, voltage, and other system variables.

Frequency stability is a long-term phenomenon. Its analysis is carried out using a long-term dynamic simulation program that accounts for fast as well as slow processes (Kundur et al. [B53], Stubbe et al. [B71]).

The models for generating units should accurately represent their responses under conditions of large variations in voltage and frequency, including the action of prime-mover and excitation system control and protective functions.

The generator rotor-circuit representation used is similar to that for transient stability analysis. However, since generators may experience sustained frequency deviations, the effect of rotor speed variations in the stator voltage equations cannot be neglected.

5.3 Modeling considerations based on rotor structure

5.3.1 Salient-pole generators

Salient-pole generators with laminated rotors are usually constructed with copper-alloy damper bars located in the pole faces. These damper bars are often connected with continuous end-rings and thus, form a squirrel-cage damper circuit that is effective in both the direct axis and the quadrature axis. The damper circuit in each axis may be represented by one circuit; hence, Model 2.1 is recommended for most salient-pole generators.

Salient-pole machines with solid-iron poles may justify a more detailed model structure with two damper circuits in direct axis. In such cases, Model 3.1 would be more appropriate. IEEE [B36] discusses various aspects of salient-pole machine modeling. Some of the above considerations are also touched upon in Canay [B3]. More information on these particular topics is discussed in Kilgore [B46].

Data supplied by manufacturers is usually based on the Model 2.1 structure. For situations justifying the Model 3.1 structure, the parameters may have to be derived from tests such as the standstill frequency-response tests.

5.3.2 Round-rotor generators

In round-rotor machines, slots are present over part of the circumference to accommodate the field winding. The tops of these slots contain wedges for mechanical retention of the field turns. These wedges are usually made of a nonmagnetic metal, and may be either segmented or full length. In many constructions, a conductive ring under the field end-winding retaining ring, with fingers extending under the ends of the slot wedges, is used to improve conduction at these connection points. For infrequent cases where the retaining ring is magnetic, field leakage fluxes and corresponding inductances will be affected, with noticeable differences existing in frequency-response data obtained at near full load, compared with standstill data (Jack and Bedford [B39]).

Copper strips are often inserted under the wedges to provide improved conduction between wedge segments and/or to improve damper-circuit action. In some cases, a complete squirrel-cage winding is formed, while in other cases the conductive paths contribute only marginally to damper-circuit action. The effectiveness of the slot-wedge damper circuit may vary widely depending on the wedge material, segmenting of the wedge and the design of the conductive circuit below the wedge. Jack and Bedford [B39] and Dougherty and Minnich [B17] discuss the impact of some of the above details on the direct-axis rotor model. A third-order model for the direct-axis often gives a better fit to *Ld(s)* and *sG(s)* test data than a second-order one. However, the added computational complexity of simulation cannot usually be justified. In most cases, a second-order model for the direct-axis will suffice, along with the inclusion of L_{f1d}, which reflects the differences in mutual coupling between the field, the equivalent rotor wedge, and/or damper circuits and the stator.

Turbogenerators with no conducting strips under the slot wedges and no wedges or damper bars in the pole-face region can be adequately represented by Model 2.2.

The pole-face region is often slotted circumferentially, or on occasion, may be slotted longitudinally for rotor flexing and balancing purposes. In some cases, longitudinal pole-face slots may be filled with wedges of either low-conductivity steel or, in the case of machines subject to subsynchronous resonance (SSR), high-conductivity material to form a quadrature-axis damper circuit. The q-axis equivalent circuit model must account for various current paths in the rotor iron along the pole faces. The electrical properties of these paths may be affected by circumferential slotting, or by pole-face wedges or damper bars.

However, should the pole-face area have conducting wedges or damper bars, Model 2.3 is recommended. It has also been found that for a range of rotor damper constructions, a third-order representation such as Models 2.3 and 3.3 gives a better fit between measured and calculated values of $L_q(s)$ including phase angle in the 0.1 Hz to 10 Hz range. It appears that the effects of currents in the pole-face area are more accurately represented by a third-order quadrature-axis model.

Standard data supplied by manufacturers is usually based on the Model 2.2 structure. Data for higher-order models has to be derived from appropriate tests on the generators. Alternatively, techniques such as those described in Dougherty and Minnich [B18] may be used to derive higher models from design information.

5.4 Use of simplified models

5.4.1 Neglect of damper circuits

The first order of simplification to the synchronous generator model is to neglect the effects of damper circuits. The primary reason for this approximation is that often machine parameters related to the damper circuits are not readily available, particularly for older units. This model simplification may also contribute to reduction in computational effort by reducing the order of the model and by allowing larger integration steps in time domain simulations, provided modeling of other devices in the system allow such an increase in time step.

Neglect of damper circuits effects introduces some degree of loss of accuracy. Depending on the nature and scope of the study, this may be acceptable.

5.4.2 Classical model

The “voltage-behind-transient-reactance” model offers considerable computational simplicity as it allows the transient electrical performance of the generator to be represented by a simple voltage source of fixed magnitude behind an effective reactance. It is commonly referred to as the “classical” model, since it was used extensively in early power system stability studies (Kundur [B54]).

Such a model is now used for screening studies, such as contingency screening and ranking for transient stability limit search applications (IEEE [B37]).

The classical model is also used for representing “remote” machines in the analysis of very large interconnected power systems. Podmore [B64] and Wang et al. [B81] describe dynamic-equivalencing techniques in which “coherent” groups of generators are identified and each such group of machines is represented by a single equivalent classical generator model.

6. Representation of saturation and its effect on synchronous generator performance

6.1 General

The various implications of synchronous generator saturation have been discussed extensively in the literature for many years. In general, the initial values of the synchronous generator rotor angles and excitations, on which the synchronous generator stability performance greatly depends, are significantly affected by saturation. In addition, saturation has an impact on the extent to which high-initial-response excitation could improve transient stability. In any system planning or operating policy/decision, if power system stability plays an important role, satisfactory representation of generator saturation is highly desirable.

6.2 Representation of synchronous generator saturation in the steady state

The effect of saturation on the synchronous generator steady-state performance has been recognized for at least 60 years when the initial concern was the accurate calculation of the field excitation for the exciter design and sizing. During the second half of this 60-year period, the effect of saturation on determining the internal angles of synchronous generators has received much attention as well.

In general, the effect of saturation depends not only on the saturation curve in the axis of the resultant machine ampere-turns but also on the phase angle between the resultant ampere-turns and the resultant flux due to both the saliency and the different saturation levels in the different axes (El-Serafi and Demeter [B22], El-Serafi and Wu [B23], El-Serafi et al. [B24]). Since such information is not commonly available, empirical standard methods, which seem in most of the cases to represent the effect of saturation reasonably accurately and to give relatively closer agreement with the measured values, have been used in the synchronous generator phasor diagrams. Some of these empirical standard methods were documented in 1945 with the first AIEE test code for synchronous machines. These procedures now appear essentially in the same form in IEEE Std 115-1995. Other publications and IEEE papers also treated the subject and discussed the difference in approach between salient-pole generators and round-rotor turbogenerators (El-Serafi and Abdallah [B21], Flores et al. [B30], Turner [B76]). These empirical “standard” methods depend mainly on calculating a saturation increment I_{FS} (or in another form a saturation factor K). I_{FS} (or K) is the difference between (or the ratio of) the actual excitation and the excitation on the air-gap line of the

saturation curve at the operating point. An internal voltage "behind some specific reactance" is usually used to locate the operating point on this saturation curve. For the steady-state performance calculation, either the leakage reactance or the Potier reactance is used to determine the internal voltage (a brief discussion and consideration of the use of the leakage reactance and the Potier reactance is given in Annex 5A of IEEE Std 115-1995). An alternative for locating the operating point on the saturation curve is to use the total ampere-turns, or the total summation of the currents in per-unit quantities, of the various windings on the corresponding axis.

In these empirical "standard" methods of accounting for saturation, the trend in the past was to use only one saturation factor (or increment) corresponding to the saturation in the direct axis. This trend has been shifted latter to the use of two different saturation factors (or increments) corresponding to the saturation in the direct and quadrature axes. In both cases, magnetic coupling between the direct and quadrature axes (cross-magnetizing phenomenon) is ignored, and thus, an exact simulation of the effect of saturation is not included in this d- and q-axis modeling. The relative importance of accounting for this cross-magnetizing phenomenon has, however, been recognized and an accurate or precise two-axis model of saturated synchronous generators would include the representation of this cross-magnetizing phenomenon (El Serafi et al. [B24]). In this case, consideration of the phase shift between the resultant ampere-turns and the resultant magnetic flux is included in the cross-magnetization modeling. Most research in this area has been performed on small laboratory machines.

6.2.1 Use of one saturation factor (or increment)

The use of one saturation factor or increment has been applied to both the salient-pole and the cylindrical-rotor synchronous machines using different assumptions. In the case of salient-pole machines, saturation is assumed to occur only in the direct axis and a saturation increment I_{FS} (or ΔE_p) corresponding to the voltage behind the Potier (or leakage) reactance is obtained from the generator open-circuit saturation curve (Figure 4). The excitation, including the effect of saturation, will be equal to the sum of this saturation increment plus the excitation from the air-gap line of the open-circuit saturation curve corresponding to the internal voltage "E_{GU}" calculated using the unsaturated d- and q-axis synchronous reactances (Figure 5). E_{GU} and E_I are used for the same internal voltage in Figure 4, Figure 5, Figure 6, and Figure 7.

In the case of cylindrical-rotor synchronous generators, saturation can be significant in both the direct and quadrature axes. However, the use of one saturation factor (or increment) is applied assuming that the magnetic path is homogeneous around the rotor periphery, i.e., the open-circuit saturation curve represents the magnetic relationship in any axis around the rotor periphery. Thus the open-circuit curve can be used to find the saturation correction corresponding to the total air-gap flux (corresponding to the voltage behind the leakage or Potier reactance). Adding this saturation increment in phase with the voltage behind the leakage or Potier reactance to the voltage behind the unsaturated synchronous reactance, the total excitation including saturation is obtained (Figure 6). The algebraic sum of this saturation increment and the voltage behind the unsaturated synchronous reactance is sometimes considered to be the total excitation including saturation (IEEE Std 115-199). However, such representation will result in considerable error in calculating the internal load angles especially in large turbine generators. In a second approach, the unsaturated synchronous reactance is broken into two components, and the larger component ($X_{su} - X_p$) or ($X_{su} - X_l$) is adjusted by the saturation factor to give, together with the addition of X_p or X_l, the saturated synchronous reactance. K_p or K_l is a number greater than unity.

$$X_{sat} = \frac{X_{su} - X_p}{K_p} + X_p \qquad \text{or} \qquad X_{sat} = \frac{X_{su} - X_l}{K_l} + X_l$$

An internal voltage E_{QD} is then determined using this saturated reactance as shown in Figure 7. The total excitation is then obtained by multiplying this internal voltage by the saturation factor. By comparing Figure 6 and Figure 7, it is evident that both approaches are similar. The saturated synchronous reactance method is used mostly with round-rotor machines.

6.2.2 Use of two saturation factors

In this approach, both the direct-axis and quadrature-axis saturation effects are represented by specifically adjusting the unsaturated synchronous reactances X_{du} and X_{qu} by corresponding saturation factors K_d and K_q to obtain saturated d- and q-axis synchronous reactances in the same way as discussed in 6.2.1. In this case, K_d is calculated from a direct-axis saturation function to give X_{dsat} and K_q is calculated from a quadrature-axis saturation function to give X_{qsat}. The internal voltage behind the leakage or Potier reactance is used to define the operating point on both saturation curves. Using these saturated reactances X_{dsat} and X_{qsat} instead of the unsaturated reactance X_{du} and X_{qu} in Figure 5, an internal voltage ($\equiv E_{GU}$ in Figure 5) is obtained. The total excitation is then obtained by multiplying this internal voltage by the saturation factor K_d. Empirically, the use of the two saturation factors seems to give, in at least some cases, an accurate representation of the effect of saturation in the intermediate axis of the total ampere-turns, i.e., the effect of both the saturation factor due to the total resultant ampere-turns using the saturation curve in the intermediate axis of the total resultant ampere-turns and the phase angle between the resultant flux and the resultant ampere-turns.

Annex D describes in some detail the theoretical aspects of developing K_d and K_q saturation factors. In addition, a practical method is shown for determining equivalent d- and q-axis saturation curves. This method requires measured information for field current and internal angle of a synchronous machine under various operating conditions. Values of power, reactive power, and terminal voltage should also be measured.

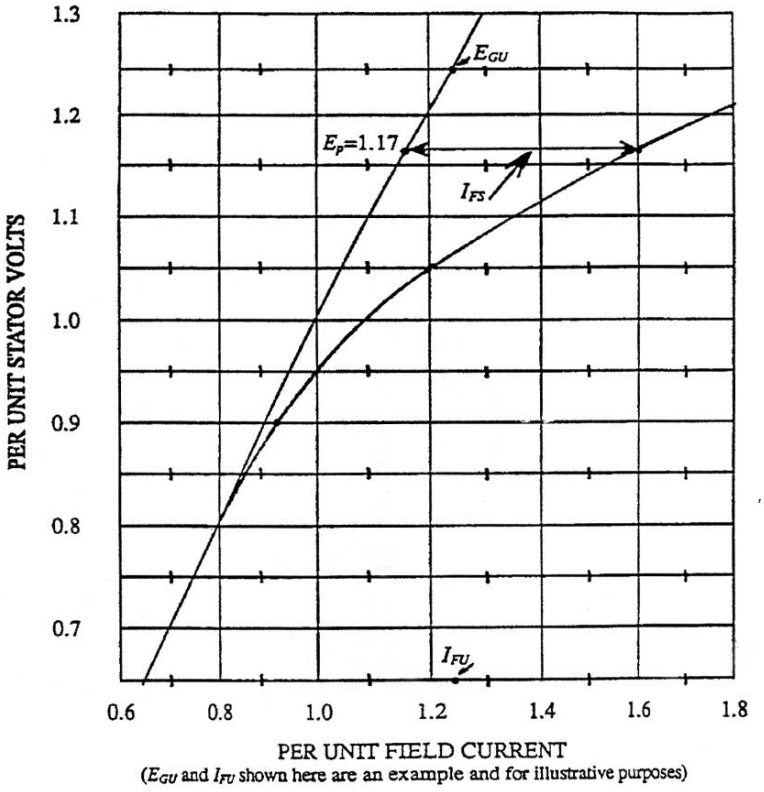

Figure 4—Typical open circuit saturation curve for a 2400 kVA generator and determination of a single saturation increment

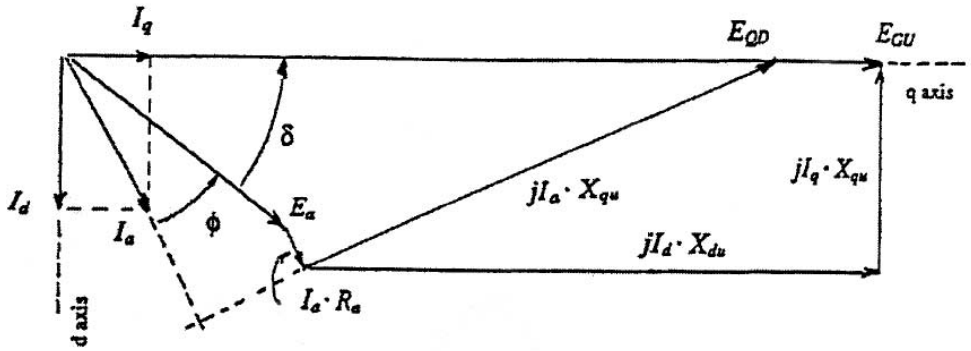

Figure 5—Phasor diagram for the calculation of the unsaturated generated voltage E_{GU} for salient-pole synchronous generators

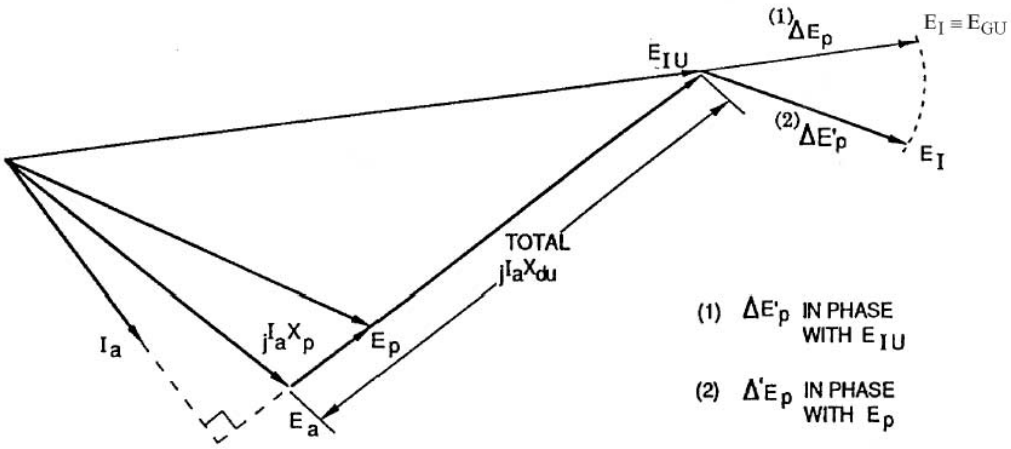

Figure 6—Phasor diagram for a cylindrical-rotor synchronous generator

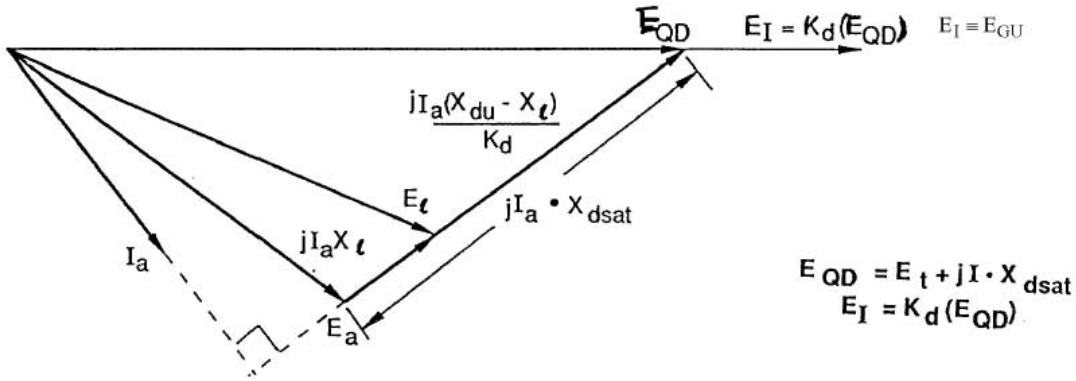

Figure 7—Saturated synchronous reactance method in phasor diagram form

6.2.3 Cross-magnetizing phenomenon

It has been recognized recently that the magnetic coupling between the direct and quadrature axes of saturated synchronous machines (cross-magnetizing phenomenon), which in effect results in the accurate representation of the saturation effect in the axis of the resultant ampere-turns, plays an important role in their analysis. This magnetic coupling causes changes in the flux linkages in their direct and quadrature axes. This could be represented in the phasor diagram in the form of two d- and q-axis voltage drops, E_{dq} and E_{qd}, which are proportional to the changes in the d- and q-axis flux linkages respectively and which can be called the cross-magnetizing voltages, Figure 8. The values of these cross-magnetizing voltages are functions of the ampere-turns of both the direct and quadrature axes (El-Serafi et al. [B24]). In this case, the projections of the internal voltage behind the leakage or Potier reactances on the direct and quadrature axes are used to define the operating point on the corresponding saturation curves to determine K_d and K_q respectively.

In a second approach, the effects of both the d- and q-axis saturation factors and the cross-magnetizing phenomenon are combined together to give the values of the saturated d- and q-axis synchronous reactances (El-Serafi and Abdallah [B21]). In this case, the values of the saturated reactances are functions of the ampere-turns of both the direct and quadrature axes and can be used as shown in the phasor diagram of Figure 5.

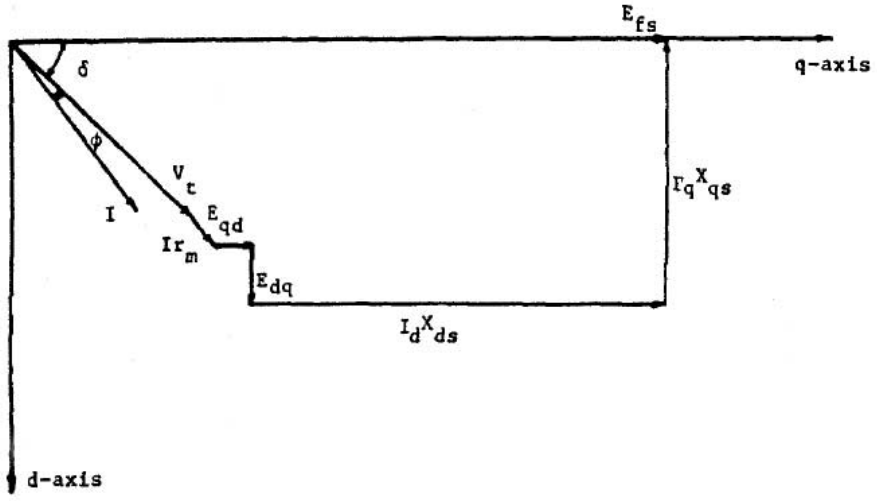

Figure 8—Inclusion of the cross-magnetizing effect in the phasor diagram of a saturated synchronous generator

The differences or improvements in stability performance of large generators, using a cross-magnetization representation have not been shown. In other words, comparing measured excitation and measured internal angle using simulations with or without the extra cross magnetization for large generators has not been documented or demonstrated.

6.3 Representation of saturation effect during large disturbances

6.3.1 Current approaches and assumptions

By their very nature, large-disturbance studies represent operating conditions that vary significantly from their steady-state values to the extent that a complete nonlinear time-dependent model is desirable. However, the current state of the art does not allow for the simple implementation of a complete nonlinear, time-dependent stability model. Moreover, this would be far too time consuming and costly for all but a few specialized studies.

More specifically, the magnetic saturation of a generator is, in principle, dependent on the electrical current in every "circuit" (as well as the recent magnetic history of the steel). For the three-rotor circuit configuration of Model 3.3, one ought to know four currents as inputs in each axis. Therefore, there may be in total eight values of circuit parameters or inductances to be adjusted for saturation (four in each axis). Such an approach appears difficult and impractical to implement principally due to the lack of input data and it is usually assumed that the leakage inductances are independent of saturation and that the saturation corrections during the simulation process of large disturbances are to be limited to the adjustment of the magnetizing inductances, L_{ad} and L_{aq}. In this case, this is done using essentially the same techniques as for the steady-state saturation discussed in 6.2.

Although this simplified method for accounting for saturation in this case usually gives satisfactory results which agree reasonably well with on-site measurements recorded during actual disturbances, it is still the opinion of some analysts that during severe system disturbances, when generator currents are usually several times the normal, the stator leakage inductance L_l should also be adjusted. Appropriate background material is noted in Flores et al. [B30] and Turner [B76], but such procedures are not common practice in current large size stability programs.

The manner in which the saturation effects can be accounted for in stability simulations depends to a degree on whether the computer codes are based on the "time constant and reactance" approach, or alternatively on the use of the d- and q-axis model structure in which the resistance and reactance values of the structure elements of stator and rotor, including the field circuit, are explicitly known. The differences between these two approaches are discussed in 6.3.2.

6.3.2 Adjustment of parameters during large disturbances

The adjustment of the parameters during these time domain calculations to account for the saturation depends to a degree on the organization of the machine flux, current, and voltage equations. As well known, the simulation codes for the time domain calculations can be organized in two distinct ways:

1) **The machine equations are stated in terms of the reactances and time constants (transient and subtransient):** Historically, these constants could be measured directly from the terminal short-circuit tests as explained in the IEEE Std 115-1995 or provided by the manufacturer from calculation. It should be noted that the q-axis parameters cannot be obtained from a short-circuit test. However, calculated values of these q-axis reactances and time constants are frequently furnished as discussed in 7.3 of Clause 7.

   In the stability programs using this simulation format, all the generator parameters input data, namely the various reactances and time constants, are the unsaturated values. During the simulation process, the saturated values of these parameters have to be adjusted as a function of the operating conditions as described in Annex D.

2) **The machine equations are stated in a circuit-model form:** In this case, the parameters required are the stator and field leakage inductances, the magnetizing inductances, L_{ad} and L_{aq}, and the leakage inductances and resistances for each equivalent rotor body branch. These may be derived from frequency-response measurements as specified in the IEEE Std 115-1995, or by analytical procedures. The field circuit resistance r_{fd} should also be known.

   In this case of machine equations format, L_{ad} and L_{aq} are adjusted for saturation at each time step. The saturation function used will be the same one that is used for the calculation of these parameters when the initial values of excitation and load angle are calculated. The values for L_{ad} and L_{aq} that are input to the simulation will be the unsaturated values. The adjustment to account for saturation is done using essentially the same techniques for the steady-state saturation discussed in 6.2. EPRI [B25] and Kundur and Dandeno [B50] demonstrate how the accounting for saturation in this case has been done in one of the available commercial stability programs. Kundur [B54] describes in detail the basis for this method of saturation representation.

Irrespective of the apparent differences, relatively minor variations in results of stability simulations between the two above approaches have been detected for situations where comparisons have been made.

6.4 Generator saturation in small-disturbance modeling

6.4.1 General comments and theoretical background

Small-disturbance theory involves concepts of linear responses of a generator to perturbations in the generator armature and field currents. This means that the permeability describing the behavior of the generator iron can be considered constant relative to the magnitude of the small-signal swings in flux density. However, as a result of the hysteretic nature of iron, the magnetization (B-H) path for small disturbances is different from the path followed for steady-state operation in a solid iron rotor, that is, the apparent permeability of the rotor is different. This means that the generator small-signal circuit parameters are somewhat different from the steady-state circuit parameters (L_d and L_q). The latter parameters are used solely for small-signal study initialization purposes. The rotor permeance is only one component of the entire generator magnetic circuit, so that the effect of the small-signal permeability on circuit parameters can be determined only by detailed magnetic analysis or by test. Thus, the small-signal operational inductances (or circuit parameters) cannot be deduced in any way from steady-state data.

Figure 9 is a schematic representation of the B-H path in rotor iron for both steady-state and small-signal behavior. The continuous curve represents the normal (steady-state) magnetization curve. The small loops show the B-H path for small deviations. The normal permeability is defined as the quotient B/H at any point on the normal curve. The incremental permeability is defined as the slope of the incremental loop. This slope depends on signal amplitude; for simplicity, the limiting value for zero signal is usually used. The loops depicted are those that would result after many cycles of small signal perturbations. The actual B-H path in arriving at a small signal-steady condition is more complicated. For conceptual (and analytical) purposes, it is sufficient to assume that for each value of steady-state flux density in the rotor, there is a corresponding value of incremental permeability. The analysis of small-signal behavior can be done by replacing the steady-state permeability by the corresponding value of incremental permeability in every region of the rotor. The incremental permeability is about 1/10 of the normal (steady-state) permeability for points on the "air-gap" portion of the normal B-H characteristic. The so-called "initial permeability," that is measured around the toe of the normal B-H curve, is a special case of incremental permeability (Minnich [B59]. This condition applies when standstill-frequency-response measurements are made. Under these test conditions, the operating flux density is zero over the entire rotor cross section. Because the incremental permeability is smaller at high (and normal) operating flux densities, it would be expected that the small-signal inductance parameters would be different between standstill conditions and rated operating conditions. This has been confirmed by both analysis and test, as discussed below.

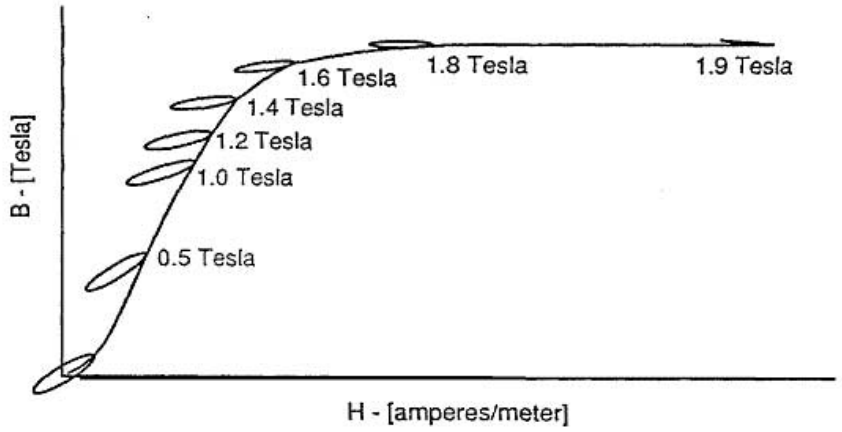

Figure 9—Schematic examples of incremental minor loops

Figure 10 shows the small-signal frequency response of the field-to-armature mutual inductance (both calculated and measured) for a turbogenerator. Two pairs of curves are shown; one at zero excitation (standstill), and one for running on open-circuit under rated-voltage conditions. These latter tests have become known as open-circuit frequency-response (OCFR) tests. Since these characteristics were measured for small-signal excitations around their respective steady-state operating points, circuit parameters derived from them are entirely appropriate for small-signal (eigenvalue) analysis. The zero frequency intercept of the magnitude of L_{ad} is the small-signal value of this mutual inductance. At the rated-voltage operating point, the value is about 80% to 90% of the steady-state value (L_{adu}).

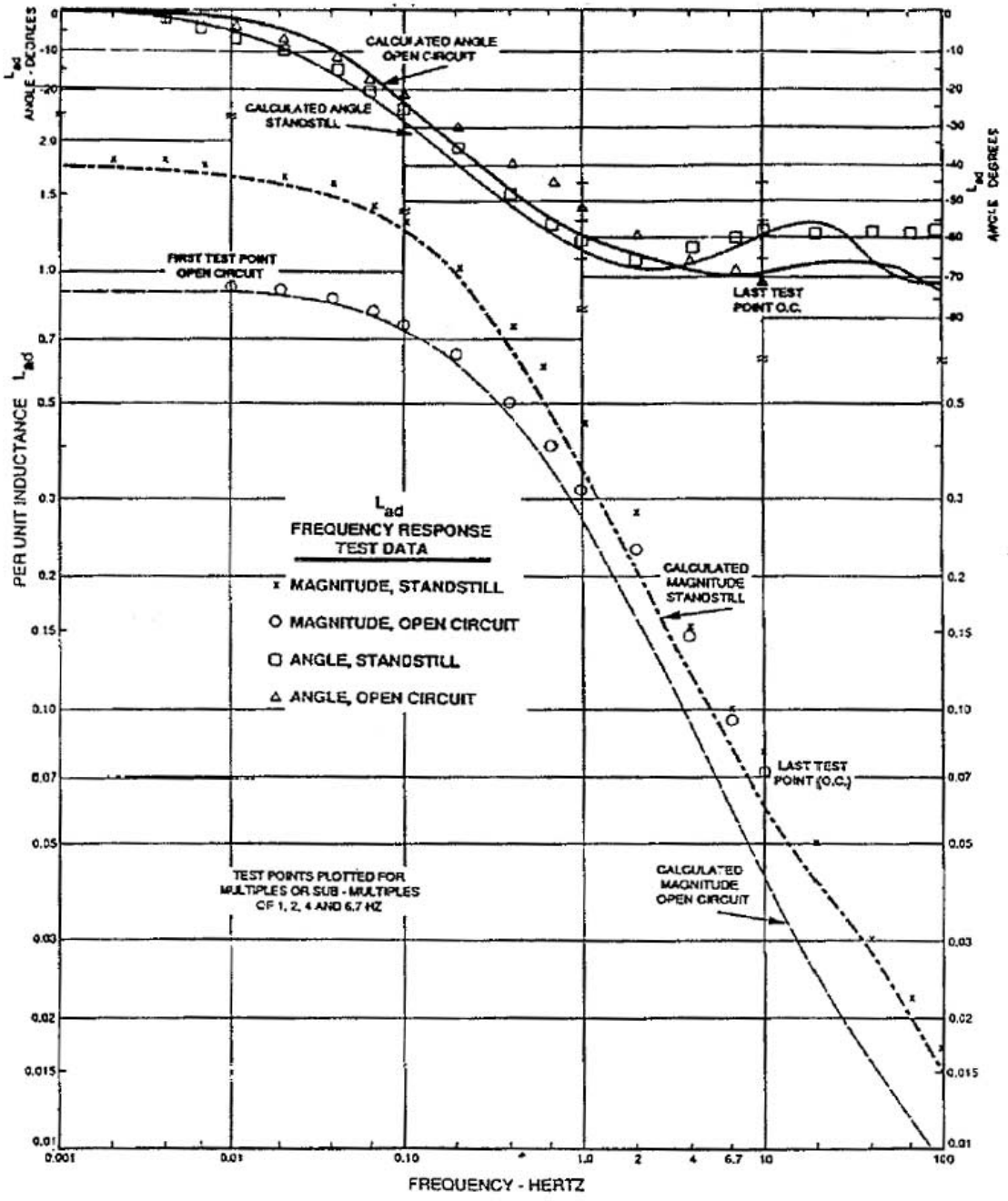

Figure 10—Comparison of the d-axis armature field mutual inductance, L_{ad} at open circuit rated voltage and at standstill: test data and finite-element calculated data

Most small-signal analysis of power systems is concerned with oscillation modes in the 0.1 Hz to about 3 Hz range. When considering the effects of saturation in general, and based on existing on-line small signal OCFR test data, it would appear that the actual small-signal value or incremental saturation effects, even if they are modeled differently from the incremental permeability concept, should have a relatively minor impact on small-signal analyses. The justification for this statement is that the rotor values of R_{1d}, L_{1d}, R_{2d}, L_{2d} are considered the important factors in the machine representation under analysis conditions in the frequency range from 0.1 Hz to about 3 Hz. This concept has been confirmed to some extent by the test data referred to above where one 500 megawatts, two-pole machine had no amortisseurs, while the other 500 megawatts, two-pole machine had amortisseurs in both axes. The machine without the amortisseurs is also the same one whose finite element analyses is partly shown in Figure 10.

7. Determination of generator stability parameters

7.1 Introduction

The objective of this clause is to summarize techniques for deriving parameters for the model structures of Clause 4 to be used to represent generators in studies of power systems stability. Typically these parameters are derived from data obtained by measurements made upon a given machine, although numerical methods can also be used to obtain equivalent data.

A wide range of test methods have been devised over the years from which data can be obtained to characterize synchronous machines. These methods tend to fall into three categories:

Steady-state tests. During these tests, the machine is operated at constant load and the various steady-state voltages and currents are measured. Methods for conducting a wide-range of steady-state tests are described in IEEE Std 115-1995.

Transient tests. During these tests, the machine is typically operating at an initial steady-state condition when a step change in some operating condition is made. Often such changes involve the sudden introduction or removal of a short circuit at the armature terminals. Procedures for conducting a range of commonly accepted transient tests are described in IEEE Std 115-1995. Alternative transient test methods such as stator-decrement testing have also been proposed (EPRI [B27], [B28].

Frequency-response tests. Steady-state frequency-response testing has gained acceptance in recent years (Dandeno and Iravani [B9]) and such test methods have been incorporated into IEEE Std 115-1995. Although on-line frequency responses were discussed in Dandeno et al. [B14], the most common of such tests are conducted with the machine at standstill by the application of sinusoidal-steady-state currents or voltages to the terminals (armature and/or field winding) of the machine. The frequency of these applied signals is varied over a wide range (e.g., 0.001 Hz to 200 Hz) with the objective of fully characterizing the machine behavior over the full range of frequencies which are likely to be encountered during the operation of the machine. The data obtained from these tests is typically saved as ratios of the resultant voltages and currents, corresponding to transfer functions (magnitude and phase) needed for the determination of machine model parameters. Clause 12 of IEEE Std 115-1995 presents specific procedures for the analysis of such standstill frequency responses.

It is important to recognize that the process of combining a model structure (Clause 4) with measurements or analytical data to obtain a machine model is neither trivial nor unique. The ultimate objective is to obtain a model which best represents the behavior of a machine for a particular situation under investigation. It should be understood that:

— Although they have been shown to perform very well in studies of a wide range of phenomena, the lumped-parameter model structures which are described in Clause 4 are based upon approximations to the physical phenomena which occur in actual machines. Techniques for modeling nonlinear phenomena such as saturation effects are not well developed at this time and this may limit the applicability of the models in some situations.

— The range of complexity of the physical phenomena in synchronous machines in combination with the relative crudeness of the lumped-parameter model structures is such that it is likely that different types of tests (and hence different data sets) made upon the same machine will yield different parameters for the same model structure. Although such differences may not be of significance in some cases, it is likely that modeling of synchronous machines will remain somewhat of an art and that experience and judgement will be invaluable in obtaining accurate representations of machine performance for many types of stability analyses which may be investigated. For example, frequency-response testing grew out of experience which indicated that the models derived from transient (open- and short-circuit) tests were inadequate to predict the behavior of synchronous generator behavior under the influence of excitation-system controls.

— Similarly, even when the same set of data is used to determine the required parameters, different model structures are likely to result in differing predictions of machine performance when analyzing any specific situation. Here again, experience and judgement will be invaluable to obtain the most accurate simulation results.

— In order to accurately represent excitation-system effects, it is necessary to derive models from test data which specifically measures the characteristics of the generator field-winding terminals. Such data are not readily obtained from transient tests and represent a significant advantage of frequency-response testing.

— Characterization of the rotor quadrature axis is essential for the derivation of accurate models. Since traditional transient tests provide little information about this axis, the capability to provide quadrature-axis data represents an additional advantage of frequency-response testing.

The basic method used to determine parameters for synchronous generator models is to find those parameters which result in the best match between the behavior of the model and the measured behavior of the generator as represented by the data from which the model parameters are being derived. For many years, suddenly-applied-short-circuit test data represented the standard measure of transient performance and various commonly accepted approximations formed the basis of model parameter derivation. For example, the rotor was assumed to behave as if there were two windings in the direct axis and the test methods were focused upon reinforcing this viewpoint; the tests were specifically aimed at deriving the corresponding transient and subtransient parameters. In this viewpoint, there was little distinction between model parameters and machine characteristics.

With the advent of computers and high-speed computational capability, it is now possible to fit measured data to a wide range of models. Recognizing that the model can only approximate the measured behavior of the generator, it is now possible to use digital techniques to “adjust” the model parameters to obtain a “best fit” between the model and the data.

For example, some sort of weighted-least-squares technique is typically used in the parameter-derivation process. The various model parameters (either time constants or resistances and inductances) are varied until the best fit with test data is obtained. In such a technique, some sort of weighting is used to adjust the fit with respect to the relative importance given to each measurement. In this context the model parameters are no longer unique functions of the data and the model structure. Experience and judgement can be expected to be helpful in achieving the best parameter values for a given application.

In this clause, various techniques for model parameter derivation are summarized.

7.2 Parameter determination by tests

7.2.1 Models structures and parameterization

Model formats that are assumed, either explicitly or implicitly in most stability studies, usually fall in one of the following two categories:

— Equivalent circuits (EC)
— Operational inductances (OI)

For convenient reference, equivalent circuit models are summarized in Figure 11 and Figure 12. The parameters needed in order to use these models are listed in the vector $\theta_{EC(2,1)}$ and $\theta_{EC(3,3)}$ below:

$$\theta_{EC(2.1)} = \left[R_{fd} R_{1d} R_{1q} L_{fd} L_{1d} L_{1q} L_l L_{ad} L_{aq} L_{f1d} N_{afd}\right] \tag{27}$$

for the Model 2.1 and

$$\theta_{EC(3.3)} = \left[R_{fd} R_{1d} R_{2d} R_{1q} R_{2q} R_{3q} L_l L_{fd} L_{1d} L_{2d} L_{1q} L_{2q} L_{3q} L_{ad} L_{aq} L_{f1d} L_{f2d} N_{afd}\right] \tag{28}$$

for the Model 3.3.

Notice that the last parameter of these vectors is the armature-to-field turn-ratio N_{afd}, which relates the actual field-winding variables (voltage, current, resistance, inductance) to their values referred to the stator winding as in Figure 1. Some of the parameters in Equation (27) and Equation (28), such as N_{afd} and the leakage inductance L_1 cannot be uniquely determined from terminal tests.

The operational inductance model incorporates three transfer functions in the direct axis, $\{L_d(s), sG(s), Z_{fd}(s)\}$, and one in the quadrature axis, $L_q(s)$, which were defined in Clause 4. However, the field input impedance with armature short-circuited, $Z_{fd}(s)$, can be replaced in the direct-axis representation, without any loss of generality, by the armature-to-field transfer impedance with armature open, $Z_{afo}(s)$ (IEEE Std 115-1995, Kamwa et al. [B45]):

$$Z_{afo}(s) \equiv \left.\frac{s\,\psi_d}{i_{fd}}\right|_{i_d = 0} \tag{29}$$

where i_{fd} is the field-current, referred to the stator winding while ψ_d and i_d are respectively the direct-axis armature flux and current.

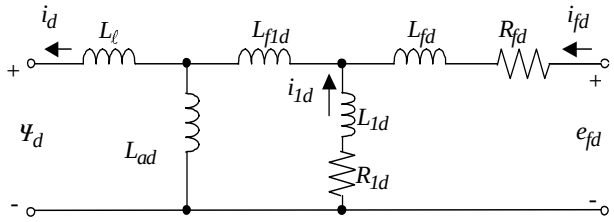

(a)—Direct axis: Two rotor windings/defined for a given armature-to-field turn-ratio N_{afd}

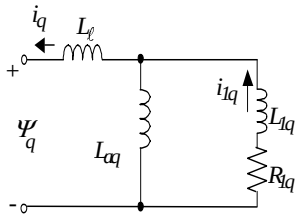

(b)—Quadrature axis: Single rotor winding

Figure 11—Model 2.1: Equivalent circuits referred to the stator terminals

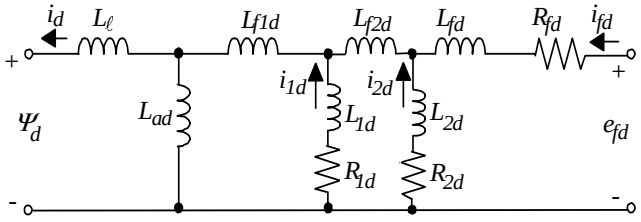

(a)—Direct axis: Three rotor windings/defined for a given armature-to-field turn-ratio N_{afd}

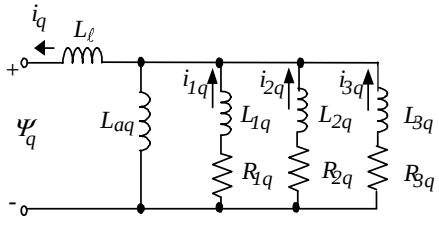

(b)—Quadrature axis: Three rotor winding

Figure 12—Model 3.3: Equivalent circuits referred to the stator terminals

For Model 2.1, the operational inductances can be expressed as follows (with time constants in seconds; resistances and inductances in per unit):

$$L_d(s) = (L_{ad} + L_l)\frac{(1 + sT_{1d})(1 + sT_{2d})}{(1 + sT_{3d})(1 + sT_{4d})} \tag{30}$$

$$G(s) = \frac{(L_{ad} / \omega_{rated})}{R_{fd}}\frac{(1 + sT_{5d})}{(1 + sT_{3d})(1 + sT_{4d})} \tag{31}$$

$$Z_{fd}(s) = R_{fd}\frac{(1 + sT_{1d})(1 + sT_{2d})}{(1 + sT_{6d})} \qquad \text{or} \qquad Z_{afo}(s) = L_{ad}\frac{(s1 + sT_{5d})}{(1 + sT_{7d})} = sL_{afo}(s) \tag{32}$$

for the direct axis and

$$L_q(s) = (L_{aq} + L_l)\frac{(1 + sT_{1q})}{(1 + sT_{2q})} \tag{33}$$

for the quadrature axis.

Based on the various unknown quantities appearing in Equation (30), Equation (31), Equation (32), and Equation (33), the parameter vector associated to the operational inductances of a Model 2.1 is therefore:

$$\theta_{OI(2.1)} = \left[R_{fd}T_{1d}T_{2d}T_{3d}T_{4d}T_{5d}T_{6d}T_{1q}T_{2q}L_lL_{ad}L_{aq}N_{afd}\right] \tag{34}$$

Notice that with 13 parameters, $\theta_{OI(2.1)}$ has two more components than $\theta_{EC(2.1)}$, which means that the two representations are not fully equivalent without further assumptions. The direct- and quadrature-axis input operational inductances, $L_d(s)$ and $L_q(s)$, are often expressed in terms of transient and subtransient quantities used, for instance in the IEEE Std 115-1995, to describe the synchronous machine short-circuit test results:

$$\frac{1}{L_d(s)} = \frac{1}{L_{ad} + L_l} + \left(\frac{1}{L'_d} - \frac{1}{L_{ad} + L_l}\right)\frac{sT'_d}{1 + sT'_d} + \left(\frac{1}{L''_d} - \frac{1}{L'_d}\right)\frac{sT''_d}{1 + sT''_d} \tag{35}$$

$$\frac{1}{L_q(s)} = \frac{1}{L_{aq} + L_l} + \left(\frac{1}{L''_q} - \frac{1}{L_{aq} + L_l}\right)\frac{sT''_q}{1 + sT''_q} \tag{36}$$

In a similar way, four operational inductances are defined in Equation (37), Equation (38), Equation (39), and Equation (40) for a 3.3 equivalent circuit structure:

$$L_d(s) = (L_{ad} + L_l)\frac{(1 + sT_{1d})(1 + sT_{2d})(1 + sT_{3d})}{(1 + sT_{4d})(1 + sT_{5d})(1 + sT_{6d})} \tag{37}$$

$$G(s) = \frac{(L_{ad} / \omega_{rated})}{R_{fd}}\frac{(1 + sT_{7d})(1 + sT_{8d})}{(1 + sT_{4d})(1 + sT_{5d})(1 + sT_{6d})} \tag{38}$$

$$Z_{fd}(s) = R_{fd}\frac{(1 + sT_{1d})(1 + sT_{2d})(1 + sT_{3d})}{(1 + sT_{9d})(1 + sT_{10d})} \tag{39}$$

$$\text{or} \quad Z_{afo}(s) = L_{ad}\frac{s(s1 + sT_{7d})(s1 + sT_{8d})}{(1 + sT_{11d})(1 + sT_{12d})} = sL_{afo}(s)$$

for the direct axis and

$$L_q(s) = (L_{aq} + L_l)\frac{(1 + sT_{1q})(1 + sT_{2q})(1 + sT_{3q})}{(1 + sT_{4q})(1 + sT_{5q})(1 + sT_{6q})} \tag{40}$$

for the quadrature axis.

The parameter vector associated to the operational inductances of a Model 3.3 is then given by:

$$\theta_{OI(3.3)} = \left[R_{fd}L_lL_{ad}L_{aq}T_{1d}T_{2d}T_{3d}T_{4d}T_{5d}T_{6d}T_{7d}T_{8d}T_{9d}T_{10d}T_{1q}T_{2q}T_{3q}T_{4q}T_{5q}T_{6q}N_{afd}\right] \tag{41}$$

With a total of 21 parameters, $\theta_{OI(3.3)}$ has five more components than $\theta_{EC(3.3)}$, which again means that the two representations are not fully equivalent without further assumptions.

The corresponding transient, subtransient and sub-subtransient quantities are defined as follows:

$$\frac{1}{L_d(s)} = \frac{1}{L_{ad} + L_\ell} + \left(\frac{1}{L'_d} - \frac{1}{L_{ad} + L_\ell}\right)\frac{sT'_d}{1 + sT'_d} + \left(\frac{1}{L''_d} - \frac{1}{L'_d}\right)\frac{sT''_d}{1 + sT''_d} + \left(\frac{1}{L'''_d} - \frac{1}{L''_d}\right)\frac{sT'''_d}{1 + sT'''_d} \tag{42}$$

$$\frac{1}{L_q(s)} = \frac{1}{L_{aq} + L_\ell} + \left(\frac{1}{L'_q} - \frac{1}{L_{aq} + L_\ell}\right)\frac{sT'_q}{1 + sT'_q} + \left(\frac{1}{L''_q} - \frac{1}{L'_q}\right)\frac{sT''_q}{1 + sT''_q} + \left(\frac{1}{L'''_q} - \frac{1}{L''_q}\right)\frac{sT'''_q}{1 + sT'''_q} \tag{43}$$

In contrast with the more classical transient and subtransient quantities, sub-subtransient quantities were introduced in the last two decades only Canay [B2], [B9], [B11] and are therefore not yet used in commercial stability computer programs.

Although generator testing is often motivated by thermal, mechanical, or performance considerations, it can also provide dynamic data that are detailed enough for determining the elements of one of the above vectors θ_{EC} and θ_{OI} at a suitable level of accuracy, generally assessed through a graphical "goodness-of-fit" criterion. As will be shown in 7.4 (data translation), these two parameter vectors are closely related.

The models in Figure 11 and Figure 12 and in Equation (30), Equation (31), Equation (32), Equation (33) Equation (34), Equation (35), Equation (36), Equation (37), Equation (38), Equation (39), Equation (40) Equation (41), Equation (42), and Equation (43) share in common three inductances and one resistance that characterize the machine steady-state behavior:

- L_l, the armature leakage inductance: it is generally computed by the manufacturer at the design stage. There is no standard test that allows its determination in a practical manner (IEEE Std 115-1995).
- $L_d = L_{ad} + L_l$, the direct-axis synchronous inductance: it is found by performing an open-circuit test (IEEE Std 115-1995, 10.3) and a sustained or steady-state short-circuit test. The per-unit unsaturated value, L_{du}, is the ratio of the field current required to produce rated armature current under sustained armature terminal short-circuit, to the field current required to produce rated armature voltage on the air-gap line extrapolation of the open-circuit saturation curve.
- $L_q = L_{aq} + L_l$, the quadrature-axis synchronous inductance: it is found by performing a slip test (IEEE Std 115-1995, 10.4.2). Alternatively, its unsaturated value can be determined according to 10.8.2 of IEEE Std 115-1995.
- R_{fd} is the field resistance referred to the stator.

Determination of the remaining elements of the parameter vectors θ_{EC} or θ_{OI} requires dynamic tests, the most common of which are described next.

7.2.2 Three-phase, no-load, sudden-short-circuit test

The short-circuit test (IEEE Std 115-1995, Kamwa et al. [B43]) has a long history, with its standardized form dating back to 1945. Since it is the best way of assessing the overall electrical/mechanical condition of a machine, the incentive to use this test extends beyond the scope of parameter determination. Usually, one machine is selected from a group of similar machines, with the test results being carefully recorded using high-speed data-acquisition systems for later use in determining model parameters as well as other aspects of machine performance. Several tests are performed at various pre-fault, open-circuit voltage levels. It is generally felt that a well-built machine should be able to sustain at least a 70% rated-voltage test without any damage, but testing levels up to 100% are not infrequent on hydrogenerators. The maximum test voltage is dictated by the risk of overcurrents, limited during the test only by the subtransient reactance X_d''.

The armature and field currents from a sudden-three-phase short-circuit applied to the terminals of a 361.4-MVA, 20-kV, 2-pole turbine-alternator are shown in Figure 13. Clause 11.12 of IEEE Std 115-1995 describes the most commonly used computerized method for obtaining synchronous machine parameters from the test data illustrated in Figure13. However, this method of obtaining parameters completely ignores the quadrature axis (which is poorly excited during a sudden-three-phase short-circuit test) and presupposes a second-order direct-axis model of the synchronous machine. In effect, based on six simplifying assumptions Kamwa et al. [B43], the armature-current variation following a sudden-three-phase short-circuit is assumed to be described by the following expression:

$$i_a(t) = I_{ac}(t)\sin(\omega_r t + \lambda) - I_h(t)\sin(2\omega_r t + \lambda) - I_{dc}(t)\sin(\lambda) \tag{44}$$

where

$$I_{ac}(t) = V_o\sqrt{2}\left[\frac{1}{X_d} + \left(\frac{1}{X'_d} - \frac{1}{X_d}\right)e^{-\frac{t}{T'_d}} + \left(\frac{1}{X''_d} - \frac{1}{X'_d}\right)e^{-\frac{t}{T''_d}}\right] \tag{45}$$

$$I_{dc}(t) = \frac{V_o\sqrt{2}}{2}\left(\frac{1}{X''_d} + \frac{1}{X''_q}\right)e^{-\frac{t}{T_a}} \quad \text{and} \quad I_h(t) = \frac{V_o\sqrt{2}}{2}\left(\frac{1}{X''_d} - \frac{1}{X''_q}\right)e^{-\frac{t}{T_a}} \tag{46}$$

are respectively, the ac, dc and 2nd-harmonic components, with $V_o\sqrt{2}$ the peak pre-fault value of the terminal voltage in per unit and ω_r the machine rotor speed in electrical radians/seconds (assumed constant during the test.). For graphical illustration of the ac and dc components, see Figure 14, which corresponds to the 361.4-MVA, 20-kV, 2-pole turbine-alternator oscillograms shown in Figure 13.

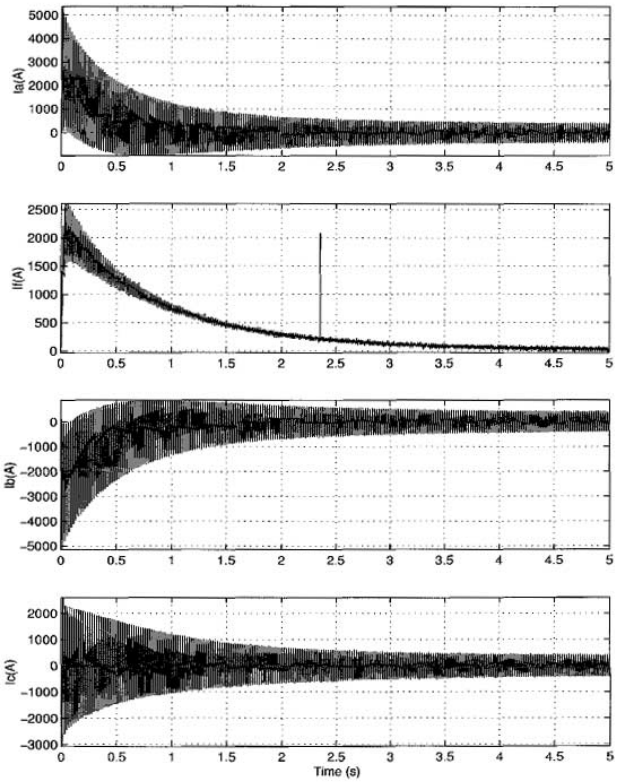

Figure 13—Oscillograms of a 361.4-MVA/20-kV, two-pole turbine generator during sudden-three-phase short-circuit at 10% rated voltage

The parameters appearing in Equation (44), Equation (45), and Equation (46) are the well-known reactances (in p.u.) and time constants (in seconds) associated with the sudden-three-phase short-circuit test, while T_a is the armature winding time constant. Assuming that the direct- and quadrature-axis subtransient reactances are very close to each other, which causes the second harmonic term in Equation (46) to vanish (as is normally the case for symmetrical-rotor machines) a simple computerized method for determining the parameter vector $\{X_{ad},\ X_l,\ X'_d,\ X''_d,\ X''_q,\ T'_d,\ T''_d,\ T_a\}$ characterizing the armature short-circuit current Equation (44) is described in Clause 11 of IEEE Std 115-1995. However, for salient-pole machines such as hydraulic generators, neglecting the second-harmonic term in Equation (44) may result in appreciable errors, especially for the subtransient and transient time constants, since a subtransient saliency $(X''_d - X''_q)/\ X''_d$ of between 10% and 20% is common for hydraulic generators (Kamwa et al. [B43]). Recognizing this pitfall, Kamwa et al. [B44] propose a nonlinear least-squares procedure for determining the parameter vector $\{X_{ad},\ X_l,\ X'_d,\ X''_d,\ X''_q,\ T'_d,\ T''_d,\ T_a\}$, which is much more effective for salient-pole machines.

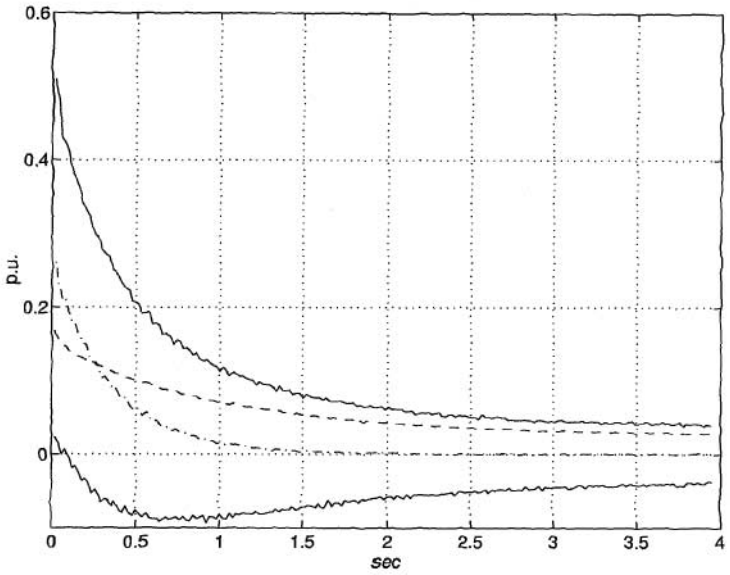

Figure 14—Decomposition of the armature current in Figure 13. (a) Upper/lower envelopes of $i_a(t)$: ____; (b) ac component $I_{ac}(t)$: -----; (c) dc component $I_{dc}(t)$: -.-.-.-.

Example 7.1: Short-circuit parameters of typical hydrogenerators

Table 2 summarizes typical information about three different hydrogenerators from test reports jointly produced by a utility and a manufacturer for contract assessment purposes. The following observations can be made:

— The quadrature-axis data is limited (and generally unreliable).
— There is no subtransient open-circuit time constant.
— The transient open-circuit time constant is derived from a different test than the sudden-three-phase short-circuit with the result that it may be inconsistent with other data such as $\{X'_d,\ X''_d,\ T'_d,\ T''_d\}$.

The following typical approximate relationships

$$\frac{X'_d}{X_d} = \frac{0.386}{1.021} = 0.378 \qquad \frac{T'_d}{T'_{do}} = \frac{1.92}{7.36} = 0.26 \qquad \text{(Machine 1)}$$

$$\frac{X'_d}{X_d} = \frac{0.323}{1.104} = 0.316 \qquad \frac{T'_d}{T'_{do}} = \frac{1.419}{5.62} = 0.252 \qquad \text{(Machine 2)}$$

hold with a 30% error for the first machine and 20% for the second. Similar inconsistencies can be established for the equally common approximate relationship $X''_d \ / \ X'_d \cong T''_d \ / \ T'$.

If the open-circuit time constants (T'_{do} and T''_{do}) are not available and are to be derived exactly in order to avoid data inconsistencies, they can be obtained as the roots of the following second-order equation (Canay [B2], Shackshaft and Henser [B68]:

$$1 + b_1 p + b_2 p^2 = 0 \qquad T'_{do} = -\frac{b_1}{2} + \frac{1}{2}\sqrt{b_1^2 - 4b_2} \qquad T''_{do} = -\frac{b_1}{2} - \frac{1}{2}\sqrt{b_1^2 - 4b_2} \qquad (47)$$

with

$$b_1 = X_d T'_d / X'_d + (X_d / X_d'' - X_d / X'_d + 1) T''_d \qquad \text{and} \qquad b_2 = X'_d \, T'_d \, T''_d \, / X''_d \tag{48}$$

Generally, the value of T'_{do} obtained from the field short-circuit decrement test should be used when available, instead of the reconstructed value from Equation (47). However, in such a case, if T''_{do} is not available from the manufacturer calculations, this value can be determined consistently with the remaining short-circuit data using the following relationship Canay [B2]:

$$X''_d = X_d \frac{T'_d \, T''_d}{T'_{do} \, T''_{do}} \Rightarrow T''_{do} = \frac{X_d}{X''_d} \frac{T'_d \, T''_d}{T'_{do}} \tag{49}$$

Table 2—Typical unsaturated parameters available from a sudden-three-phase short-circuit test (IEEE Std 115-1995, Clause 11) or manufacturer calculations[(a)]

	Machine 1 310 MVA/13.8 kV/ 60 Hz/128.6 rpm		**Machine 2 202 MVA/13.8 kV/ 60Hz/112.5 rpm**		**Machine 3 187 MVA/13.8 kV/ 60 Hz/180 rpm**	
	Measured (1986)	**Manufacturer**	**Measured (1985)**	**Manufacturer**	**Measured (1992)**	**Manufacturer**
T'_{do}	7.36	6.6	5.62	5.7	6.22	6.5
T'_d	1.92	2.2	1.419	1.5	1.01	1.12
T''_{do}	undefined	0.05	undefined	0.09	undefined	0.06
T''_d	0.068	0.046	0.0669	0.03	0.053	0.04
T_a	0.289	0.26	0.186	0.15	0.23	0.22
T''_{qo} [(b)]	undefined	0.10	undefined	0.09	undefined	0.10
X'_d	0.386	0.33	0.323	0.28	0.296	0.35
X''_d	0.307	0.25	0.229	0.22	0.252	0.23
X''_q [(c)]	0.302	0.33	0.212	0.29	0.243	0.31
X_d	1.021	1.14	1.104	1.0	1.305	1.32
X_q	0.541	0.63	0.416	0.62	0.474	0.80

[a]Time in seconds, reactance/resistance in p.u.
[b]Field short-circuit test (IEEE Std 115-1995, 11.10.1.1) and value adjusted for 75 °C.
[c]Line-to-line short-circuit test (IEEE Std 115-1995, 11.13.5.3)

7.2.3 Decrement tests (load rejection)

Shackshaft ([B69], [B70]) was an early proponent of decrement tests, describing up to four different types:

— Stator-decrement test with field-winding short-circuited, and then open-circuited: the machine under test is operating at zero load and is excited totally from the power system, i.e., its field current is zero. The generator is then disconnected from the power system and the subsequent variations of

stator voltage and, if the field is short-circuited, the current in the field winding can be used to determine the machine parameters.

— Rotor-decrement test with stator short-circuited, and then open-circuited: the machine is excited via its field winding and the excitation supply is then suddenly shorted out; from the decay of field current and stator voltage, or if the stator is short-circuited, the stator current, some machine parameters can be determined.

Although De Mello and Ribeiro [B16], EPRI [B28], and Shackshaft [B69] made use of all the above described decrement tests, stator-decrement tests are considered more acceptable than rotor-decrement tests by some experience personnel. Otherwise known as load-rejection tests, they were pioneered in North America (De Mello and Hannet [B15], De Mello and Ribiero [B16], EPRI [B28]) and later investigated in the EPRI project RP-2308 [B28]. Comparisons between load-rejection and SSFR based models can be found in Rankin [B65]. Japanese utilities have also reported on the use of load-rejection tests (Hurley and Schwenk [B34], Sugiyama et al. [B72]). In particular, Hirayama [B33] discusses the role of the AVR and derives a saturated second-order equivalent-circuit model from such tests.

Several special operational considerations are required for the load-rejection tests:

— The first event for the test should be the isolation of the synchronous machine from the power system. Ideally, then, the test should be initiated by tripping the circuit breakers connecting the machine to the system, followed by automatic turbine tripping. A simultaneous circuit breaker and turbine trip is also suitable.
— To eliminate the effects of the voltage regulator on the transient behavior of the machine following load rejection, it should be in the manual position.
— Excitation must be maintained following load rejection. However, most units' relaying schemes trip the field breaker following load rejection. This automatic trip should be temporarily disabled.

Although measurement of the rotor angle allows the derivation of direct and quadrature fluxes from a single rejection, provided the operating point has sufficient initial flux levels in each axis, it is generally preferable to perform separate direct-axis and quadrature-axis load rejections. However, alignment in the quadrature axis is more complicated.

The analysis for deriving parameter values can be based on a computerized graphical procedure as in IEEE Std 115-1995, Clause 11, since a proper alignment of the rotor in a given axis allows the voltage response to obey a similar expression as Equation (44). Hence, assuming no quadrature-axis current, a second order model $\theta_{OI(2,1)}$ yields the following terminal voltage:

$$V_a(t) = \left\{ V_0\sqrt{2} - I_0\sqrt{2}\left[(X'_d - X_d)e^{-\frac{t}{T'_{do}}} + (X''_d - X'_d)e^{-\frac{t}{T''_{do}}} \right] \right\} \sin(\omega_r t) \qquad (50)$$

where $V_0\sqrt{2}$ and $I_0\sqrt{2}$ are the pre-fault crest values of the load voltage and current while ω_r is the machine rotor speed in electrical radians per seconds, assumed constant during the test.

The main problem encountered with load rejection tests is that, ideally, the field voltage should be kept constant. For certain excitation systems this is not possible, for instance, in excitation systems whose source is an alternator. The test requires recording of the field voltage, whose dynamics must be included in the simulation. However, in some excitation systems, such as rotating brushless exciters, it is not possible to measure field voltage.

7.2.4 Standstill-frequency-response tests

This method of arriving at parameters for generator models has only been developed within the past 15 years. The actual procedures for testing are described in IEEE Std 115-1995, Clause 12, but basically involve exciting the stator or field of a generator when it is at standstill and is disconnected from the usual generator step-up transformer. Hence, the method is described as standstill-frequency-response (SSFR) testing. Although earlier work focused on turbogenerators, a recent IEEE working group reported on initial testing performed on salient-pole machines, including three utility hydrogenerators (Dandeno [B10]).

The exciting currents are quite low and the exciting frequencies recommended in the standard range from .001 Hz up to between 100 Hz and 200 Hz. By positioning one of the stator windings relative to the field winding in one of two ways, either direct-axis or quadrature-axis stator operational impedances may be obtained. The direct-axis quantities may be measured with the field open- or short-circuited. Stator-to-field and field-to-stator transfer functions or impedances for the range of exciting frequencies quoted above are also measured. Some brief comments on the interpretation of the results are given below.

The models obtained are small-signal models. Because of the low magnitude of the measuring signals, the magnetic behavior of the generator at standstill is most likely determined by the incremental permeability of the rotor iron. The values of $L_{ad}(0)$ and $L_{aq}(0)$ obtained from the "zero-frequency" intercepts of the operational inductance curves will be incremental values, corresponding to the incremental permeability at the toe of the B-H curve of the steel used in the machine. Therefore, to reflect flux levels corresponding to normal operating conditions, the value of L_{adu} from the air-gap line is generally substituted for $L_{ad}(0)$. It has been observed that this empirical adjustment of $L_{ad}(0)$ to ensure compatibility with the air-gap line in the direct-axis model results in a relatively minor correction. Based on recent test results from about 10 machines, it has amounted to somewhere between 8% to 18% increase and the average is about 12% for turbine-generators (IEEE Std 115-1995). The values of L_{adu} from the air-gap line are subsequently corrected for steady-state saturation in most stability programs in the initialization processes, as discussed in Clause 6. The same comments also apply to the values obtained for $L_{aq}(0)$. It is currently assumed that the correction factor for the quadrature axis is proportional to the $L_{adu}/L_{ad}(0)$ correction factor. Further motivations and approaches for such corrections are discussed in greater detail in Verbeeck et al. [B80].

The actual derivation of the model parameter values from frequency-response results is discussed in Clause 12 of IEEE Std 115-1995. It deals with derivation of parameters for models based on "standstill" test data. The approach used, but not the only one possible, starts with a choice of equivalent-circuit structures for both axes. Figure 11 and Figure 12 are examples for illustration.

Starting with a value for stator leakage inductance, L_l, the remaining direct and quadrature axes rotor parameters are calculated by assuming some initial value and calculating the error between the frequency response of the resulting equivalent circuit and each measured test point. The value of each undetermined element is then changed by a small amount and if the error between calculation and test is reduced, the process is continued until the error begins to increase again. The process is repeated for all other undetermined elements until the error at each test point for both magnitude and phase, between calculation and test, cannot be reduced further.

Different weights can be assigned to the amount of error that is allowed at different specific exciting frequencies. The frequency range between 0.01 Hz and 100 Hz is often chosen to obtain models which are especially suited for studying stability and subsynchronous resonance phenomena (Dandeno and Iravani [B9]. In this frequency band, the chosen model should achieve the closest fit to the measured data with consistent values of the low-frequency asymptotes of the operational-inductances, $L_{ad}(0)$, R_{fd} and $N_{afd}(0)$ (IEEE Std 115-1995, Kamwa and Viarouge [B42]). It should be stressed again that this procedure is just one of several options for parameter fitting.

Example 7-2: 1101MVA/22kV-turbine-generator (Ontario Hydro's Darlington nuclear plant)

We assume for convenience that the available measurements are: $L_d(s)$ and $L_q(s)$ expressed in ohms (at fundamental frequency), $sG(s)$ expressed as a direct ratio of field current (in A) to armature current (in A) with field shorted, and $Z_{afo}(s)$, the given ratio of the field voltage (in V) to the armature current (in A) with field open. The latter network parameter $Z_{afo}(s)$ is more frequently measured in SSFR testing than $Z_{fd}(s)$.

The objective of the analysis is to determine from these data the parameter values for a third-order direct-axis equivalent circuit referred to the stator, with resistances and inductances in p.u., as in Figure 12. From a standard short-circuit test, the unsaturated value of the synchronous reactance L_{du} has been determined to be 1.58 p.u. while the quadrature-axis reactance is L_{qu} = 1.56 p.u. and the armature leakage reactance is L_l=0.188 p.u. At rated armature voltage on the air-gap line of the open-circuit saturation curve, the field current is I_{fdo} = 2494*A*. Therefore, in the Rankin "x_{ad}" base, the base field current and the corresponding turns ratio are calculated as follows (see IEEE Std 115-1995 for more details):

$$\text{Base impedance} = Z_b = \frac{22^*22}{1101} = 0.4396\Omega \tag{51}$$

$$\text{Base voltage} = V_b = \sqrt{\frac{2}{3}}22\times 10^3 = 17963\text{V} \tag{52}$$

$$\textit{Base armature current} = I_b = \frac{V_b}{Z_b} = \frac{17963}{0.4396} = 40862\text{A} \tag{53}$$

$$L_{adu} = L_{du} - L_l = 1.58 - 0.188 = 1.39 \text{ p.u.} \tag{54}$$

$$L_{aqu} = L_{qu} - L_l = 1.56 - 0.188 = 1.37 \text{ p.u.} \tag{55}$$

$$\text{Base field current} = I_{fb} = I_{fdo}L_{adu} = 2494\times 1.39 = 3467\text{A} \tag{56}$$

$$\text{Rated turns ratio} = N_{afdu} = \frac{3}{2}\frac{I_b}{I_{fb}} = 1.5\frac{40862}{3467} = 17.68 \tag{57}$$

Since the networks in the direct and quadrature axes are decoupled, it is possible to determine their parameters in two distinct steps. In addition, during the direct-axis model identification, advantage can be taken of the field-to-armature transfer function data based on the following two stage process:

1) Perform an accurate fitting of the low-frequency asymptotes of $\{L_d(s), sG(s), Z_{afo}(s)\}$ to obtain the correct values of $L_{ad}(0)$, R_{fd} and $N_{afd}(0)$. To this end, only data in the frequency range of say 0 to 0.5 Hz are used in an iterative optimization procedure (Matlab [B58]).
2) Keep $L_{ad}(0)$, R_{fd}, and $N_{afd}(0)$ fixed. By varying the remaining network parameters iteratively, perform a global fit of the two transfer functions $\{L_d(s), sG(s)\}$, based on all relevant test data in the frequency range of interest (0.001Hz to 100 Hz). This yields the so-called two-transfer-function based equivalent circuit established in IEEE Std 115-1995.

However, a more consistent approach would be to formulate step 2 above based on the global fitting of the remaining network parameters on the three transfer functions $\{L_d(s), sG(s), Z_{afo}(s)\}$ (as in step 1), leading to a three-transfer function based equivalent circuit (Jin and El-Serafi [B40], Kamwa et al. [B45], Umans et al. [B77]), which describes more accurately the two terminal behavior of the machine direct axis (see Clause 4).

In the first fitting stage, the unknown parameters are as follows:

$$\theta_{EC(3.3d)} = \left[R_{fd}L_{f1d}L_{f2d}L_{fd}L_{1d}L_{f2d}R_{1d}R_{2d}L_{ad}(0)N_{afd}(0)\right] \tag{58}$$

while in the second step, they reduce to the following:

$$\theta_{EC(3.3d)} = \left[L_{f1d}L_{f2d}L_{fd}L_{1d}L_{2d}R_{1d}R_{2d}\right] \tag{59}$$

The quadrature-axis equivalent circuit is obtained by fitting the test data $L_q(s)$ to the following unknown vector, in the frequency range 0.001 Hz to 100 Hz:

$$\theta_{EC(3.3q)} = \left[R_{1q}R_{2q}R_{3q}L_{1q}L_{2q}L_{3q}L_{aq}(0)\right] \tag{60}$$

The optimum parameters obtained upon convergence of the fitting process (Matlab [B58]) are given in Table 3, while Figure 15, Figure 16, and Figure 17 illustrate graphically their "goodness-of-fit." In Table 3, the two low-frequency asymptotes of the operational inductances, $L_{ad}(0)$ and $N_{afd}(0)$, are significantly lower than their rated values, L_{adu} and N_{afdu}. Since the latter are derived from the open-circuit air-gap line under full excitation and rotating conditions, the discrepancies can be ascribed to the lower incremental permeability achieved at standstill, under very low magnetizing current levels (see Verbeeck et al. [B80] and the discussion above in 7.2.4).

Table 3—Per unit parameters for the Darlington's turbine generator (Model 3.3)

Direct axis				Quadrature axis			
R_{fd}	0.0067	L_{fd}	0.1766	R_{1q}	0.0046	L_{1q}	1.5205
R_{1d}	0.0211	L_{1d}	0.0006	R_{1q}	0.0074	L_{2q}	0.1725
R_{2d}	0.0336	L_{2d}	0.0241	R_{3q}	0.0686	L_{3q}	0.0991
L_{f1d}	0.0400	$L_{ad}(0)$	1.206	$L_{aq}(0)$	1.165	L_l	0.1880
L_{f2d}	0.0200	$N_{afd}(0)$	13.79				

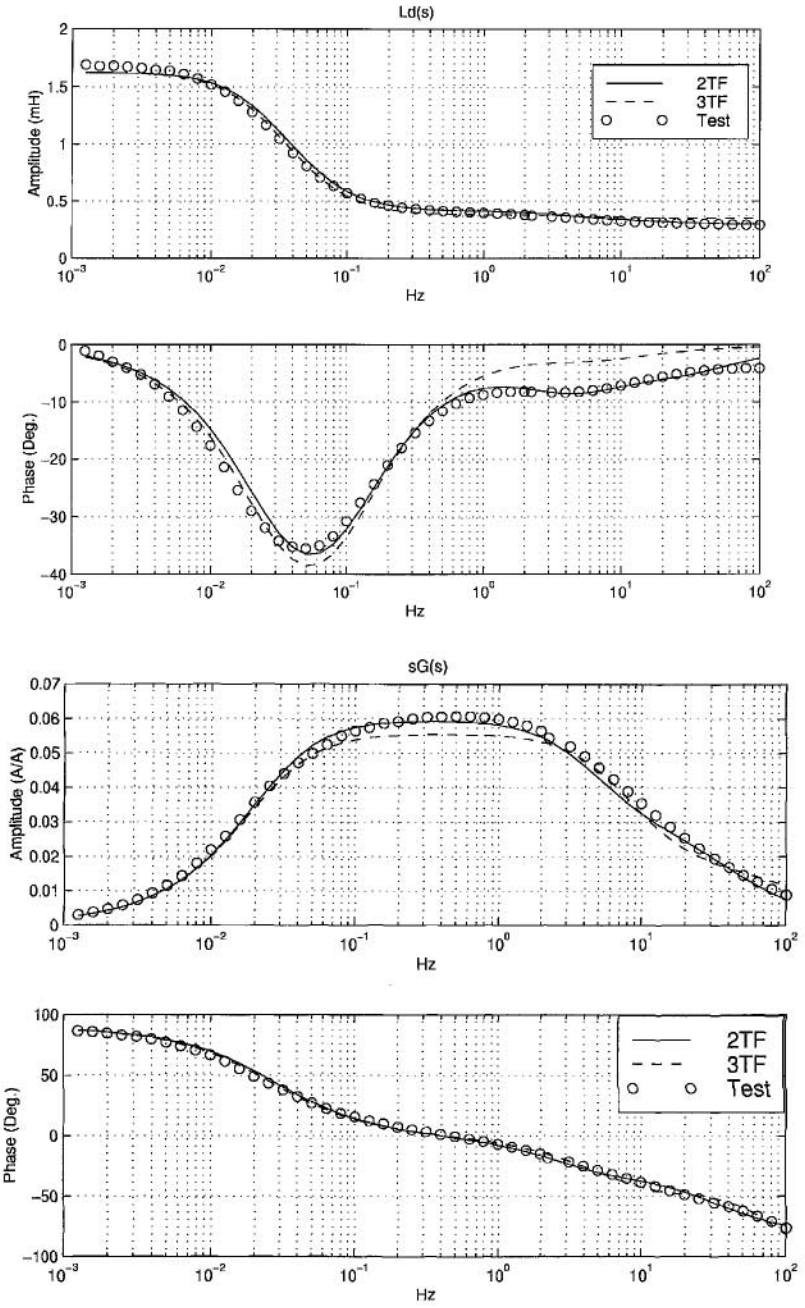

NOTE—"2TF" and "3TF" means two and three transfer function respectively

Figure 15—Goodness of fit of the Darlington direct-axis equivalent circuits based on SSFR test data

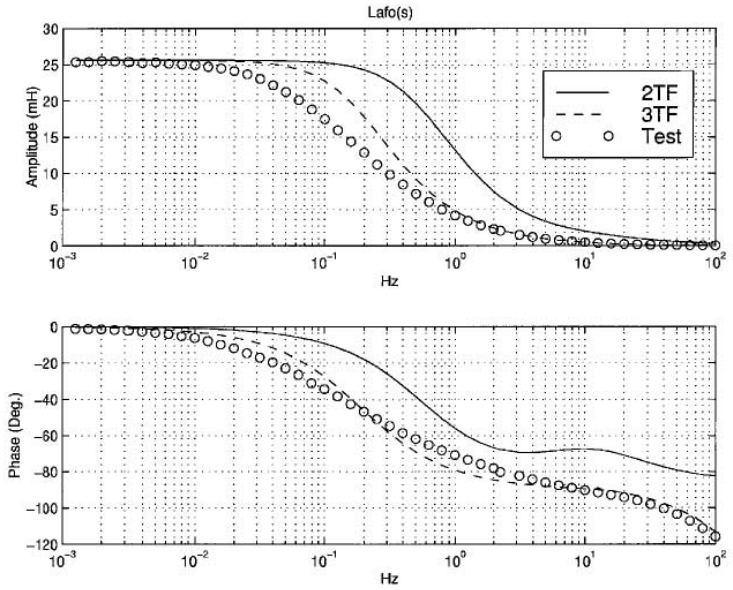

Figure 16—Goodness of fit of the Darlington direct-axis equivalent circuits based on SSFR test data

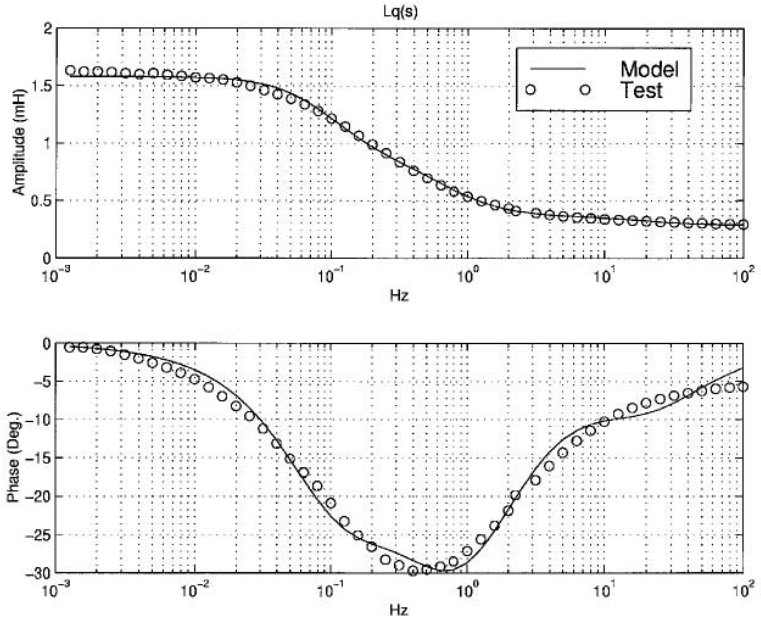

Figure 17—Goodness of fit of the Darlington quadrature-axis equivalent circuit based on SSFR test data

It is noticed from Figure 16 that the two-transfer-function based model is unable to fit $L_{afo}(s)$ [or equivalently $L_{fd}(s)$] adequately in the useful frequency range, the third-order, three transfer-function based model achieves a significantly improved fit of all the available test data, although some discrepancies still exist between test data and the $L_{afo}(s)$ model. Experience indicates that much of these can only be removed by adding one more equivalent dampers in the direct axis (Kamwa et al. [B45]). However, this additional degree of freedom adds to the model complexity, making the parameter estimation problem significantly more challenging.

7.3 Parameters derived by manufacturers

The following discussion relates to the derivation of parameters for large steam turbine and hydroelectric generators. While the detailed calculation procedures used by the manufacturers may be different, there are similarities in the steps used to determine these parameters and the meanings ascribed to them. The intent of this discussion is not to examine the detailed calculation methods. Rather, it is hoped that an explanation of the meanings of the parameters and basic assumptions implicit in their calculation will prove useful to the systems analysts applying these parameters for obtaining dynamic machine models.

7.3.1 Manufacturers' current procedures

Manufacturers' design procedures currently include running a set of computer software packages which often include a routine or module for calculation of equivalent circuit parameters. The parameters usually include the direct- and quadrature-axis reactances and time constants that can be used by the system analysts to derive the model parameters values of interest.

Manufacturers may provide subtransient, transient and synchronous reactances in the form X''_{di}, X''_{dv}, X'_{di}, X'_{dv} and X_{du} for the direct axis. The quadrature-axis quantities have similar analogous forms. Subscript "*i*" denotes quantities that would be obtained from short-circuit current equal to rated armature current and these quantities are often designated as unsaturated parameters. Subscript "*v*" applies to quantities appropriate for large current variations associated with faults; for example, sudden three-phase short circuit from rated terminal voltage. Saturation effects are included during calculation of these parameters' values by correlation studies performed on large samples of past machines with reliable test data.

If necessary, rigorous modeling of machines may also be performed by using time-stepping finite-element analyses including rotor motion and external circuit elements to simulate the fault conditions and the parameters are derived using procedures described in Clause 11 of IEEE Std 115-1995. The effects of saturation on the machine parameters can be obtained by simulating a sudden-three-phase short-circuit for different pre-fault voltage levels, ranging from very small voltages, e.g., 0.05 p.u. to 0.10 p.u., giving unsaturated values, to large voltage levels, e.g., 1.2 p.u. which would give saturated values.

Since most stability studies are carried out with flux conditions (pre-fault or pre-disturbance) corresponding to rated terminal voltage, rated-voltage values of the transient and subtransient reactances (X'_{dv} and X''_{dv}) are usually implied when X'_d and X''_d are specified.

Calculated values for direct-axis quantities are intended to simulate the operating conditions for the short-circuit tests described in 7.2.2 of this standard. Generally, manufacturers determine the parameters for the direct axis by first calculating their values for a circuit structure similar to Model 2.2 (Table 1 in Clause 4) for turbogenerators and Model 2.1 for hydrogenerators (Figure 11). They then convert these circuit parameters to synchronous, transient and subtransient reactances, and time constants.

The direct-axis open-circuit time constants provided by the manufacturer are intended to be consistent with the reactances and time constants that would be obtained from a full-voltage short-circuit test as mentioned above. It is typically assumed that these values satisfy the following approximate relationships:

$$T'_{do} \cong T'_d \frac{X_{du}}{X'_{du}} \qquad \text{and} \qquad T''_{do} \cong T''_d \frac{X'_{dv}}{X''_{dv}} \tag{61}$$

With the advent of modern numerical methods, such as time-stepping finite element analysis using commercial and in-house software packages, the dynamic performance of the machine under various fault and operating conditions may now be simulated at the design stage. The derived equivalent-circuit parameters are used to predict the maximum fault currents in order to calculate the end-winding forces and

obtain an optimum design of the winding supports. The manufacturers also use the generator equivalent-circuit model to calculate damper-winding temperatures for unbalanced-load and terminal-fault conditions.

7.3.2 Possible alternatives to present practices for providing machine parameters

Based on the various approaches described in 7.2, the manufacturers could now supply machine parameters as follows.

— Derivation of the direct-axis quantities using existing "standard" procedures, such as those described in IEEE Sd 115-1995. Time constants and reactances could be based on actual tests involving a sudden three-phase armature short-circuit applied from open circuit, which may also be simulated by time-stepping finite-element analysis.
— Derivation of quadrature-axis subtransient quantities using phase-to-phase short-circuit tests described in Clause 11 of IEEE Std 115-1995. Sometimes, "non-standard" proprietary procedures are used to obtain the quadrature-axis time constants, T'_q and T'_{qo}, based on an operational expression of the following form:

$$X_q(s) = X_{qu}\frac{(1 + T'_q\, s)}{(1 + T'_{qo}\, s)} \qquad \text{and} \qquad T'_q = T'_{qo}\,\frac{X'_q}{X_q} \tag{62}$$

It should be noted that the above expressions are based on the impedance seen in the rotor quadrature axis at some specified per-unit current and some specified hunting frequency, along with knowledge of the synchronous quadrature reactance X_{qu}. Due to solid-iron rotor effects, $X_q(s)$ normally attenuates between 4 to 6 dB per decade in the range from about 0.5 Hz to about 5 Hz for turbogenerators. Giving a steady-state value of X_{qu} and the impedance of X_q at a specific frequency in the above-mentioned range, $X_q(s)$ can be approximated with a breakpoint and a 4 to 6 dB per decade drop off for frequencies up to about 5 Hz. A transfer function with two or three poles could then be used to approximate this $X_q(s)$ characteristic. In the case of hydrogenerators, the quadrature-axis current paths in the damper bars can be well described, and one value of calculated reactance and time constant is usually acceptable to describe sudden flux changes in this axis (usually given as X''_q and T''_{qo}). However, one of the ambiguities in providing information as above is apparent: the direct-axis parameters are based on assumed short-circuit conditions, while that of the quadrature axis rely on a specific value of impedance, as seen at one specified frequency.

— Use of recently established calculations or measurement techniques, based on small-signal theory. These techniques result in direct- and quadrature-axis equivalent circuit forms with models ranging from first-order Model 1.1 to third-order Model 3.3, with Models 2.1 and 2.2 being the most common. They may be obtained in two ways, assuming flux conditions corresponding to normal or reduced voltages:
  a) From operational expressions for both axes based on finite element two-dimensional calculations (Dougherty and Minnich [B17]).
  b) From operational expressions for both axes based on frequency-response measurements as described in 7.2.4.

Most often, the parameters based on the above approaches are supplied by manufacturers by contractual arrangements with the customers.

7.4 Data translation

Using the notations of 7.2, data translation consists in solving the following problem: How to translate a time-constant-based, operational-inductance model θ_{OI} into an equivalent-circuit-based model θ_{EC} and, inversely, how to translate an equivalent-circuit-based model into a time-constant-based model.

In effect, two conceptually distinct approaches exist for extracting synchronous-machine stability models from test data. In the first approach (Canay [B2], EPRI [B26], Shackshaft and Henser [B68], Verbeeck et al. [B79]), dynamic reactances and/or time constants are fitted to measurements and the network parameters are then computed using analytical formulas. The second approach (Kamwa et al. [B43], [B45], Tsai et al. [B75]), which is recommended in Clause 12 of the IEEE Std 115-1995, reverses this process by fitting the network parameters directly to data and then computing the dynamic quantities numerically or using closed-form formulas. Naturally, each approach combines strengths and pitfalls (Table 4).

The non-uniqueness of the equivalent-circuit parameter values representing the terminal behavior of a synchronous machine is proved in Verbeeck et al. [B79] for structures with at least two damper windings on the rotor and having the same values of leakage inductance L_l, magnetizing inductance L_{ad}, and turns ratio N_{afd}. This result sheds more light on some common sources of confusion:

1) The equivalent circuit is unique only when a single damper winding is assumed for each axis. This uniqueness property is achieved by fixing the values of L_l, N_{afd}, and R_{fd}. The physical interpretation usually associated to equivalent circuits is strictly valid for this one-damper per axis model only.
2) In contrast with Kirtley [B48], the non-uniqueness of third-order equivalent circuits claimed in Verbeeck [B79] is not obtained by varying the leakage inductance value arbitrarily. It is a purely mathematical property, built into the assumed topology and which can be demonstrated using network theory.
3) The physical interpretation associated with the direct-axis two-damper equivalent circuit (see for instance the last discussion in Kirtley [B48]) is not without ambiguity, since two distinct equivalent circuits with the same values of L_l, L_{ad}, N_{afd}, and R_{fd} can be found that have the same terminal behavior $\{L_d(s), sG(s), Z_{afo}(s)\}$ (c.f. the example in 7.4.1.1).

Table 4—Comparison of the operational inductance and equivalent circuits models for power system studies

	Operational-inductance model	Equivalent-circuit model
Advantages	— Uniquely defined from a theoretical point of view, whatever the system order. — Simpler procedures for parameter determination from SSFR tests data, especially for low-order systems. — Most common for commercially available stability programs.	— Exact and easy translation into operational inductances and flux-current models whatever the given system order. — Better numerical properties for high order models (i.e., more than two rotor circuits per axis). — Best suited for software such as the EMTP or the Matlab Power System Blockset.
Pitfalls	— Poor numerical properties for high-order representation (i.e., more than two rotor circuits per axis). — No practical means for translating time constants into the corresponding equivalent circuits when the system has more than three rotor circuits.	— The model is uniquely defined for structure restricted to two rotor circuits or less. — For structure with n>2 rotor circuits, there exist (n–1) strictly equivalent solutions for each axis (i.e., two solutions exist when n=3). — For high-order system, parameter determination from SSFR tests is complicated by the fact that the model is not unique.

7.4.1 From operational inductances to equivalent circuits

Umans et al. [B77]] and EPRI [B25] provided the first comprehensive solutions to this problem, at least for the second- and third-order representations. It should be underlined that the analytical solutions in Umans et al. [B77] are exact for the direct axis and yield equivalent circuits which match precisely the original time constants describing $L_d(s)$, $L_q(s)$, and $L_{afo}(s)$ [or $L_{fd}(s)$]. Similarly, the quadrature-axis formulas used in EPRI [B25] were rigorously derived to yield an equivalent circuit of two or three damper windings which match $L_q(s)$, without any formal approximation. Another analytical method was introduced in Canay [B2] which yields an equivalent circuit fitting exactly the input operational inductance in a given axis, $L_d(s)$ or $L_q(s)$, for an arbitrary number of damper windings. However, extension of the resulting direct-axis network to fit the transfer function $sG(s)$ requires a nonlinear iteration and lacks generality since it is limited to a single frequency, i.e., ω_{ated}. In what follows, two examples will be used to illustrate the recommended translation procedures, which, for convenience, are provided in Annex E in the form of Matlab scripts [B58].

7.4.1.1 Application to a third-order direct-axis model

Let consider the following operational-inductance representation presumably obtained by fitting SSFR test data using for instance the methods in Canay [B2], EPRI [B25], Umans et al. [B77].

$$\begin{cases} L_d(s) = 1.65\dfrac{(1+0.6564s)(1+0.04615s)(1+0.00436s)}{(1+7.910s)(1+0.0463s)(1+0.0044s)} \\ G(s) = 7.958\dfrac{(1+0.0460s)(1+0.00419s)}{(1+7.910s)(1+0.0463s)(1+0.00440s)} \\ Z_{afo}(s) = 1.5\dfrac{s(1+0.0460s)(1+0.00419s)}{(1+0.0655s)(1+0.0192s)} \end{cases} \quad (63)$$

All time constants are in seconds while the inductances and impedances are in per unit. From the definition of the above transfer functions given in Equation (37), Equation (38), and Equation (39), it follows that: $L_{ad} = 1.5$, $R_{fd} = 0.0005$, and $L_l = 0.125$. Application of the procedure in Annex E to the time constants describing $L_d(s)$ and $sG(s)$ yields the equivalent circuit No. 2 in Table 5.

Table 5—Sample translation from time constants to a direct-axis equivalent circuit

Equivalent circuits 1 and 2 yield the same operational inductances $\{L_d(s), sG(s), Z_{afo}(s)\}$

Equivalent circuit No. 1				Equivalent circuit No. 2			
R_{fd}	0.0005	L_{fd}	0.0252	R_{fd}	0.0005	L_{fd}	0.0671
R_{1d}	0.5080	L_{1d}	8.8096	R_{1d}	0.2948	L_{1d}	0.4653
R_{2d}	0.2979	L_{2d}	0.4701	R_{2d}	0.5171	L_{2d}	8.9680
L_{f1d}	–0.0795	L_{ad}	1.5	L_{f1d}	–0.0382	L_{ad}	1.5
L_{f2d}	0.0415	L_l	0.15	L_{f2d}	–0.0417	L_l	0.15

The equivalent circuit No. 1 given in the table is an alternative solution to this problem, derived according to network realization theory (Verbeeck [B79]). It is noted that the two circuits differ significantly in terms of L_{f1d}, L_{f2d} and L_{fd}, with the value of the latter varying from 0.0252 to 0.0671. However, quite remarkable is that the sum of these three quantities is the same for the two circuits: $L_{f1d} + L_{f2d} + L_{fd} = –0.0128$ p.u.

On the other hand, although the equivalent damper resistances (R_{1d}, R_{2d}) and inductance (L_{1d}, L_{2d}) values are similar in the two networks, their topological location is interchanged in Figure 12, where the value of R_{1d} becomes that of R_{2d}. Therefore, the physical interpretation associated to this model structure is lost, or appears ambiguous, since two different set of parameters are able to describe the same physical reality (Dandeno and Iravani [B9], Kamwa and Viarouge [B42], Kirtley [B48]).

7.4.1.2 Application to a third-order quadrature-axis model

Consider the following third-order quadrature-axis operational inductance:

$$L_q(s) = (L_{aq} + L_l)\frac{(1 + 0.975s)(1 + 0.116s)(1 + 0.0067s)}{(1 + 7.90s)(1 + 0.276s)(1 + 0.0085s)} \quad (64)$$

with L_{aq} = 1.165 and L_l = 0.188. It actually achieves a fairly good fit to the Darlington's turbine-generator test data already considered for illustration purposes in 7.2. Applying the translation procedure in Annex E to these time constants yields the three-damper windings equivalent circuit No. 1 in Table 6. Interestingly, this circuit is identical to that given in Table 3, which resulted from a direct identification of the quadrature-axis equivalent-circuit model from SSFR test data, according to IEEE Std 115-1995.

Table 6—Sample translation from time constants to a quadrature-axis equivalent circuit

Three-damper network for a full order $L_q(s)$ and two-damper network for a reduced-order $L_q(s)$.

Equivalent circuit No. 1				Equivalent circuit No. 2			
R_{1q}	0.00461	L_{1q}	*1.520*	R_{1q}	0.00671	L_{1q}	2.2130
R_{2q}	0.00738	L_{2q}	*0.1725*	R_{2q}	0.00460	L_{2q}	0.1023
R_{3q}	0.0685	L_{3q}	*0.0991*	*	*	*	*
L_{aq}	1.165	L_l	*0.188*	L_{aq}	1.165	L_l	0.188

If the smaller time constants 0.0067s and 0.0085s are neglected in the above expression of $L_q(s)$, the following reduced-order operational inductance is obtained:

$$L_q(s) \cong (L_{aq} + L_l)\frac{(1 + 0.975s)(1 + 0.116s)}{(1 + 1.790s)(1 + 0.276s)} \quad (65)$$

Then, application of the second-order procedure in Annex E allows one to derive the corresponding two-damper winding equivalent circuit No. 2 in Table 6.

However, such an order reduction by simply truncating the third-order model is not a recommended approach, since it generally yields an approximate second-order model that is less accurate than the full second-order model derived by a direct fitting of SSFR test data (Kamwa and Farzaneh [B41]).

7.4.2 From short-circuit parameters to equivalent circuits

In this clause, the objective is to assume the well-known second-order dynamic constants, $\{L_d, L_d'', T_d', T_d'', etc.\}$, obtained from the analysis of standard commissioning tests such as the sudden-three-phase short-circuit test, and then compute a second-order equivalent circuit with the same dynamic behavior.

It was shown in Salvatore and Savino [B67] that this problem has an exact solution only if the damper winding time constant T_{5d} is known, which is never the case if only the short-circuit armature current is analyzed, as evidenced by the absence of T_{5d} in Equation (44). Even if its determination is theoretically possible by analyzing the short-circuit field-current (Kamwa et al. [B43]), such a procedure is not recommended in IEEE Std 115-1995. However, based on relationships from Takeda and Adkins [B73], an **approximate** value of T_{5d} can be obtained as:

$$T_{5d} = \frac{b}{c} \tag{66}$$

with

$$b = a\frac{L_{ad}(L''_d - L_l)}{aL_d + L_l L_{ad} - (a + L_{ad})L''_d} \tag{67}$$

$$c = \frac{1}{T''_d}\left(b + \frac{aL_l L_{ad}}{L_l L_{ad} + aL_d}\right) \qquad \text{and} \qquad a = \frac{(L'_d - L_l)}{(L_d - L'_d)}L_{ad} \tag{68}$$

For instance, applying the above formulas to Machine 2 of Table 2 yields:

$$a = 0.1450 \qquad b = 0.04122 \qquad \text{and} \qquad c = 1.7616 \Rightarrow T_{5d} = 0.0234s \tag{69}$$

where $L_d = 1.104$ p.u. $L_l = 0.198$ p.u. $L'_d = 0.323$ p.u. $L''_d = 0.229$ p.u. and $T''_d = 0.669s$.

Now given a full data set $\{T'_d,\ T''_d,\ T'_{do},\ T''_{do},\ T_{5d},\ X_d,\ X_l\}$ in the direct axis and $\{T'_{qo},\ X''_q,\ X_q,\ X_l\}$ in the quadrature axis, where the time constants (in seconds) and reactances (per unit) were determined as in 7.2.1, it is possible to compute a unique second-order equivalent circuit that faithfully replicates the starting parameters without any additional approximations (Canay [B2], EPRI [B25], Salvatore and Savino [B67], Umans et al. [B77]). This exact procedure has been implemented in a computer program (cf. Annex E). For machine 2 of Table 2, it yields the stator-referred equivalent circuit in Table 7.

An exact reverse calculation process described in 7.4.4 can be used to verify that the open- and short-circuit time constants associated with this network are identical to those given in Table 2. However, the associated transient and subtransient reactances, $X'_d = 0.282$ and $X''_d = 0.207$, are not identical to those in Table 2, because the T'_{do} and T''_{do} in that table are not the actual roots of Equation (47).

Table 7—Equivalent circuits of machine 2 from Table 2 data (values in p.u.)

L_{ad}	0.906	L_{f1d}	–0.01783	L_{fd}	0.1281	R_{fd}	0.00053
L_{aq}	0.218	L_l	0.198	L_{1d}	0.0344	R_{1d}	0.0039
L_{1q}	0.0150	R_{1q}	0.00687				

7.4.3 From equivalent circuits to operational inductances and dynamic reactances

For equivalent circuits with more than two rotor circuits, no closed-form analytical formulas have been published so far for determining, without undue approximation, the time constants and related quantities, from the resistances and inductances. However, Kamwa and Farzaneh [B41] describe a general numerical procedure, based on a straightforward state-space formulation of the network equations which effectively solves this problem for the case of general multiple-rotor-winding equivalent circuits. It especially allows

one to compute the third-order time constants based representation in Equation (37), Equation (38), Equation (39), Equation (40), Equation (41), Equation (42), and Equation (43) from the equivalent-circuit parameters (Figure 12).

For the second-order model, closed-form formulas for computing the time constants $\{T_{1d}, T_{2d}, T_{3d}, T_{4d}, T_{5d}\}$ in Equation (30), Equation (31), Equation (32), and Equation (33) from the equivalent-circuit parameters can be derived without any approximation (EPRI [B25], Salvatore and Savino [B67], Umans et al. [B77]). Using the notations in Figure 11, the following factors are first calculated:

$$a_1 = \frac{L_d\{R_{fd}(L_{1d} + L_{f1d}) + R_{1d}(L_{fd} + L_{f1d})\} + L_{ad}L_l(R_{1d} + R_{fd})}{L_d R_{1d} R_{fd}} \tag{70}$$

$$a_2 = \frac{L_d\{L_{f1d}(L_{1d} + L_{fd}) + L_{1d}L_{fd}\} + L_{ad}L_l(L_{1d} + L_{fd})}{L_d R_{1d} R_{fd}}$$

$$b_1 = \frac{(L_{ad} + L_{f1d} + L_{fd})R_{1d} + R_{fd}(L_{ad} + L_{f1d} + L_{1d})}{R_{1d} R_{fd}}$$

$$b_2 = \frac{(L_{ad} + L_{f1d})(L_{1d} + L_{fd}) + L_{1d}L_{fd}}{R_{1d} R_{fd}}$$

where $L_d = L_{ad} + L_l$. From a_1, a_2, b_1, and b_2 the relationships which define the operational inductances $L_d(s)$ and $sG(s)$ can be developed:

$$a_1 = T_{1d} + T_{2d} \qquad a_2 = T_{1d}T_{2d} \qquad b_1 = T_{3d} + T_{4d} \qquad b_2 = T_{3d}T_{4d} \tag{71}$$

In addition, $T_{5d} = (L_{1d}/\omega_{rated})/R_{1d}$. Rearranging the equations for T_{1d}, T_{2d}, T_{3d}, and T_{4d} gives:

$$T_{1d} = \frac{a_1}{2} + \frac{1}{2}\sqrt{a_1^2 - 4a_2} \qquad T_{2d} = \frac{a_1}{2} - \frac{1}{2}\sqrt{a_1^2 - 4a_2} \tag{72}$$

$$T_{3d} = \frac{b_1}{2} + \frac{1}{2}\sqrt{b_1^2 - 4b_2} \qquad T_{4d} = \frac{b_1}{2} - \frac{1}{2}\sqrt{b_1^2 - 4b_2}$$

When all the time constants $\{T_{1d}, T_{2d}, T_{3d}, T_{4d}, T_{5d}\}$ are given, a reverse relationship between the transfer function quantities and the equivalent-circuit form can be developed without any approximation (EPRI [B25], Umans et al. [B77]) (see 7.5).

Once the time constants intervening in the operational-inductance model are determined, dynamic inductances are easily computed (Kamwa and Farzaneh [B41]]) from the formal definitions given in 7.2. For example, the third-order direct-axis definition looks like:

$$\frac{1}{L_d(s)} = A_{0d} + \frac{A_{1d}}{1 + sT'_d} + \frac{A_{2d}}{1 + sT''_d} + \frac{A_{3d}}{1 + sT'''_d} \tag{73}$$
$$= \frac{1}{L_{ad} + L_\ell} + \left(\frac{1}{L'_d} - \frac{1}{L_{ad} + L_\ell}\right)\frac{sT'_d}{1 + sT'_d} + \left(\frac{1}{L''_d} - \frac{1}{L'_d}\right)\frac{sT''_d}{1 + sT''_d} + \left(\frac{1}{L'''_d} - \frac{1}{L''_d}\right)\frac{sT'''_d}{1 + sT'''_d}$$

Hence, by simple identification of the corresponding terms in Equation (73), we obtain:

$$A_{1d} = \frac{1}{L_d} - \frac{1}{L'_d}\ , \quad A_{2d} = \frac{1}{L'_d} - \frac{1}{L''_d}\ , \quad A_{3d} = \frac{1}{L''_d} - \frac{1}{L'''_d} \qquad \text{and} \qquad A_{0d} = 1/\ L'''_d \tag{74}$$

The relations above show that a one-to-one relationship exists between L'_d , L''_d , L'''_d and the coefficients A_i appearing in the pole/residue expansion Equation (). The latter can therefore be used as the basis for determining the dynamic reactances:

$$L'_d = 1/\ [1/\ L_d - A_{1d}] \qquad L''_d = 1/\ [1/\ L'_d - A_{2d}] \qquad \text{and} \qquad L'''_d = 1/\ A_{0d} \tag{75}$$

Although the pole/residue expansion is cumbersome to perform analytically, it poses no difficulty on a computer. In addition, this procedure applies to both second- and third-order models.

Example 7.4.1: Dynamic constants from a third-order operational inductance

Consider the operational inductance Equation (64), rewritten here in the following form:

$$\frac{1}{L_q(s)} = \frac{1}{1.353}\frac{(1 + 1.790s)(1 + 0.276s)(1 + 0.0085s)}{(1 + 0.975s)(1 + 0.116s)(1 + 0.0067s)} = \frac{1}{L_q}\frac{(1 + T'_{qo}s)(1 + T''_{qo}s)(1 + T'''_{qo}s)}{(1 + T'_q s)(1 + T''_q s)(1 + T'''_q\ s)} \tag{76}$$

with therefore the following association for the transient, subtransient and sub-subtransient time constants in short- and open-circuit:

$$T'_q = 0.975s \qquad T'_{qo} = 1.790s \tag{77}$$

$$T''_q = 0.116s \qquad T''_{qo} = 0.276s$$

$$T'''_q = 0.0067s \qquad T'''_{qo} = 0.0085s$$

Expanding the operational inductance Equation (76) into pole-residue yields:

$$\frac{1}{L_q(s)} = 4.0959 - \frac{0.51467}{s + 1.0256} - \frac{16.844}{s + 8.6207} - \frac{134.48}{s + 149.25} \tag{78}$$

$$= 4.0959 + \frac{-0.5018}{1 + 0.975s} + \frac{-1.954}{1 + 0.116s} + \frac{-0.90101}{1 + 0.0067s}$$

Then, comparing Equation (78) with Equation (73) results by exchanging subscript *d* by *q* in the following relationships:

$$A_{1q} = -0.5018 \qquad A_{2q} = -1.954 \qquad A_{3q} = -0.90101 \qquad \text{and} \qquad A_{0q} = 4.0959 \tag{79}$$

From Equation (75), we finally obtain the following dynamic inductances:

$$L'_q = 1/\ [1/\ L_q - A_{1q}] = 1/\ [1/ 1.3530 + 0.5018\ ] = 0.802 \text{ p.u.} \tag{80}$$

$$L''_q = 1/\ [1/\ L'_q - A_{2q}] = 1/\ [1/\ 0.80186 + 1.954] = 0.312 \text{ p.u.}$$

$$L'''_q = 1/\ A_{0q} = 1/\ 4.0959 = 0.244 \text{ p.u.}$$

7.4.4 Comparison of the numerical and analytical determination of time constants and dynamic reactances from equivalent circuits

Table 8 shows sample results of data translation applied to a 444 MVA, 20 kV, 2 poles, 60 Hz turbine-generator, using some of the methods discussed in 7.4.3. The analytical method selected for benchmarking (EPRI [B25]) is very representative of the common practice in this area (Dandeno and Service [B11]). It strongly relies on the following basic assumptions:

— $R_{fd} \ll R_{1d}$, $T''_d \ll T'_d$, etc. However, applying similar logic does not mean any thing for a third-order quadrature-axis equivalent circuit.
— $L_{f2d} = 0$ and therefore cannot apply to the equivalent circuits data given in Table 8.

Table 8—Numerical[a] vs. closed-form computations of dynamic constants for third-order equivalent circuits[b]

	3d		3q		Numerical	Closed-form		Numerical	Closed-form
R_{fd}	0.00127	R_{1q}	0.009	L'_d	0.426	0.46	L'_q	0.869	1.0
R_{1d}	0.0065	R_{2q}	0.021	L''_d	0.345	0.32	L''_q	0.466	0.49
R_{2d}	0.0953	R_{3q}	0.096	L'''_d	0.217	0.22	L'''_q	0.2695	0.27
L_{fd}	0.196	L_{1q}	2.340	T'_{do}	4.65	4.65	T'_{qo}	1.057	1.31
L_{1d}	1.136	L_{2q}	0.573	T''_{do}	0.4546	0.45	T''_{qo}	0.166	0.19
L_{2d}	0.057	L_{2q}	0.162	T'''_{do}	0.00576	0.006	T'''_{qo}	0.0124	0.012
L_{f1d}	0.015	L_{aqu}	1.044	T'_d	0.8276		T'_q	0.7324	
L_{f2d}	0	L_l	0.162	T''_d	0.4537		T''_q	0.0897	
L_{adu}	1.663			T'''_d	0.00387		T'''_q	0.0074	

[a]Kamwa and Farzaneh [B41].
[b]Dandeno and Service [B11], Dandeno et al. [B14], EPRI [B25].

Comparing the results of the analytical formulas of Dandeno and Service [B11] with the numerical method (Kamwa and Farzeneh [B41]) leads to the following observations:

— Analytical formulas and numerical calculations yield similar open-circuit time constants but slightly different dynamic reactances. However, it is not clear how to derive the associated short-circuit time constants using analytical formulas.
— The discrepancies for the quadrature axis are larger (Figure 18). It seems that in this case, given the inductance and resistance values at hand, the various assumptions underlying the derivation of analytical formulas hold to a lesser extent.

Although the dynamic responses obtained from approximate dynamic constants globally make sense (see Figure 18), the latter contain significant systematic errors that may prohibit their blind use for third-order models.

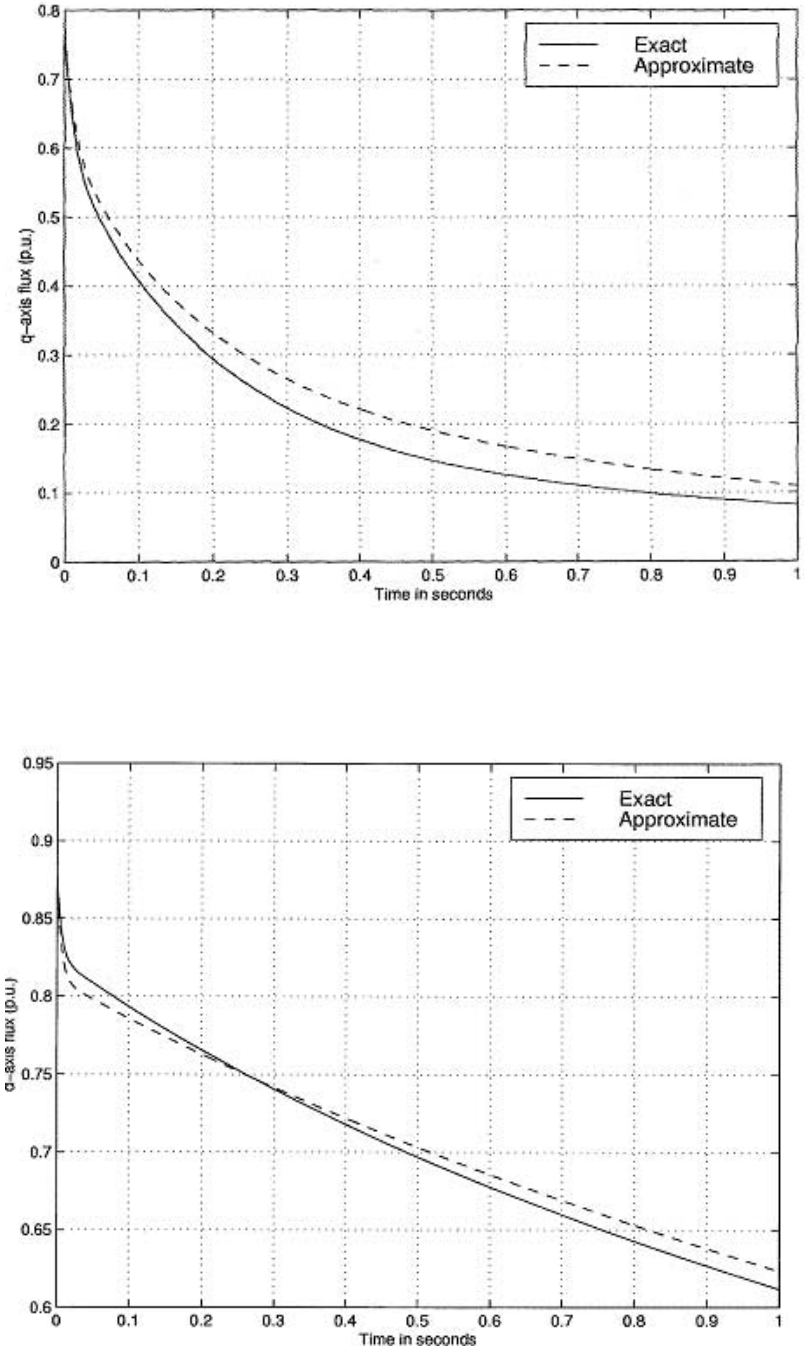

Figure 18—Assessment of numerical (exact) and closed-form (approximate) computations of time constants and related quantities

Annex A

(informative)

Bibliography

[B1] Blondel, A., "The Salient Pole Synchronous Machine," *L'Elcairage Elec.*, 1895. Also, *Trans. International Elec. Congress,* St. Louis, vol. 1, p. 635, 1904.

[B2] Canay, I. M., "Determination of the Model Parameters of Machines from the Reactance Operators, (Evaluation of Standstill Frequency Response Test)," *IEEE Transactions*, EC-8(2), pp. 272–279, June 1993.

[B3] Canay, I. M., "Equivalent Circuits of Synchronous Machines for Calculating Quantities of the Rotor During Transient Processes and Asynchronous Starting, Part II, Salient Pole Machines," *Brown Boveri Review,* vol. 57, March 1970.

[B4] Canay, I. M., "Extended Synchronous Machine Model for Calculation of Transient Processes and Stability," *Electrical Machines and Electromechanics (International Quarterly),* no. 1, pp. 137–150, 1977.

[B5] Canay, I. M., "Identification and Determination of Synchronous Machine Parameters," *Brown Boveri Review,* June/July 1984.

[B6] Chorlton, A., and Shackshaft, G., "Comparison of Accuracy of Methods for Studying Stability-Northfleet Exercise," CIGRE Study Committee 32, Working Group 3 Report, February 1971.

[B7] Concordia, C., "Steady State Stability of Synchronous Machines as Affected by Voltage-Regulator Characteristics," *AIEE Transactions,* vol. 63, p. 215–220, May 1944.

[B8] Concordia, C., Crary, S. B., and Lyons, J. M., "Stability Characteristics of Turbine Generators," *AIEE Transactions,* vol. 57, pp. 732–744, 1938.

[B9] Dandeno, P. L., and Iravani, M. R., "Third Order Turboalternator Electrical Stability Models with Applications to Subsynchronous Resonance Studies," *IEEE Transactions,* vol. EC-10, No. 1, pp. 78–86, March 1995.

[B10] Dandeno, P. L. (IEEE Working Group Chair), Karmaker, H.C. (Secretary), Azuaje, C., Glinkowski, M., Kamwa, I., Oliveira, S., Salon, S. J., Saunders, R. M., and Umans, S., "Experience with Standstill Frequency Response (SSFR) Testing and Analysis of Salient Pole Synchronous Machines," *IEEE Transactions,* EC-14(4), pp. 1209–1217, December 1999.

[B11] Dandeno, P. L., and Service, J. R., "Experience with Translation of Turbogenerator Operational Test Data and Corresponding d and q Axis Stability Models into Standard Inductances and Time Constants Forms," *10th Power Syst. Comp. Conf. (PSCC),* pp. 371–378, 1990.

[B12] Dandeno, P. L., Hauth, R. L., and Schulz, R. P., "Effects of Synchronous Machine Modeling in Large Scale Stability Studies," *IEEE Transactions on PAS,* vol. 92, pp. 574–582, March/April 1973.

[B13] Dandeno, P. L., Kundur, P., Poray, A. T., and Coultes, M. E., "Validation of Turbo-Generator Stability Models by Comparison with Power System Tests," *IEEE Transactions on PAS,* vol. PAS-100, pp. 1637–1645, 1981.

[B14] Dandeno, P. L., Kundur, P., Poray, A. T. and Zein-el-Din, H. M., "Adaptation and Validation of Turbo-generator Model Parameters Through On-Line Frequency Response Measurements," *IEEE Transactions on Power App. & Syst.*, PAS-100, p. 1656–1665, April 1981.

[B15] De Mello, F. P., and Hannet, L. H., "Validation of Synchronous Machine Models and Derivation of Model Parameters from Tests," *IEEE Transactions*, PAS-100(2), pp. 662–672, February 1981.

[B16] De Mello, F. P., and Ribeiro, J. R., "Derivation of Synchronous Machine Parameters from Tests," *IEEE Transactions*, PAS-96(4), pp. 1211–1218, July/August 1977.

[B17] Dougherty, J. W., and Minnich, S. H., "Operational Inductances of Turbine Generators, Test Data vs. Finite-Element Calculations," *IEEE Transactions on PAS*, vol. PAS-102, pp. 3393–3404, 1983.

[B18] Dougherty, J. W., and Minnich. S. M., "Finite Element Modeling of Large Turbine Generators: Calculation versus Load Test Data," *IEEE Transactions on PAS*, vol. PAS-100, pp. 3921–3929, August 1981.

[B19] *Electrical Transmission and Distribution Reference Book*, Westinghouse Electric Corp., Pittsburgh, pp. 147–152, 1964.

[B20] El-Serafi, A. M., and Abdallah, A. S., "Effect of Saturation on the Steady-State Stability of a Synchronous Machine Connected to an Infinite Bus System," *IEEE Transactions on Energy Conversion*, vol. 6, pp. 514–521, 1991.

[B21] El-Serafi, A. M., and Abdallah, A. S., "Saturated Synchronous Reactances of Synchronous Machines," *IEEE Transactions on Energy Conversion,* vol. 7, pp. 570–579, 1992.

[B22] El-Serafi, A. M., and Demeter, E., "Determination of the Saturation Curves in the Intermediate Axes of Cylindrical-Rotor Synchronous Machines," *Proceedings of the International Conference on Electrical Machines*, Istanbul, Turkey, vol. 3, pp. 1060–1065, September 2–4, 1998.

[B23] El-Serafi, A. M., and Wu, J., "Determination of the Parameters Representing the Cross-magnetizing Effect in Saturated Synchronous Machines," *IEEE Transactions on Energy Conversion*, vol. 8, pp. 333–342, 1993.

[B24] El-Serafi, A. M., Abdallah, A. S., El-Sherbiny, M.K. and Badawy, E.H., "Experimental Study of the Saturation and the Cross-Magnetizing Phenomenon in Saturated Synchronous Machines," *IEEE Transactions on Energy Conversion*, vol. EC-3, pp. 815–823, 1988.

[B25] EPRI Report, EL-1424, *Determination of Synchronous Machine Stability Study Constants*, vol. 1, Westinghouse Electric Corporation, 1980.

[B26] EPRI Report, EL-1424, *Determination of Synchronous Machine Stability Study Constants*, vol. 2, Ontario Hydro, 1980.

[B27] EPRI Report, EL-1424, *Determination of Synchronous Machine Stability Study Constants*, vol. 3, prepared by Power Technologies Inc., 1980.

[B28] EPRI report, EL-5736, *Confirmation of Test Methods for Synchronous Machine Dynamic Performance Models*, prepared by Consumers Power Inc., August 1988.

[B29] Ewart, D. N., and De Mello, F. P., "A Digital Computer Program for the Automatic Determination of Dynamic Stability Limits," *IEEE Transactions on PAS*, vol. 86, pp. 867–875, July 1967.

[B30] Flores, J. F., Buckley, G. W., and McPhereson, G., Jr., "The Effects of Saturation of the Armature Leakage Reactance of Large Synchronous Machines," *IEEE Transactions on PAS,* vol. PAS-103, pp. 593–600, 1984.

[B31] Harley, R. G., Limebeer, D. J. and Chirricoeei, E., "Comparative Study of Saturation Methods in Synchronous Machine Models," *Proceedings IEE,* vol. 127, Part B, pp. 1–7, 1980.

[B32] Heck, C., *Magnetic Materials and their Applications,* Crane Russak, 1974.

[B33] Hirayama, K., "Practical Detailed Model for Generators," *IEEE Transactions,* EC-10(l), pp. 105–110, March 1995.

[B34] Hurley, J. D. and Schwenk, H. R., "Standstill Frequency Response Modeling and Evaluation by Field Tests on a 645 MVA Turbine Generator," *IEEE Transactions on PAS,* vol. PAS-100, pp. 828–836, 1981.

[B35] IEEE Committee Report, "Second Benchmark Model for Computer Simulation of Subsynchronous Resonance," *IEEE Transactions on PAS,* vol. PAS-104, no. 5, pp. 1057–1066, May 1985.

[B36] IEEE Committee Report: "Current Usage and Suggested Practices in Power System Stability Simulations for Synchronous Machines," *IEEE Transactions on Energy Conversion,* vol. EC-1, pp. 77–93, March 1986.

[B37] IEEE Special Publication prepared by the Power System Stability Committee, "Techniques for Power System Stability Limit Search, TP-138-0, 1999.

[B38] IEEE 100, *The Authoritative Dictionary of IEEE Standards Terms,* Seventh Edition.

[B39] Jack, A. G., and Bedford, T. J., "A Study of the Frequency Response of Turbogenerators with Special Reference to Nanticoke GS," *IEEE Transactions,* vol. EC-2, no. 3., pp. 496–505, Sept. 1987.

[B40] Jin, Y., and El-Serafi, A. M., "A "Three Transfer Function" Approach for the Standstill Frequency Response Test of Synchronous Machine," *IEEE Transactions,* EC-5(4), pp.740–749, December 1990.

[B41] Kamwa, I., and Farzaneh, M., "Data Translation and Order Reduction for Turbine-Generator Models Used in Network Studies," *IEEE Transactions,* EC-12(2), pp. 118–126, June 1997.

[B42] Kamwa, I., and Viarouge, P., "On Equivalent-Circuit Structure for Empirical Modeling of Turbine-Generators," *IEEE Transactions,* EC-9(3), pp. 579–592, September 1994.

[B43] Kamwa, I., Pilote, M., Viarouge, P., Mpanda-Mabwe, B., Crappe, M., and Mahfoudi, R., "Experience with Computer-Aided Graphical Analysis of Sudden-Short-Circuit Oscillograms of Large Synchronous Machines," *IEEE Transactions,* EC-10(3), pp. 407–414, September 1995.

[B44] Kamwa, I., Viarouge, P., and Mahfoudi, R., "Phenomelogical Models of Large Synchronous Machines from Short-Circuit Tests During Commissioning—A Classical/Modern Approach," *IEEE Transactions,* EC-9(l), pp. 85–97, March 1994.

[B45] Kamwa, I., Viarouge, P., Le Huy, H., and Dickinson, J., "The Three-Transfer-Function Approach for Building Phenomenological Models of Synchronous Machines," *IEE Proc. Gener. Transm. Distrib.*, 141(2), pp. 89–98, 1994.

[B46] Kilgore, L. A., "Calculation of Synchronous Machine Constants—Reactances and Time Constants Affecting Transient Characteristics," *AIEE Transactions,* vol. 50, pp. 1201–1213, Dec. 1931.

[B47] Kimbark, E. W., *Power System Stability, Vol. III: Synchronous Machines,* pp. 118–128, 1956.

[B48] Kirtley, J. L., "On Turbine-Generator Equivalent Circuits," *IEEE Transactions,* PWRS-9(1), pp. 262–271, March 1994.

[B49] Krause, P. C., Nozari, F., Skvarenina, J. L., and Olive, D. W., "The Theory of Neglecting Stator Transients," *IEEE Transactions on PAS,* vol. 98, no. 1, pp. 141–148, Jan/Feb 1979.

[B50] Kundur, P., and Dandeno, P. L., "Implementation of Advanced Generator Models into Power System Stability Programs," *IEEE Transactions on PAS,* vol. PAS-102, pp. 2047–2054, 1983.

[B51] Kundur, P., and Morison, G. K., "A Review of Definitions and Classification of Stability Problems in Today's Power Systems," Panel Session on Stability Terms and Definitions, IEEE PES Winter Meeting, NY., Feb. 1997.

[B52] Kundur, P., Lee, D. C., and Zein El-Din, H. M., "Power System Stabilizers for Thermal Units: Analytical Techniques and On-Site Validation," *IEEE Transactions,* vol. PAS-100, pp. 81–95, January 1981.

[B53] Kundur, P., Morison, G. K., and Balu, N. J., "A Comprehensive Approach to Power System Analysis," CIGRE Paper 38–106, presented at the 1994 Session, Paris, France.

[B54] Kundur, P., *Power System Stability and Control,* New York: McGraw Hill, 1994.

[B55] Kundur, P., Rogers, G. J., Wong, D. Y., and Lauby, M., "A Comprehensive Computer Program Package for Small Signal Stability Analyses of Power Systems," *IEEE Transactions on Power Systems,* vol. 5. no. 4, pp. 1076–1083, Nov. 1990.

[B56] Lee, D. C. and Kundur, P., "Advanced Excitation Control for Power System Stability Enhancement," CIGRE Paper 38–01, 1986.

[B57] Manchur, G., Lee, David C., Coultes, M. E., Griffin, J.D.A., and Watson, W., "Generator Models Established by Frequency Response Tests on a 555 MVA Machine," *IEEE Transactions on PAS,* vol. 91, No. 5, pp. 2077–2084, September/October 1972.

[B58] *Matlab User's Guide* (Version 6) and *Matlab Optimization Toolbox User's Guide* (Version 3), The Mathworks Inc., Natick, MA, 2000: http://www.mathworks.com.

[B59] Minnich, S. H., "Small Signals, Large Signals and Saturation in Generator Modeling," *IEEE Transactions on Energy Conversion,* vol. EC-1, pp. 94–102, 1986.

[B60] Minnich, S. H., Schulz, R. P., Baker, D.H., Sharma, D. K., Farmer, R.G., and Fish, J. H., "Saturation Functions of Synchronous Generators from Finite Elements," *IEEE Transactions on Energy Conversion,* vol. EC-2, pp. 680–692, Dec. 1987.

[B61] Morison, G. K., Gao, B., and Kundur, P., "Voltage Stability Analysis using Static and Dynamic Approaches," *IEEE Transactions on Power Systems,* vol. 8, no. 3, pp. 1159–1171, August 1993.

[B62] Park, R. H., "Two-Reaction Theory of Synchronous Machines," Part I, *AIEE Transactions*, vol. 48, p. 716, 1929.

[B63] Park, R. H., "Two-Reaction Theory of Synchronous Machines," Part II, *AIEE Transactions,* vol. 52, p. 352, 1933.

[B64] Podmore, R., "Identification of Coherent Generators for Dynamic Equivalents," *IEEE Transactions*, vol. PAS-97, pp. 754–763, July/August 1978.

[B65] Rankin, A. W., "Per-Unit Impedances of Synchronous Machines," *AIEE Transactions*, vol. 64, (I) pp. 569-572 and (ii) pp. 839–841, 1945.

[B66] Rusche, P. A. E., Brock, G. J., Hannet, L. N., and Willis, J. R., "Test and Simulation of Network Dynamic Response Using SSFR and RTDR Derived Synchronous Machine Models," *IEEE Transactions*, EC-5(l), pp. 145–155, March 1990.

[B67] Salvatore, L., and Savino, M., "Exact Relationships Between Parameters and Test Data for Models of Synchronous Machines," *Elec. Machines & Power Syst.*, 8, pp. 169–184, 1983.

[B68] Shackshaft, G., and Henser, P. B., "Model of Generator Saturation for Use in Power System Studies," *Proceedings IEE*, vol. 126, pp. 759–763, 1979.

[B69] Shackshaft, G., "Implementation of New Approach to Determination of Synchronous-Machine Parameters from Tests," *Proceedings IEE*, 124(12), pp. 1170–1177, December 1977.

[B70] Shackshaft, G., "New Approach to the Determination of Synchronous-Machine Parameters from Tests," *Proceedings IEE*, 121(11), pp. 1385–1392, November 1974. Discussion: *Proceedings IEE*, 123(5), pp. 429–432, 1976.

[B71] Stubbe, M., Bihain, A., Deuse, J., Baader, J. C., "STAG, a New Unified Software Program for the Study of Dynamic Behaviour of Electrical Power Systems," *IEEE Transactions on Power Systems*, vol. 4, no. 1, pp. 129–138, 1989.

[B72] Sugiyama, T., Nishiwaki, T., Takeda, S., and Abe, S., "Measurements of Synchronous Machine Parameters Under Operating Conditions," *IEEE Transactions*, PAS-101(4), pp. 895–904, April 1982.

[B73] Takeda, Y., and Adkins, B., "Determination of Synchronous-Machine Parameters Allowing for Unequal Mutual Inductances," *Proceedings IEE*, 121(12), pp.1501–1504, Dec. 1974. Discussion: *Proceedings. IEE*, 123(5), pp. 429–432, May 1976.

[B74] Taylor, C. W., Mechenbier, J.R., and Mathews, C. E., "Transient Excitation Boosting at Grand Coulee Third Power Plant: Power System Application and Field Test," *IEEE Transactions on Power Systems*, vol. 8, No. 3, pp.1291–1298, August 1993.

[B75] Tsai, H., Keyhani, A., Demcko, J., and Farmer, R. G., "On-Line Synchronous Machine Parameter Estimation from Small Disturbance Operating Data," *IEEE Transactions*, EC-10(1), pp. 25–36, March 1995.

[B76] Turner, P. J., "Finite Element Simulation of Turbine Generator Terminal Faults and Application of Machine Parameter Prediction," *IEEE Transactions on Energy Conversion*, vol. EC-2, pp. 122–131, 1987.

[B77] Umans, S. D., Mallick, J. A., and Wilson, G. L., "Modeling of Solid Rotor Turbogenerators—Parts I & II," *IEEE Transactions*, PAS-97(1), pp. 269–291, Jan./Feb. 1978.

[B78] Van Cutsem, T., Jacquemart, Y., Marquet, J. N., and Pruvot, P., "Comprehensive Analysis of Mid-Term, Voltage Stability," *IEEE Transactions on Power Systems*, vol. 10, pp. 1173–1182, August 1995.

[B79] Verbeeck, J., Pintelon, R., and Guillaume, P., "Determination of Synchronous Machine Parameters Using Network Synthesis Techniques," *IEEE Transactions*, EC-14(3), pp. 310–314, September 1999.

[B80] Verbeeck, J., Pintelon, R., and Lataire, P., “Influence of Saturation of Estimated Synchronous Machine Parameters in Standstill Frequency Response Tests,” *IEEE Transactions*, EC-15(3), pp. 277-283, September 2000.

[B81] Wang, L., Klein, M., Yirga, S. and Kundur, P., “Dynamic Reduction of Large Power Systems for Stability Studies,” *IEEE Transactions on Power Systems*, vol. 12, no. 2, pp. 889–895, May 1997.

[B82] Xu, X., Mathur, R. M., Rogers, G. J., and Kundur, P., “Modeling of Generators and their Controls in Power System Simulations Using Singular Perturbations,” *IEEE Transactions on Power Systems*, vol. 13, no. 1, pp.109–114, February 1998.

Annex B

(normative)

List of main symbols

General conventions:

a) Subscripts *a*, *b*, *c*, and *fd* refer to the three armature phases and the field winding, respectively.
b) Subscripts *d* and *q* refer to the direct- and quadrature-axis equivalent armature windings, respectively.
c) Subscripts *u* and *sat* refer to the unsaturated and saturated values of parameters such as inductances.

model N.M	a model-numbering scheme, where "N" represents the number of equivalent rotor windings on the direct axis and "M" the number of equivalent rotor windings on the quadrature axis
ψ	winding flux linkage
i	winding current
v	armature-winding voltage
N_p	number of magnetic poles on the machine
N_{afd}	armature to field turn ratio: N_{afdu} measured in unsaturated conditions; $N_{afd}(0)$ measured at zero frequency during SSFR tests
L_a, R_a	armature-phase self inductance and armature phase resistance
L_{ab}	armature phase-phase mutual inductance
L_m	peak armature-phase to field-winding mutual inductance
L_f	field-winding self inductance
Ψ_d, Ψ_q	d- and q-axis stator flux linkages
i_d, i_q	d- and q-axis stator terminal currents
ω_m, ω	rotor mechanical and electrical angular velocity
e'_{fd}, i'_{fd}	actual values of field voltage and current measured at the field-winding terminals
e_{fd}, i_{fd}	field voltage and current reflected to the armature winding through the field to direct-axis armature winding turns ratio, N_{afd}
L_l	stator leakage inductance (both d- and q-axis)
X_l	stator leakage reactance (both d- and q-axis)

L_{ad}, L_{aq}	d- and q-axis stator to rotor mutual inductance: L_{adu}, L_{aqu} measured in unsaturated conditions; $L_{ad}(0)$, $L_{aq}(0)$ measured at zero frequency during SSFR tests
X_{ad}, X_{aq}	d- and q-axis stator to rotor mutual reactance: X_{adu}, X_{aqu} measured in unsaturated conditions; $X_{ad}(0)$, $X_{aq}(0)$ measured at zero frequency during SSFR tests
L_d, L_q	d- and q-axis synchronous inductance: L_{du}, L_{qu} measured in unsaturated conditions; $L_d(0)$, $L_q(0)$ measured at zero frequency during SSFR tests
X_d, X_q	d- and q-axis synchronous reactance: X_{du}, X_{qu} measured in unsaturated conditions; $X_d(0)$, $X_q(0)$ measured at zero frequency during SSFR tests
$L_d(s)$, $L_q(s)$	d- and q-axis operational inductance, as viewed from the stator terminals
$L_{afo}(s)$	armature to field transfer inductance with armature open
$sG(s)$	stator to field operational transfer function
$Z_{fd}(s)$	field input impedance with armature short-circuited
R_{fd}, L_{fd}	field winding resistance and leakage inductance referred to the stator
R_{kd}, L_{kd}	d-axis damper winding resistance and leakage inductance referred to the stator, $k=1,2,...,n_d$
R_{kq}, L_{kq}	q-axis damper winding resistance and leakage inductance referred to the stator, $k=1,2,...,n_d$
L_{fkd}	mutual inductance between field winding and a d-axis damper winding referred to the stator, $k=1,2,..., n_d$
T_{kd}	time constants in the numerator and denominator of the d-axis operational inductance and transfer impedances $\{L_d(s), sG(s), Z_{fd}(s)\}$, $k=1,2,...$ (in seconds)
T_{kq}	time constants in the numerator and denominator of the q-axis operational inductance $L_q(s)$, $k=1,2,..., 2n_q$ (in seconds)
L'_d, L'_q	d- and q-axis transient inductance
L''_d, L''_q	d- and q-axis subtransient inductance
L'''_d, L'''_q	d- and q-axis sub-subtransient inductance
X'_d, X'_q	d- and q-axis transient reactance
X''_d, X''_q	d- and q-axis subtransient reactance
X''_d, X''_q	d- and q-axis sub-subtransient reactance
T'_{do}, T'_{qo}	d- and q-axis transient open-circuit time constants in seconds
T''_{do}, T''_{qo}	d- and q-axis subtransient open-circuit time constant in seconds
T'''_d , T'''_q	d- and q-axis sub-subtransient open-circuit time constant in seconds

T'_d , T'_q	d- and q-axis transient short-circuit time constants in seconds
T''_d, T''_q	d- and q-axis subtransient short-circuit time constants in seconds
T'''_d, T'''_q	d- and q-axis sub-subtransient short-circuit time constants in seconds
X_p	Potier reactance
X_{su}	unsaturated synchronous reactance (cylindrical machine)
X_{sat}	saturated synchronous reactance (cylindrical machine)
X_{dsat}, X_{qsat}	saturated synchronous reactances in the d and q axes
X_{adsat}, X_{aqsat}	saturated d- and q-axis stator to rotor mutual inductance
K	saturation factor: ratio of the actual excitation and the excitation on the air-gap line of the open-circuit saturation curve at the operating point
K_d, K_q	saturation factors in the d and q axes
E_a, I_a	terminal voltage and current (in phasor diagrams)
E_l, E_p	voltage behind the leakage and Potier reactance
E_{QD}	voltage behind the quadrature-axis synchronous reactance X_q
δ	phase displacement between the terminal voltages E_a and E_{QD}, i.e., between E_a and the quadrature magnetic axis of the machine (positive for a generator and negative for a motor)
E_{GU}	voltage behind the unsaturated synchronous reactance X_{su} (i.e., unsaturated internal voltage)
I_{FU}	field current (in p.u.) required to induce a voltage E_{GU} on the air-gap line of the open-circuit saturation curve
I_{FS}	difference between the actual excitation (I_F) and the excitation (I_{FU}) on the air-gap line of the open-circuit saturation curve at the operating point (in p.u.)
I_{FG}	base field current (in amperes) required to induce 1.0 per unit terminal voltage on the air-gap line of the open-circuit saturation curve

Annex C

(informative)

Calculation of generator electrical torque or power

In a majority of stability programs, synchronous machine torque is calculated in terms of the machine's direct- and quadrature-axis currents and fluxes. Such calculations can be performed either in engineering-units or in per unit. As is commonly found in engineering analyses, the choice of per-unit notation results in equations that are more concise. Thus, per-unit equations will be presented in this annex, although an alternate formulation in engineering units would be equally valid.

Per-unit electromagnetic torque is given by

$$T_e = \Psi_d i_q - \Psi_q i_d \tag{C.1}$$

in terms of the per-unit direct- and quadrature-axis fluxes, Ψ_d and Ψ_q, and the per-unit direct- and quadrature-axis currents, i_d and i_q.

Accuracy in simulation of synchronous machine performance requires accurate representation of these currents and fluxes. The effects of damper and rotor-body currents should be included in transient simulations, since these currents play a significant role both in determining the magnitudes of the transient electromagnetic torque and in determining the damping of the electromechanical oscillations associated with the transient.

For Model 2.2, which includes the effects of the field winding, an additional damper winding on the direct-axis and two damper windings on the quadrature axis, the per-unit direct- and quadrature-axis stator fluxes are given by

$$\Psi_d = -L_d i_d + L_{ad} I_{fd} + L_{ad} i_{1d} \tag{C.2}$$

$$\Psi_q = -L_q i_q + L_{aq} i_{1q} + L_{aq} i_{2q} \tag{C.3}$$

Similar expressions may be derived for higher- or lower-order models, or for Model 2.2 with the differential leakage reactance L_{f1d} included, as in Figure 1 of 4.1.

As discussed in 4.1, the per-unit differential equations for the direct- and quadrature-axis voltage are

$$v_d = -R_a i_d + \frac{1}{\omega_b}\frac{d\Psi_d}{dt} - \frac{\omega_m}{\omega_{mo}}\Psi_q \tag{C.4}$$

$$v_q = -R_a i_q + \frac{1}{\omega_b}\frac{d\Psi_q}{dt} + \frac{\omega_m}{\omega_{mo}}\Psi_d \tag{C.5}$$

Here, ω_m is the rotor speed (in radians per second), ω_b is the synchronous electrical speed, and ω_{mo} is the synchronous rotor speed (radians per second), and time (t) is in seconds. The above sign convention for voltages, currents and flux linkages also conforms to the convention that the quadrature-axis leads the direct-axis, when the field is assumed rotating counterclockwise relative to the armature. The above convention is also preferred in the widely used stability programs referred to in Annex D.

In large-size transient stability programs, the rate of change of stator flux linkages is usually neglected. This is done primarily to be consistent with the practice of neglecting power system network transients. Omission of the $\frac{d\Psi_q}{dt}$ and $\frac{d\Psi_d}{dt}$ terms implies that stator dc offsets during faults or other unbalances are ignored. This simplification permits a positive sequence representation of both generator and power network. It also results in a conservative answer, i.e., a transient power limit, for a given disturbance, would be lower with this omission.

The resulting equations, then, would become

$$v_d = -R_a i_d - \frac{\omega_m}{\omega_{mo}}\Psi_q \tag{C.6}$$

$$v_q = -R_a i_q + \frac{\omega_m}{\omega_{mo}}\Psi_d \tag{C.7}$$

Solving for Ψ_d and Ψ_q (above) and substituting into Equation (C.1) for T_e gives

$$T_e = \{v_d i_d + v_q i_q + i_a^2 R_a\}\frac{\omega_{mo}}{\omega_m} \tag{C.8}$$

or

$$T_e = \{P_e + i_a^2 R_a\}\frac{\omega_{mo}}{\omega_m} \tag{C.9}$$

where P_e = electrical output power = $v_d i_d + v_q i_q$ and $i_a^2 = i_d^2 + i_q^2$.

It is sometimes customary to ignore changes in electrical machine speed, ω_m. Exceptions would occur when sustained system frequency deviates noticeably from the normal 50 Hz or 60 Hz. This is most likely with small isolated power systems, or where “islanding” conditions suddenly are encountered in a portion of a large power system. Normally ω_m is very close in value to ω_{mo}. Assuming then that ω_m/ω_{mo} = 1.0, Equation (C.8) simplifies to:

$$T_e = P_e + I_a^2 R_a \tag{C.10}$$

Neglecting the instantaneous changes in speed tends to give an optimistic result. IEEE [B36] and Canay [B4] indicate that neglecting both $\frac{d\Psi}{dt}$ terms compensates for the omission of changes in instantaneous speed. Both of these simplifications appear to be justified, not only from a practical consideration of the orders of magnitude of the quantities involved, but also due to the fact that measured test results show good agreement with simplified calculations, such as that of Equation (C.10).

This issue is further discussed in Canay (C.5). The authors treat the general case of any machine and then specifically discuss Park's equations for a synchronous machine, where their arbitrary reference frame of electrical speed is replaced by the rotor reference frame as in Equation (C.4) and Equation (C.5). They finally conclude that both neglecting the rate of change of flux linkages in the rotor reference frame and setting the rotor speed equal to the system electrical speed is required in order to neglect the electrical transients due to the stator windings of the synchronous machine.

Annex D

(informative)

Procedures in a widely used stability program to account for saturation when adjusting mutual reactances

D.1 Theoretical and practical aspects

These concepts are described in Kundur and Dandeno [B50]. Generator equations are written initially by calculating direct- or quadrature-axis flux linkages in terms of direct- or quadrature-axis circuit elements, and with the appropriate direct- or quadrature-axis stator and rotor currents. X_d and X_{ad} used in Equation (D.1), Equation (D.2), and Equation (D.3) are unsaturated values.

Thus, for example, in the general case,

$$\Psi_d = -L_d i_d + L_{ad} i_{fd} + L_{ad} i_{1d} + L_{ad} i_{2d} \tag{D.1}$$

and the process may be continued for Ψ_{fd}, Ψ_{1d}, Ψ_{2d}, Ψ_{1q}, Ψ_{2q}...etc.

The stability program then eliminates stator flux linkages and rotor currents by expressing them in terms of components of rotor flux linkages and stator currents. The resulting differential equations describe the electrical dynamics of the machine rotor circuits with rotor flux linkages chosen as the state variables.

When using this approach, it is also customary to convert i_{fd} and e_{fd} per-unit field quantities, which are in the reciprocal system, into non-reciprocal quantities. This is done to permit interfacing with excitation system per-unit relationships. These conversions are discussed in Kundur and Dandeno [B50] and Minnich et al. [B60], which cover the theory of this particular program.

In the steady state, rotor currents i_{1d}, i_{2d}, i_{1q}, i_{1q} ...etc., are equal to zero. The direct-axis flux linkage equation simplifies to

$$\Psi_d = -L_d i_d + L_{ad} i_{fd} \qquad \text{(all quantities per unit)} \tag{D.2}$$

For actual operating conditions, (referring to the phasor diagram of Figure D.1, and noting that $\Psi_d = E_q$), the above equation can be rewritten:

$$X_{ad} i_{fd} = E_q + i_d X_d \tag{D.3}$$

i_{fd} will be in per unit using the reciprocal system. Then with saturation included,

$$X_{adsat} i_{fd} = E_q + i_d X_{dsat} \tag{D.4}$$

X_{adsat} (and X_{aqsat}) are adjusted values and depend on the initial operating point.

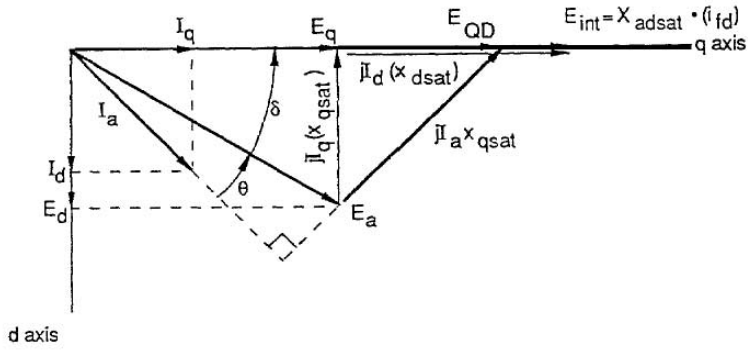

Figure D.1—Phasor diagram for commercial stability program

The steps for specifically adjusting X_{adu} and X_{aqu} to obtain X_{dsat} and X_{qsat} are given below.

Step number

1) Determine a q-axis saturation function K_q, for a calculated air-gap voltage E_l. This value of depends on machine power, reactive power, and terminal voltage (q-axis saturation curve is assumed to be known for the calculation of K_q).
2) Determine X_{qsat} where

$$X_{aqsat} = \frac{X_{aqu}}{K_q} \qquad \text{and} \qquad X_{qsat} = X_{aqsat} + X_l$$

3) Determine δ, the internal machine angle, located by the phasor E_{QD}, where

$$E_{QD}\angle\delta = E_a\angle 0^\circ + jI_aX_{qsat} \tag{D.5}$$

4) For the same E_l calculated in step (1) above, find X_{dsat}, where $X_{adsat} = \frac{X_{adu}}{K_d}$
5) K_d is determined from a known saturation curve, or from the open circuit saturation curve.
6) Determine field current i_{fd}, where $i_{fd} = \frac{E_q + i_dX_{dsat}}{X_{adsat}}$ (All values in per-unit reciprocal).

D.2 Use of on-site measurements to derive under load saturation factors

One basic approach to determining K_q and K_d factors can be through the use of on-site measurements of generator quantities. The values of armature voltage, current and power factor (or MW, MVAR, and kV) are measured. In addition, field current and internal angle are measured (EPRI [B25], Minnich et al. [B60]).

From the phasor diagram shown in Figure. D.1, E_d, the projection of the terminal voltage on the direct axis also has the magnitude of a vector corresponding to $I_q(X_{qsat})$. Note that I_q is the projection of the armature current I_a on the quadrature axis. The power angle θ and the internal angle δ have been measured, as have E_a and I_a.

An examination of the phasor diagram in Figure D.1 shows that $E_d = i_qX_{qsat}$ and it follows that $X_{qsat} = \frac{E_d}{I_q}$

An internal voltage behind the leakage reactance is determined and its magnitude is called E_l. (E_l is not shown on Figure D.1). The equivalent excitation for this particular operating point is I_{exq} and, by definition

$$I_{exq} = \frac{E_l}{X_{aqsat}}$$

Repeating Equation (D.4) as an algebraic quantity, $X_{adsat} i_{fd} = E_q + i_d X_{dsat}$ and noting that $X_{dsat} = X_{dsat} - X_l$ it follows that $(X_{dsat} - X_l) i_{fd} = E_q + i_d X_{dsat}$.

Collecting X_{dsat} terms and solving for X_{dsat} it follows that $X_{dsat} = \frac{E_q + X_l i_{fd}}{i_{fd} - I_d}$.

Finally $X_{exd} = \frac{E_l}{X_{adsat}}$

The various values of I_{exd} or I_{exq} can be plotted against the corresponding test values of E_l, from which they were derived. Some kind of exponential or power function can be tried to develop a smooth curve through the test points, as shown in Figure D.2.

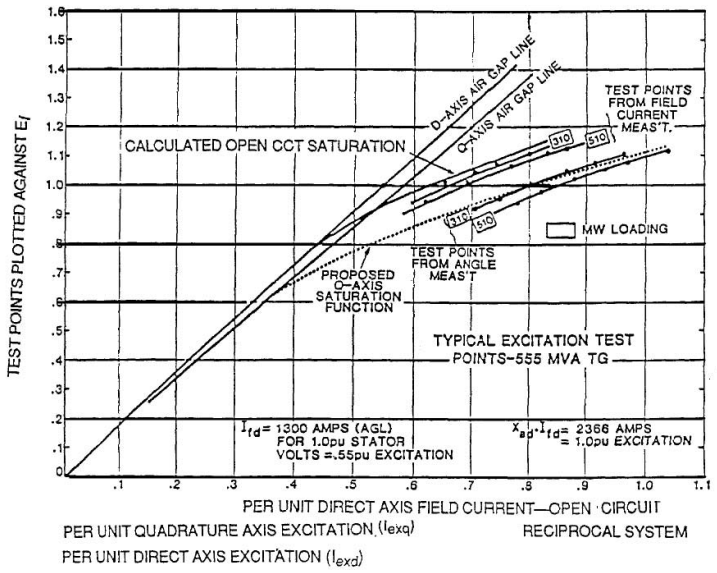

Figure D.2—Typical excitation test points 555 MVA turbogenerator

Figure D.2 shows several I_{exq} and I_{exd} points obtained from readings for a turbogenerator at power loadings of 310 MW and 510 MW at various power factors, overexcited and under-excited. Curve fitting procedures may be used to obtain functions which, when plotted, will fall close to the test points. The shape of the function curves is similar to that of the open-circuit saturation curve that is also plotted here on a reciprocal base. Note that the test points for both d-axis and q-axis calculations vary with MW loadings.

Figure D.3 is an example of how to determine K_d and K_q factors from the function information plotted in Figure D.2.

The determination of K_d and K_q factors is based on the arbitrary assumption that the total air-gap flux corresponding to E_l is presumed to act first in one axis alone, and then in the other axis. The method, while pragmatic, is simple to apply and provides reasonable agreement between test and calculation.

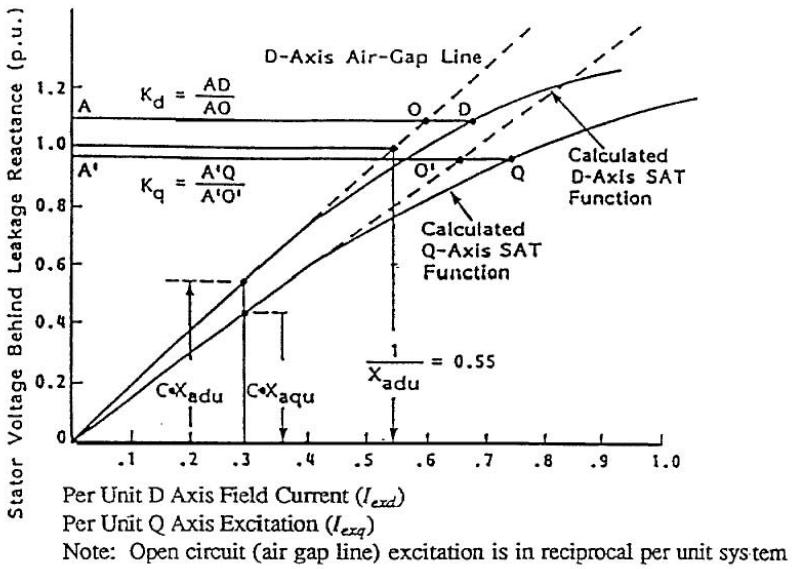

Figure D.3—D and Q axes saturation functions

Note from Figure D.3 that the values of K_d and K_q are unity or greater, depending upon the value of E_l, which is a function of X_l, armature voltage current and power factor, and also depending upon where the "break point" from the air-gap line is assumed. Different values of E_l are assumed to more easily identify the K_d and K_q ratios.

Annex E

(informative)

Sample matlab listing

Table E.1(a)—Translation of operational inductances into equivalent-circuits (resistances/ inductances in p.u., time in sec, wn = nominal frequency in rad/sec)

Equivalent circuit with two rotor circuits in each axis

Direct axis [a]	Quadrature axis[b]

`%Set the time constants in Ld(s),sG(s)`
`%See (eq. 7.2.4-7.2.5)`
`T1=1.419;`
`T2=0.0669;`
`T3=5.62;`
`T4=0.09;`
`T5=0.0234;`
 	
`Ld= 1.104; %Synchronous inductance`
`Ll=0.198;  %Stator leakage inductance`
`Lad=Ld-Ll; %Mutual inductance`
`wn=2*pi*60;%Rated frequency in rad/sec`
 	
`%Implementation of the formulas in [B77]`
`Ro=wn*Ld*(T3+T4-T1-T2);`
`Ro=Lad*Lad/Ro;`
 	
`a=Ld*(T1+T2)-Ll*(T3+T4);a=a/Lad;`
`b=Ld*T1*T2-Ll*T3*T4; b=b/Lad;`
`c=(T3*T4-T1*T2)/(T3+T4-T1-T2);`
 	
`Lf1d=b-a*T5+T5*T5;  %in p.u.`
`Lf1d=Ro*Lf1d/(c-T5);  %in p.u.`
 	
`Rfd=Ro*(Lf1d+Ro*(2*T5-a));`
`Rfd=Rfd/(Lf1d+Ro*(T5+c-a));%in p.u.`
`Lfd=Rfd*(a-T5-Lf1d/Ro);  %in p.u.`
`R1d=Ro*Rfd/(Rfd-Ro);  %in p.u.`
 	
`%Inductances in p.u.`
`L1d=R1d*T5; L1d=L1d*wn;`
`Lfd=Lfd*wn; Lf1d=Lf1d*wn;`
	`%Set the time constants in Lq(s)`
	`%See (eq. 7.2.14)`
	`Tq1=.975;`
	`Tq2=.116;`
	`Tq3=1.790;`
	`Tq4=.276;`
	
	`Laq=1.165; %Mutual inductance`
	`Ll=.188;  %Stator leakage inductance`
	`Lq=Laq+Ll; %Synchronous inductance`
	`wn=2*pi*60;%Rated frequency in rad/sec`
	
	`%Implementation of the formulas in [B25]`
	`%conv(x,y)= polynomial multiplication`
	`N=conv([Tq1 1],[Tq2 1]);`
	`D=conv([Tq3 1],[Tq4 1]);`
	`Nz=conv(N-D*Ll/Lq,[Laq/wn 0]);`
	`Dz=D-N;  Nz=Nz(1:3);  Dz=Dz(1:2);`
	`Req=Nz(3)/Dz(2);`
	`Nz=Nz/Nz(3);  Dz=Dz/Dz(2);`
	
	`%compute polynomial roots and sort them`
	`Tab=sort(abs(roots(Nz)));  Tab=1./Tab;`
	`Tm=sort(abs(roots(Dz)));  Tm=1/Tm(1);`
	
	`%Solve a system of two linear equations`
	`x=[1 1;Tab(1) Tab(2)]\[1 ;Tm]/Req;`
	
	`%Results`
	`R1q=1/x(1); L1q=wn*R1q*Tab(1); %in p.u.`
	`R2q=1/x(2); L2q=wn*R2q*Tab(2); %in p.u.`

[a]Umans et al. [B77]
[b]EPRI [B25]

Table E.1(b)—Translation of operational inductances into equivalent-circuits (resistances/ inductances in p.u., time in sec, wn = nominal frequency in rad/sec)

Equivalent circuit with two rotor circuits in each axis

Direct axis[a]	Quadrature axis[b]

%Set the time constants in Ld(s),sG(s)
%See eqs. (7.2.11-7.2.12)
T1=6.5637e-001; %in seconds
T2=4.6153e-002; %in seconds
T3=4.3605e-003; %in seconds
T4=7.9098; %in seconds
T5=4.6295e-002; %in seconds
T6=4.3995e-003 ;%in seconds
T7=4.6003e-002; %in seconds
T8=4.1867e-003; %in seconds
 	
Wn=2*pi*60;%Rated frequency in rad/sec
Ld=1.65; %Synchronous inductance
Ll=.15; %Stator leakage inductance
Lad=Ld-Ll; %Mutual inductance
 	
%Implementation of the formulas in [B77]
Ro=wn*Ld*(T4+T5+T6-T1-T2-T3);
Ro=Lad*Lad/Ro;
A=Ld*(T1+T2+T3)-Ll*(T4+T5+T6);a=a/Lad;
B=Ld*(T1*(T2+T3)+T2*T3)-Ll*(T4*(T5+T6)+T5*T6); b=b/Lad;
C=Ld*T1*T2*T3-Ll*T4*T5*T6;c=c/Lad;
D=(T4*(T5+T6)+T5*T6-T1*(T2+T3)-T2*T3);
D=d/(T4+T5+T6-T1-T2-T3);
E=(T4*T5*T6-T1*T2*T3)/(T4+T5+T6-T1-T2-T3);
 	
Lf1d=c-T7*(b-T7*(a-T7));
Lf1d=Ro*Lf1d/(e+T7*(T7-d));
A=a-T7-Lf1d/Ro;
B=b-A*T7-d*Lf1d/Ro;
 	
R1d=Ro*(A*T7-B-T7*T7)/(d*T7-e-T7*T7);
L1d=R1d*T7;
Rp=R1d*Ro/(R1d-Ro);
Tp=Rp*(e/Ro-B/R1d)/T7;
Lf2d=Rp*(A*T8-B-T8*T8)/(T8-Tp);
Tf=A-T8-Lf2d/Rp;
 	
R2d=Rp*(Tf-T8)/(Tp-T8);
L2d=R2d*T8;
Rfd=R2d*Rp/(R2d-Rp);
Lfd=Rfd*Tf;
 	
%Inductances in p.u.
Lfd=wn*Lfd;L1d=wn*L1d;L2d=wn*L2d;
Lf1d=wn*Lf1d;Lf2d=wn*Lf2d;
	%Set the time constants in Lq(s)
	%See eq. (7.2.14)
	Tq1=.975; %in seconds
	Tq2=.116; %in seconds
	Tq3=.0067; %in seconds
	Tq4=1.790; %in seconds
	Tq5=.276; %in seconds
	Tq6=.0085; %in seconds
	
	wn=2*pi*60; %in seconds
	Laq=1.165; %Mutual inductance
	Ll=.188; %Stator leakage inductance
	Lq=Laq+Ll; %Synchronous inductance
	
	%Implementation of the formulas[B25]
	%conv(x,y)= polynomial multiplication
	N=conv([Tq1 1],[Tq2 1]);
	N=conv(N,[Tq3 1]);
	D=conv([Tq4 1],[Tq5 1]); D=conv(D,[Tq6 1]);
	Nz=conv(N-D*Ll/Lq,[Laq/wn 0]);
	Dz=D-N; Nz=Nz(1:4); Dz=Dz(1:3);
	Req=Nz(4)/Dz(3);
	Nz=Nz/Nz(4); Dz=Dz/Dz(3);
	
	%compute polynomial roots and sort them
	Tab=sort(abs(roots(Nz))); Tab=1./Tab;
	Tm=sort(abs(roots(Dz))); Tm=1./Tm ;
	
	M=[1 1 1 ;
	Tab(2)+Tab(3) Tab(1)+Tab(3)
	Tab(1)+Tab(2);
	Tab(2)*Tab(3) Tab(1)*Tab(3)
	Tab(1)*Tab(2);];
	
	%Solve a system of three linear equations
	x=M\[1 ;Tm(1)+Tm(2) ; Tm(1)*Tm(2)];
	x=x/Req;
	
	%Results
	R1q=1/x(1); L1q=wn*R1q*Tab(1); %in p.u.
	R2q=1/x(2); L2q=wn*R2q*Tab(2); %in p.u.
	R3q=1/x(3); L3q=wn*R3q*Tab(3); %in p.u.

[a]Umans et al. [B77]
[b]EPRI [B25]